

# **Optimization of Claudin-11 Removal by Anti-Claudin Peptide NT11 in the Mouse Blood-Testis Barrier**

Sayaka Grace Hansen

Department of Human Genetics  
McGill University, Montreal, Canada  
June 2024



A thesis submitted to McGill University in partial fulfillment of the requirements of the degree  
of Master of Science

© Sayaka Grace Hansen 2024

## Abstract

Male infertility in cancer survivors is a prevalent consequence. Currently, sperm banking is the only method for preserving fertility in male patients; however, this option is unavailable for prepubertal boys who are exposed to sterilizing anti-cancer therapies before sperm production begins. Thus, researchers are exploring post-therapy transplantation of spermatogonial stem cells (SSCs) as a potential avenue to restore patient fertility. Studies in mice revealed a significant challenge to this approach: only a limited number of transplanted SSCs successfully reach their niche due to their inability to pass through the blood-testis barrier (BTB). Various studies have shown that individual claudin family members, notably Claudin-11, contribute uniquely to the paracellular properties of the BTB. Thus, targeting claudins to transiently disrupt the BTB structure may enhance SSC engraftment. Anti-claudin peptide NT11 was developed by modifying the C-terminal fragment of *Clostridium perfringens* enterotoxin (C-CPE), designed to transiently remove Claudin-11 from the BTB. Using an *ex vivo* air-liquid interface model to culture mouse testis tissue with NT11, I observed the removal of Claudin-11 after 16 and 72 hours of culture, as detected by wholemount immunofluorescent staining. This effect was observed in two mouse infertility models (W/W<sup>v</sup> and busulfan-treated 129/B6 mice testis tubules) and quantified using colocalization analyses with Pearson's correlation coefficient and by comparison of signal intensities using integrated sum intensities. Moreover, following the removal of NT11, there was a gradual restoration of Claudin-11 localization in the BTB over 72 hours. These studies will be expanded to observe the effect of NT11 on human testis biopsies after optimization of the purification processes of our peptide. To achieve this, I have focused on improving the purification, induction, and solubility of our peptide using several different methods such as adjusting buffer concentrations, employing Amicon centrifugal filters, and utilizing size exclusion chromatography. This process has proven to be quite a challenge due to NT11's insolubility, which did not improve despite alternative sonication methods, induction conditions, auto-induction media, and buffer additives. The structure of the protein suggests that NT11's insolubility likely results from modifications of the  $\beta 8$  and  $\beta 9$  center strands of C-CPE, leading to protein instability. Therefore, I propose future investigations for increasing NT11 stability and alternative methods for BTB disruption. Ultimately, my study demonstrates the effectiveness of our current peptide in disrupting mouse BTB *ex vivo*. However, prior to moving forward to human studies, it is essential that we improve the purification and solubility of NT11.

My study serves as a valuable resource for the evaluation of peptides capable of disrupting cellular barriers for potential drug delivery, as well as investigating methods of improving protein induction, solubility, and purification for insoluble proteins.

## Résumé

L'infertilité masculine est une conséquence fréquente chez les survivants du cancer. Actuellement, la congélation du sperme avant le début du traitement est la seule méthode permettant de préserver la fertilité chez les patients. Néanmoins, cela n'est pas possible pour les garçons prépubères qui sont exposés à des thérapies anticancéreuses stérilisantes avant le début de la production de spermatozoïdes. Par conséquent, les chercheurs explorent la transplantation post-thérapeutique de cellules souches spermatogonies (SSC) comme voie potentielle pour restaurer la fertilité des patients. Des études chez la souris ont révélé un défi important pour cette approche: le nombre de SSC qui réussissent à atteindre leur niche est limité en raison de leur incapacité à traverser la barrière hémato-testiculaire (BTB). Plusieurs études ont démontré que les membres individuels de la famille des claudines, notamment Claudine-11, contribuent de manière unique aux propriétés paracellulaires du BTB. Ainsi, cibler les claudines pour perturber la structure du BTB de manière transitoire pourrait améliorer la greffe de SSC. Le peptide anti-claudine NT11 a été développé en modifiant le fragment C-terminal de l'entérotoxine *Clostridium perfringens* (C-CPE), conçu pour éliminer de manière transitoire la Claudine-11 du BTB. En utilisant un modèle d'interface air-liquide *ex vivo* pour cultiver du tissu testiculaire de souris avec NT11, j'ai observé l'élimination de Claudine-11 après 16 et 72 heures de culture, détectée par immunofluorescence. Cet effet a été observé dans deux modèles d'infertilité chez la souris (tubes testiculaires de souris W/W<sup>v</sup> et 129/B6 traitées au busulfan) et a été quantifié à l'aide d'analyses de colocalisation avec le coefficient de corrélation de Pearson et des comparaisons d'intensités de signaux utilisant les intensités de somme intégrées. De plus, suite à la suppression de NT11, une restauration progressive de localisation de Claudin-11 dans le BTB a eu lieu sur 72 heures. Ces études seront développées pour observer l'effet du NT11 sur les biopsies de testicules humains après l'optimisation de la purification de notre peptide. Pour atteindre cet objectif, je me suis concentrée sur l'amélioration de la purification, de l'induction et de la solubilité de notre peptide en utilisant différentes méthodes, telles que l'ajustement des concentrations de tampon, l'utilisation de filtres centrifuges Amicon et l'utilisation de la chromatographie d'exclusion de taille. Ce processus est devenu un défi en raison de l'insolubilité du NT11, qui ne s'est pas améliorée malgré les méthodes alternatives de sonication, les conditions d'induction, les milieux d'auto-induction et les additifs tampons. La structure de la protéine suggère que l'insolubilité de NT11 provient vraisemblablement des modifications des

feuillet  $\beta 8$  et  $\beta 9$  du C-CPE, provoquant une instabilité protéique. Par conséquent, je propose de futures études pour augmenter la stabilité de NT11 et des méthodes alternatives pour la perturbation du BTB. Pour finir, mon étude démontre l'efficacité de notre peptide actuel pour perturber la BTB de souris *ex vivo*. Cependant, une amélioration supplémentaire de la purification et de la solubilité de NT11 est nécessaire afin d'entreprendre les études chez l'homme. Mon étude constitue une ressource utile pour l'évaluation de peptides capables de perturber les barrières cellulaires pour l'administration de médicaments, ainsi que pour l'étude de méthodes permettant d'améliorer l'induction, la solubilité et la purification des protéines insolubles.

## Table of Contents

Abstract.....	2
Résumé.....	4
Table of Contents.....	6
List of Abbreviations .....	9
List of Figures.....	12
List of Tables .....	14
Acknowledgements.....	15
Contributions of Authors .....	16
1. Introduction .....	17
1.1 Significance and Rationale .....	17
1.2 Spermatogenesis and Spermatogonial Stem Cells.....	18
1.3 Spermatogonial Stem Cell Transplantation .....	21
1.4 The Blood-Testis Barrier .....	23
1.5 Tight Junction Proteins: Claudins.....	25
1.6 Sertoli Cell Tight Junction Remodelling .....	29
1.7 Claudin Interactions in the Blood-Testis Barrier.....	30
1.8 Disrupting the Blood-Testis Barrier.....	33
1.9 Summary and Hypothesis .....	37
2. Materials and Methods .....	39
2.1 Animal: W/W <sup>v</sup> Mice and Busulfan-Injected 129/B6 Mice .....	39
2.2 Animal Protocol Ethics.....	39
2.3 SSC culture medium .....	39
2.4 Air-Liquid Interface Culture System .....	40
2.5 Antibodies for Immunofluorescence.....	42
2.6 Whole-Mount Immunofluorescence .....	42
2.7 Confocal Imaging.....	43
2.8 ImageJ Analysis of Confocal Images .....	45
2.9 Statistical Analysis of Images.....	46
2.10 Plasmid Generation.....	47

2.11	Protein Induction.....	47
2.12	Studier Method for Auto-Induction of Protein Expression.....	48
2.13	Protein Purification .....	50
2.14	Size Exclusion Chromatography.....	52
2.15	Amicon Ultra Centrifugal Filters .....	52
2.16	Solubility Test.....	53
2.17	Antibodies for Western Blot .....	53
2.18	Western Blot Analysis and Coomassie Protein Assay.....	54
3.	Results .....	56
3.1	Aim 1: Claudin-11 Removal from the Blood-Testis Barrier by NT11 .....	56
3.1.1	Establishing an <i>Ex Vivo</i> Organ Culture System to Investigate Peptide Effects .	56
3.1.2	Decrease in Claudin-11 Localization After 16- and 72-hour NT11 Treatments	59
3.1.3	Removal of NT11 Allows Claudin-11 to Repopulate the BTB.....	63
3.1.4	Pearson’s Correlation Coefficient Supports Claudin-11 Delocalization from the Sertoli Cell Tight Junctions .....	66
3.1.5	Measuring Integrated Sum Intensities to Quantify Relative Amount of Claudin-11 at the BTB .....	68
3.1.6	Summary of Results from Aim 1 .....	70
3.2	Aim 2: Optimizing NT11 Purification.....	72
3.2.1	Assessing Purity of NT11 Protein Preparations .....	72
3.2.2	Incorporation of Size Exclusion Chromatography and Amicon Centrifugal Filters to Improve Purity of NT11 .....	74
3.2.3	Adjustment of Binding Buffers to Modify Non-Specific Interactions with Ni-NTA Agarose Beads and Improve Elution .....	76
3.2.4	Exploring Column Purification to Prevent Non-Specific Interactions with Ni-NTA Agarose Beads .....	78
3.2.5	Optimizing Sonication Methods to Extract NT11 from the Pellet .....	80
3.2.6	Lowering Induction Temperatures and Incorporating Various Detergents/ Additives to Increase Protein Solubility .....	80
3.2.7	Adjustments to Culture Conditions to Improve Induction of NT11 .....	83

3.2.8	Summary of Results from Aim 2.....	86
4.	Discussion .....	88
4.1	NT11 Mediated Claudin-11 Removal and Recovery in the Blood-Testis Barrier.....	88
4.2	Optimization of NT11 Purification, Solubility and Induction .....	89
4.3	Limitations of Study .....	95
5.	Conclusions and Future Directions .....	97
5.1	Final Conclusion .....	97
5.2	Optimizing NT11 Stability and BTB Disruption.....	97
5.3	NT11 Treatment on Human Testis Biopsies.....	99
6.	References .....	100
7.	Appendix .....	117
7.1	Animal Ethics Certificate.....	117

## List of Abbreviations

**aa:** Amino acid

**AceE:** Angiotensin Converting Enzyme 2

**ANOVA:** Analysis of Variance

**ArnA:** Bifunctional Polymyxin Resistance Protein 4-Amino-4-Deoxy-L-Arabinose

**ART:** Assisted Reproductive Technology

**β-ME:** β-mercaptoethanol

**BTB:** Blood-Testis Barrier

**BSA:** Bovine Serum Albumin

**CaCl<sub>2</sub>:** Calcium Chloride

**cdNA:** Complementary Deoxyribonucleic Acid

**CPE:** *Clostridium Perfringens* Enterotoxin

**C-CPE:** C-terminal Domain of *Clostridium Perfringens* Enterotoxin

**Cldn/ CLDN:** Claudin

**CoCl<sub>2</sub>•6H<sub>2</sub>O:** Cobalt Chloride Hexahydrate

**Coloc:** Colocalization

**CRP:** C-Reactive Protein

**CuCl<sub>2</sub>•2H<sub>2</sub>O:** Copper (II) Chloride Dihydrate

**DNA:** Deoxyribonucleic Acid

**DnaK:** Heat Shock Protein 70 kDa

**EB:** Elution Buffer

***E. coli* BL21 (DE3) pLysS:** *Escherichia coli* Strain BL21, Lysogenic for λ-DE3

**EF-Tu:** G Protein-Elongation Factor Thermal Unstable Tu

**EL1:** First Extracellular loop

**EL2:** Second Extracellular loop

**FeCl<sub>3</sub>•6H<sub>2</sub>O:** Iron (III) Chloride Hexahydrate

**FGF2:** Fibroblast Growth Factor 2

**FIJI/ Image J:** Java-based Image Processing Program

**FSH:** Follicle-Stimulating Hormone

**GDNF:** Glial Cell Line-Derived Neurotrophic Factor

**GFRA1:** GDNF Family Receptor Alpha-1

**GlmS:** Glutamine-Fructose-6-Phosphate Aminotransferase [Isomerizing]

**GST:** Glutathione S-Transferase

**h:** Hours

**HEPES:** 2-[4-(2-Hydroxyethyl) Piperazin-1-yl] Ethane-sulfonic Acid

**His:** Histidine

**HRP:** Horseradish Peroxidase

**H<sub>3</sub>BO<sub>3</sub>:** Boric Acid

**ICSI:** Intracytoplasmic Sperm Injection

**IMAC:** Immobilized Metal Affinity Chromatography

**IPTG:** Isopropyl β-D-Galactopyranoside

**IVF:** *In Vitro* Fertilization

**JAM:** Junctional Adhesion Molecules

**KCl:** Potassium Chloride

**kDa:** Kilodalton

**KH<sub>2</sub>PO<sub>4</sub>:** Potassium Dihydrogen Phosphate/ Monopotassium Phosphate (MKP)/

Monobasic Potassium Phosphate

**KO:** Knockout

**LB:** Lysogeny Broth/ Luria-Bertani  
**LD:** Loading Dye  
**LH:** Luteinizing Hormone  
**LPS:** Lipopolysaccharide  
**LSM:** Laser Scanning Microscope  
**MA:** Meiotic Arrest  
**MBP:** Maltose-Binding Protein  
**MEM $\alpha$ :** Minimum Essential Medium  $\alpha$   
**MeOH:** Methanol  
**mg:** Milligram  
**mL:** Milliliter  
**mm:** Millimeter  
**mM:** Millimolar  
**MgSO<sub>4</sub>:** Magnesium Sulfate  
**MgSO<sub>4</sub>•7H<sub>2</sub>O:** Magnesium Sulfate Heptahydrate  
**MIP:** Maximum Intensity Projection  
**MnCl<sub>2</sub>•4H<sub>2</sub>O:** Manganese (II) Chloride Tetrahydrate  
**MW:** Molecular Weight  
**MWCO:** Molecular Weight Cut Off  
**NaCl:** Sodium Chloride  
**Na<sub>2</sub>HPO<sub>4</sub>:** Disodium Phosphate (DSP)/ Disodium Hydrogen Phosphate/ Sodium Phosphate, Dibasic  
**Na<sub>2</sub>MoO<sub>4</sub>•2H<sub>2</sub>O:** Sodium Molybdate Dihydrate  
**Na<sub>2</sub>SeO<sub>3</sub>•5H<sub>2</sub>O:** Sodium Selenite Pentahydrate  
**(NH<sub>4</sub>)<sub>2</sub>SO<sub>4</sub>:** Ammonium sulfate

**NiCl<sub>2</sub>•6H<sub>2</sub>O:** Nickel (II) Chloride Hexahydrate  
**Ni-NTA:** Nickel<sup>2+</sup> ion- Nitrilotriacetic acid  
**NPS:** Media with (NH<sub>4</sub>)<sub>2</sub>SO<sub>4</sub>, KH<sub>2</sub>PO<sub>4</sub>, Na<sub>2</sub>HPO<sub>4</sub>  
**NTA:** Nitrilotriacetic Acid  
**nm:** Nanometer  
**NT:** N-terminal Domain of Spidroin Protein  
**NT11:** Peptide Targeting Claudin-11: His::NT::C-CPE $\Delta$ CBD::Cldn11EL2  
**OD:** Optical Density  
**OD<sub>600</sub>:** Optical Density at 600nm  
**PAS:** Periodic Acid Schiff  
**PBS:** Phosphate-Buffered Saline  
**PCR:** Polymerase Chain Reaction  
**PCTE:** Polycarbonate Track Etch  
**PDZ:** Post-Synaptic Density 95/Discs large/Zonula Occludens-1  
**PVDF:** Polyvinylidene Difluoride  
**RB:** Resuspension Buffer/ Lysis Buffer  
**RI-MUHC:** Research Institute- McGill University Health Centre  
**ROI:** Region of Interest  
**RNA:** Ribonucleic Acid  
**rRNA:** Ribosomal RNA  
**RT:** Room Temperature  
**SCO:** Sertoli Cell-Only  
**SD:** Standard Deviation  
**SDS-PAGE:** Sodium Dodecyl Sulfate-Polyacrylamide Gel Electrophoresis  
**SEC:** Size Exclusion Chromatography

**SlyD:** Sensitive to Lysis D Protein  
**SSC:** Spermatogonial Stem Cells  
**SUMO:** Small Ubiquitin-like Modifier  
**TB:** Terrific Broth  
**TBST:** Tris-Buffered Saline with Tween 20  
**TCA:** Trichloroacetic Acid  
**TEER:** Transepithelial/ Trans-Endothelial Electrical Resistance  
**TGFβ2:** Transforming Growth Factor-β2  
**Tris:** Tris Base (2-Amino-2-Hydroxymethyl-Propane-1,3-diol)  
**TRX:** Thioredoxin  
**WB:** Wash Buffer  
**ZnSO<sub>4</sub>•7H<sub>2</sub>O:** Zinc Sulphate Heptahydrate  
**ZO:** Zonula Occludens

**ZY:** ZY Medium with Tryptone and Yeast Extract  
**ZYP-0.8G:** Rich Medium for growth with little or no induction with 0.8% glucose  
**ZYP-5052:** Rich Medium for Auto-Induction with 0.5 % Glycerol, 0.05% Glucose, and 0.2% α-lactose  
**°C:** Degrees Celsius  
**μg:** Microgram  
**μL:** Microliter  
**μm:** Micrometer  
**μM:** Micromolar  
**50x5052:** Media containing 0.5 % Glycerol, 0.05% Glucose, 0.2% α-lactose

## List of Figures

Figure 1: Seminiferous epithelium organization.....	19
Figure 2: Segmentation of stages in human and mouse testis tubules.....	20
Figure 3: The Blood-Testis Barrier organization.....	24
Figure 4: Proteins in the Blood-Testis Barrier.....	26
Figure 5: Schematic representation of a claudin molecule. ....	28
Figure 6: Schematic representation of C-CPE interacting with a claudin molecule.....	34
Figure 7: Scheme of C-CPE::Claudin fusion proteins.....	36
Figure 8: Air-liquid interface <i>ex vivo</i> culture system.....	40
Figure 9: Scheme for claudin recovery experiment.....	41
Figure 10: Confocal imaging of mice testis tubules. ....	44
Figure 11: Creating an ROI using ZO-1 signal at the membrane. ....	45
Figure 12: Scheme of NT11 induction and purification. ....	51
Figure 13: Claudin-11 protein localization pattern in W/Wv mice testis tubules.....	56
Figure 14: NT11 treatment had no effect on localization of Claudin-11 at 5 hours and 10 hours in a submerged whole testis <i>ex vivo</i> culture system.....	57
Figure 15: Variation in Claudin-11 protein localization pattern in B6 mice testis tubules. ....	58
Figure 16: NT11 treatment decreased localization of Claudin-11 at the BTB in W/Wv testis tubules.....	61
Figure 17: NT11 treatment decreased localization of Claudin-11 at the BTB in 129/B6 busulfan-treated testis tubules.....	62
Figure 18: Decrease in Claudin-11 localization at the BTB after 16-hour NT11 treatment before removing the peptide from the media. ....	63
Figure 19: Recovery of Claudin-11 to the BTB following treatment with NT11. ....	64
Figure 20: Variation in Claudin-11 localization across tubules of the same recovery time points. ....	65
Figure 21: Claudin-11 colocalization with ZO-1 in W/Wv and 129/B6 busulfan-treated testis tubules after 16 and 72-hour NT11 treatments. ....	66
Figure 22: Claudin-11 colocalization with ZO-1 in W/Wv testis after 24, 48 and 72 hours post 16-hour NT11 treatment. ....	67

Figure 23: Integrated sum intensity of Claudin-11 over ZO-1 in W/Wv and 129/B6 busulfan-treated testis tubules after 16 and 72-hour NT11 treatments. ....	69
Figure 24: Integrated sum intensity of Claudin-11 over ZO-1 in W/Wv testis tubules after 24, 48, 72 hours post 16-hour NT11 treatment. ....	70
Figure 25: Assessing NT11 purification and comparing purified NT11s. ....	73
Figure 26: Analysis of NT11 purity after Size Exclusion Chromatography and Amicon Centrifugal Filters. ....	75
Figure 27: Comparing buffers with different additives for NT11 purification. ....	77
Figure 28: Assessing NT11 purity after column purification. ....	78
Figure 29: Solubility test on NT11 induced at lower temperature or with additives, resuspended with various detergents. ....	82
Figure 30: Assessing NT11 induction and soluble fractions from testing IPTG concentrations and auto-induction media. ....	85
Figure 31: Structural composition of C-CPE. ....	94

## List of Tables

Table 1: 1000x trace elements. ....	49
Table 2: Original and modified buffers for NT11 purification. ....	76
Table 3: Yield table for total protein loaded on Coomassie-stained denaturing polyacrylamide gel and western blot on assessing NT11 purity after column purification. ....	79
Table 4: Comparing hydrophobicity of amino acids from exchanged sequences. ....	91
Table 5: Amino acid sequences of different constructs and domains. ....	93

## **Acknowledgements**

I would like to express my sincere gratitude to Dr. Aimee Ryan and Dr. Makoto Nagano for their guidance, support, and expertise throughout the course of my research. Dr. Ryan's encouragement to explore science from different perspectives has challenged me to grow and venture beyond my comfort zone. Similarly, Dr. Nagano's support in problem-solving has honed my critical thinking skills. Their lessons and feedback have been instrumental in shaping this thesis and my development as an independent researcher. Additionally, I would like to thank my thesis committee members, Dr. Indra Gupta and Dr. Teruko Taketo, for their critical guidance and troubleshooting throughout my master's program. I would also like to thank the RI-MUHC Molecular Imaging Platform for their assistance and help throughout my project.

Furthermore, I would like to express my heartfelt appreciation to the lab members in Dr. Ryan, and Dr. Gupta's lab for their continuous support and mentorship. Especially thank you to Liz Legere, Vasikar Murugapoopathy, and Dr. Jean-François Boisclair Lachance for their tireless efforts in teaching me the foundational aspects of lab work. I am profoundly grateful for the time and effort they invested in me throughout my studies. I would also like to particularly thank Ira Lacdao for her unwavering support and guidance. Her expertise and encouragement have helped me navigate through challenges with confidence. Together, their guidance and assistance were indispensable, without which I could not have accomplished this endeavor. Moreover, their perspective and feedback have been invaluable in helping me visualize my project in new ways, especially in light of new and unexpected data. They not only helped me build my technical skills in the lab, teaching me everything from Western Blots to protein purification, but also provided a sense of warmth and comfort throughout my journey.

Finally, I would like to sincerely thank my family and especially my partner, Antoine Aubet, for their never-ending support and patience. Their constant encouragement and care have been my foundation.

## **Contributions of Authors**

This project was conducted under Dr. Makoto Nagano and Dr. Aimee Ryan's research proposal on "Effects of anti-claudin peptides on human blood-testis barrier for stem cell delivery". Dr. Enrique Gamero-Estevez designed and generated the polypeptide, NT11, along with the protein production protocol. Sayaka Hansen has since then generated the peptide used for her project with Dr. Gamero-Estevez' construct and has improved the current protein production protocol. Dr. Jean-François Boisclair Lachance and Liz Legere generated the stocks of C-CPE currently used in the lab. The Animal Resources Division at the RI-MUHC and Xiangfan Zhang helped maintain and provide animal care for experimental mice. Sayaka Hansen performed all other experiments, participated in experimental design and troubleshooting of the project. Additionally, Dr. Jean-François Boisclair Lachance and Ira Lacdao contributed to the optimization of the protein purification protocol. Data collection was conducted by Sayaka Hansen. Additionally, data analysis was performed by Sayaka Hansen with guidance from Dr. Aimee Ryan and Dr. Makoto Nagano. Dr. Aimee Ryan and Dr. Makoto Nagano supervised the work, participated in experimental design and troubleshooting.

## 1. Introduction

### 1.1 Significance and Rationale

The National Cancer Institute has projected 2,001,140 new cancer cases in 2024, with statistics estimating that one in every two men will face a cancer diagnosis in their lifetime (Siegel et al., 2024). As the number of cancer diagnoses among children and young adolescents rise and innovative therapies improve survival rates, the need for fertility preservation among male oncofertility patients has become increasingly significant (Kadam et al., 2018). Cancer treatments, while lifesaving, often have detrimental effects on fertility, posing significant challenges to individuals seeking to preserve their reproductive potential. As such, addressing the fertility concerns of male cancer patients has emerged as a critical aspect of comprehensive cancer care.

Spermatogonial stem cells (SSCs) are sensitive to anti-cancer therapies designed to target rapidly dividing cells (Lopes et al., 2020). Chemotherapy, in particular, poses a significant risk of permanent infertility by impairing the ability of testicular cells to generate healthy, mature sperm (Dohle, 2010). Studies of spermatogenesis in long-term cancer survivors, particularly those with testicular cancer and Hodgkin's disease, have shown persistent azoospermia or severe oligozoospermia in up to 24% of patients, with recovery levels being higher in younger patients compared to older patients at the time of treatment (Vakalopoulos et al., 2015). The combination of radiotherapy and chemotherapy will induce gonadotoxic effects (Vakalopoulos et al., 2015). SSCs play a crucial role in continuously replenishing germ cells, which eventually differentiate into sperm throughout a male's life (Amann & Howards, 1980; Kubota & Brinster, 2018). As a result, the efficacy of sperm production is severely compromised from these cancer treatments. Presently, sperm banking stands as the primary method of preserving fertility in male patients (Osterberg et al., 2014). The collected sperm can later be used for *in vitro* fertilization (IVF) or intracytoplasmic sperm injection (ICSI). However, for prepubertal boys undergoing sterilizing anti-cancer therapies, sperm cryopreservation is not viable as their testes do not yet produce sperm (Osterberg et al., 2014). This limitation has prompted researchers to turn their attention to SSCs, which are present in the testes from birth (Forbes et al., 2017; Hermann et al., 2012). By harvesting these cells before cancer treatment, they can be preserved and subsequently transplanted back into the patient post-therapy, thus offering a promising avenue for restoring patient fertility (Hermann et al., 2012).

Despite its potential, SSC transplantation has yet to be clinically implemented due to an important limitation: only a low number of transplanted SSCs will properly reintegrate into the stem cell niche in the testis which is required for engraftment and subsequent regeneration of spermatogenesis post-transplantation (Kadam et al., 2018; Shinohara et al., 2001; Takashima & Shinohara, 2018). This inefficiency of SSC homing can be attributed to the tight junction barrier formed between somatic cells in the seminiferous epithelium—the blood-testis barrier (BTB) (Shinohara et al., 2001). When SSCs are transplanted into the testes, they are injected into the lumen of the seminiferous tubules, necessitating their traversal of the BTB to reach their niche on the basement membrane (Kanatsu-Shinohara et al., 2008). Studies in mice indicate that only approximately 1 in 8 SSCs successfully colonize and regenerate spermatogenesis post-transplantation (Nagano, 2003). Our hypothesis is that transient disruption of the BTB could facilitate the passage of more SSCs to their niche on the basement membrane, thereby enhancing engraftment efficacy following transplantation.

In the Ryan and Nagano labs, we have developed a novel peptide with the ability to bind to claudins, critical components of tight junctions, thereby transiently removing these transmembrane proteins from the BTB. In my thesis study, I established a system to assess the effects of this peptide using mouse testis pieces *ex vivo*, while also exploring various methods of optimizing protein induction, purification, and solubility. I demonstrated that our peptide effectively removes the target claudin from the BTB in a reversible manner. Notably, upon removal of the peptide from the media, the targeted claudin was again localized to the tight junctions of the testis tubules, the BTB. Our project lays the groundwork for investigating the transient disruption of the BTB in human samples, as the fundamental structure and composition of the BTB are highly conserved between mice and humans (X.-H. Jiang et al., 2014). Ultimately, our research will contribute to defining effective peptides that disrupt the mouse BTB and encourage further investigation in the development of peptides capable of disrupting cellular barriers for potential drug delivery.

## **1.2 Spermatogenesis and Spermatogonial Stem Cells**

Spermatogenesis involves a series of intricate, cellular, proliferative, and developmental phases to produce genetically unique male gametes. This complex biological process takes place inside the seminiferous tubules; a convoluted cluster of tubules located in the testes.

Spermatogenesis can be broken down into three phases (Suede et al., 2023). The first phase involves mitotic cell division of diploid SSCs located in the niche on the basal membrane of the seminiferous epithelium. These mitotic divisions allow the SSCs to self-renew and produce a pool of committed spermatogonia that will develop into primary spermatocytes (Suede et al., 2023). In the second phase, which is known as spermatocytogenesis, primary spermatocytes will undergo meiosis to produce haploid secondary spermatocytes while leaving the basal membrane and moving towards the lumen (Sharma & Agarwal, 2011). In this process, the SSCs will undergo spermatogonial renewal (type A spermatogonia), proliferation via mitosis, differentiation and cell cycle progression from type B spermatogonia to preleptotene spermatocytes in the basal compartment, below the Blood-Testis Barrier (BTB) between Sertoli cells (Cheng & Mruk, 2012). The BTB will then go through extensive restructuring to allow the transit of preleptotene spermatocytes in the adluminal compartment above the BTB where

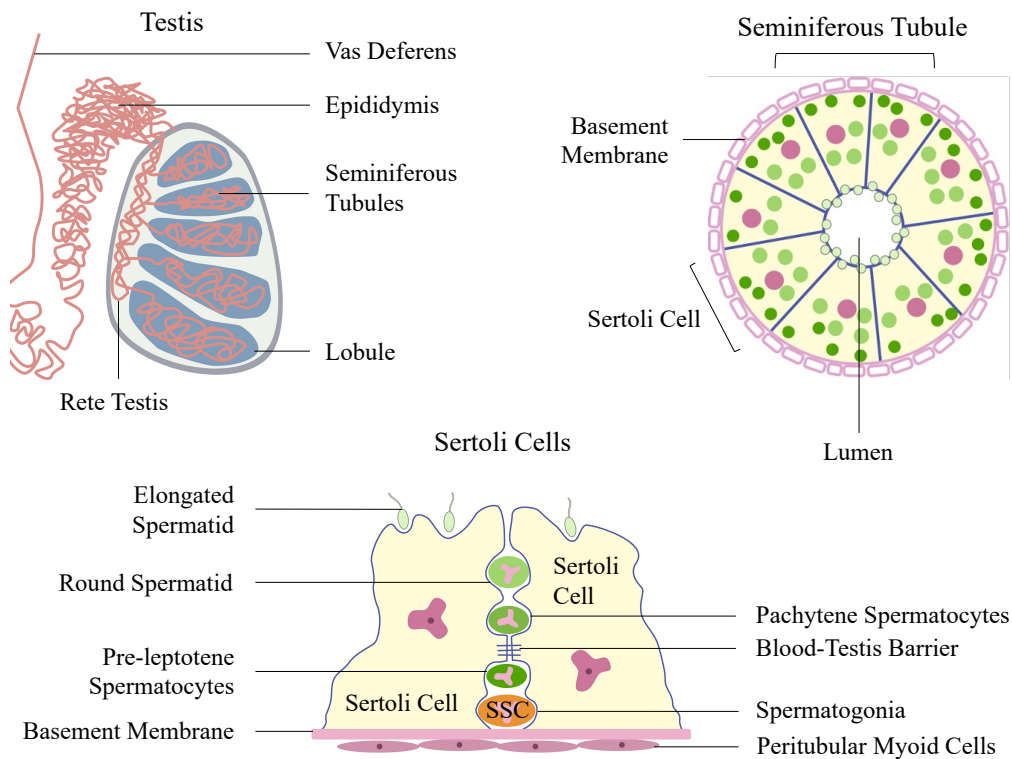


**Figure 1: Seminiferous epithelium organization.** This diagram shows cross sections through the testis, seminiferous tubule and Sertoli cells. Maturation of the SSCs into eventual spermatids starts at the basement membrane and occurs as they move towards the lumen. Adapted from Elinati, 2012.

Meiosis I and II, spermiogenesis (development of round spermatids to elongated spermatids, and to spermatozoa), and spermiation will take place (Cheng & Mruk, 2012). Thus, the third phase consists of spermatids elongating to form spermatozoa by spermiogenesis which consists of morphological development from round spermatids to mature and motile sperm cells (Figure 1) (Sharma & Agarwal, 2011; Wong et al., 2010). The spermatozoa will then travel through the lumen of the seminiferous tubules, exit through the rete testis, and be stored in the epididymis until ejaculation (Sharma & Agarwal, 2011).

The duration of spermatogenesis in humans is 74 days whereas in mice this process takes 34.5 days (Toor & Sikka, 2017). Spermatogenesis occurs within the seminiferous tubules and is regulated by several endocrine factors that include testosterone, follicle-stimulating hormone (FSH), and luteinizing hormone (LH) (Sofikitis et al., 2008). LH stimulates the proliferation and maturation of Leydig cells, which secrete testosterone, while FSH acts on Sertoli cells, promoting the production of signaling molecules essential for spermatogenesis (Oduwole et al., 2021). During spermatogenesis, the seminiferous epithelium undergoes cyclic changes as a result of germ cell development. Spermatogenesis can be broken down into seminiferous epithelium

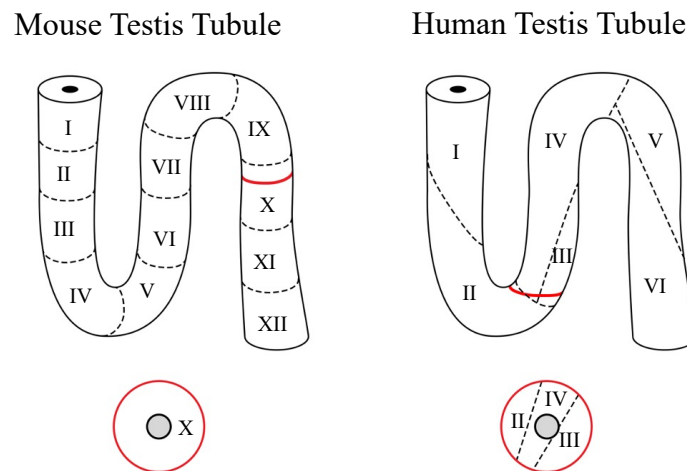


**Figure 2: Segmentation of stages in human and mouse testis tubules.** A diagram demonstrating the stages in the cycle of the seminiferous epithelium in human (I-VI) vs mouse (I-XII). In human, there is a mosaic arrangement of the stages of spermatogenesis whereas in the mouse, spermatogenesis occurs in an orderly fashion along the seminiferous tubule. The cross section outlined in red demonstrates the different stages that can be observed. Adapted from Silber, 2010.

cyclic changes stages that are characterised by the changes in morphology and relative locations of the spermatid, round spermatids, and spermatocytes when observing the cross-section of a testis tubule. Spermatogenesis is typically divided into 6 stages in human and 12 stages in mouse (Krause et al., 2008), which can be observed along a single testis tubule (Figure 2) (Ahmed & de Rooij, 2009). Most studies categorize the stages based on Periodic Acid Schiff (PAS) and hematoxylin-stained sections where they differentiate one stage from another based on the changes of the acrosome and nuclear morphology of the younger generation of spermatids (Ahmed & de Rooij, 2009; Russell et al., 1993; Xu et al., 2021).

SSCs are at the foundation of male fertility and spermatogenesis (Phillips et al., 2010). However, SSCs represent only 0.03% of all germ cells in rodent testes as they are outnumbered by the differentiating spermatogonia, spermatocytes, spermatids and sperm (Phillips et al., 2010; Song et al., 2022). SSCs are defined by their ability to balance self-renewal and differentiation, producing millions of sperm each day. Interestingly, SSC transplantation has demonstrated that SSCs have homing activity (Kanatsu-Shinohara et al., 2018). It has been previously shown that when dissociated testis cells were transplanted into the seminiferous tubules of infertile mouse recipients, donor SSCs would migrate through the BTB, thereby settling and proliferating on the basement membrane (Avarbock et al., 1996; Brinster & Zimmermann, 1994; Kanatsu-Shinohara et al., 2018). When SSCs mature under physiological conditions, they migrate from the basal compartment towards the adluminal compartment. This transition requires the formation of new tight junctions between Sertoli cells forming below the preleptotene spermatocytes, preceding by the dissolution of older junctions and the release of these cells into the adluminal compartment (B. E. Smith & Braun, 2012; Stammeler et al., 2016; Yan Cheng & Mruk, 2015). Consequently, SSC homing that is observed in SSC transplantation contrasts with the natural process of spermatogenesis.

### **1.3 Spermatogonial Stem Cell Transplantation**

Our theory regarding the potential of SSC transplantation to restore male fertility in oncofertility patients is grounded in our observation of fertility recovery in sterile mice following SSC transplantation (Nagano, 2003). The transplantation procedure involves the use of a microinjection pipet loaded with donor cells, including SSCs, which are introduced into the efferent duct of infertile recipients, facilitating injection into the rete testis where all seminiferous

tubules converge (Nagano, 2003; Takashima & Shinohara, 2018). This strategic site of injection requires the donor cells to travel in the reverse direction of spermatogenesis, dispersing into individual tubules (Nagano, 2003; Ogawa et al., 1997; Takashima & Shinohara, 2018). While the cells injected into the lumen comprise various cell types beyond SSCs, such as germ cells of later stages and different somatic cells, only the SSCs possess the capacity for self-renewal and regeneration, enabling them to survive and repopulate the recipient testes (Nagano, 2003; Zohni et al., 2012). In contrast, other cell types within the injection do not persist due to cellular death, lacking self-renewal capability (Nagano et al., 1999; Tournaye & Goossens, 2011). The presence of non-SSC cells in the injection is due to the absence of exclusive SSC biochemical or immunological markers that could be used to obtain a purified population of SSCs (Zohni et al., 2012). As stem cells are characterized by their regenerative potential rather than specific markers, SSCs cannot be identified exclusively at this time.

The Nagano lab has calculated that approximately 3000 SSCs exist in one normal adult testis, representing ~0.01% of total testis cells (Nagano, 2003). In mice, SSCs require approximately 1 week to colonize the stem cell niche after SSC transplantation (Brinster & Zimmermann, 1994; Kadam et al., 2018; Nagano, 2003; Zhao et al., 2021). In SSC transplantation, homing efficiency is defined as the proportion of injected stem cells that will colonize the recipient testis (Nagano, 2003). The number of SSCs gradually decreased during the homing process, and only 12% of SSCs successfully colonized the niche on Day 7 after transplantation (Nagano, 2003). Around 75% of injected donor SSCs were lost within 1 day while the 12% migrated to their niche on the basement membrane (Nagano, 2003).

Recipients of these injections in our experiments are genetically infertile W/W<sup>v</sup> mutant mice. The dominant-white spotting (W) locus encodes the *c-KIT* proto-oncogene which is a membrane-bound tyrosine kinase (Ogawa et al., 2000; Yuan et al., 2015). *c-KIT* plays an important role in male germ cell development and dysfunctional c-KIT will lead to azoospermia in mice (Jin et al., 2023; Ogawa et al., 2000). The W mutation is located in the transmembrane domain and the W<sup>v</sup> mutation is located in the kinase domain of the c-KIT protein (Yuan et al., 2015). The Kit<sup>W</sup>/Kit<sup>W-v</sup> compound heterozygous mutations will lead to infertility in W/W<sup>v</sup> mice as their testes do not generate spermatogenesis while heterozygous W/+ and W<sup>v</sup>/+ are fertile (Ogawa et al., 2000). This specific strain of mice carrying the compound heterozygous mutations are used as they mimic the phenotype of male infertility in human (Yuan et al., 2015).

Alternatively, busulfan-treated 129/B6 mice can also be used as an induced infertile mouse model. Busulfan is a chemotherapeutic alkylating agent that destroys endogenous spermatogenesis (Qin et al., 2016). Busulfan treatment has been studied and often used for the preparation of SSC transplantation recipients in mice. Thus, W/W<sup>v</sup> mice and busulfan-injected 129/B6 mice both serve as models to verify the efficacy of SSC transplantation (Azizi et al., 2021). With successful SSC transplantation, SSCs from the donor injection will engraft and establish spermatogenesis in recipients, producing offspring carrying the donor genotype (Li et al., 2018).

In future clinical application, our research will facilitate SSC transplantation following the harvesting and cryopreservation of SSCs prior to cancer therapy. By collecting the cells before exposure to cytotoxic agents, we aim to regenerate and sustain healthy spermatogenesis, thereby enabling patients to achieve conception naturally (Diao et al., 2022). Unlike conventional sperm banking methods, which often necessitate reliance on assisted reproductive technologies (ART), our approach offers a more direct route to restoring fertility in male oncofertility patients (David & Orwig, 2020). Unfortunately, this method is not ready for clinical application due to an important limitation: the low number of SSCs that will reach their niche due to the Blood-Testis Barrier.

#### **1.4 The Blood-Testis Barrier**

The BTB is essential for male germ cell development. This barrier is a highly dynamic structure made up of adhesion junctions, gap junctions, basal ectoplasmic specialization, and co-existing tight junctions basally located between adjacent Sertoli cells that limit paracellular and transcellular transport of substances (Figure 3) (Li et al., 2018). The gap junctions include connexin-based complexes such as Connexin 43 which interact with scaffolding proteins (Lee et al., 2009). Moreover, the basal ectoplasmic specialization includes cadherins such as N-cadherin with catenins, such as  $\beta$ -catenin, and  $\alpha$ -catenin (Lee et al., 2009). Ectoplasmic specializations, in conjunction with Sertoli cell tight junctions, are present at the periphery of the cell, with actin filament bundles hexagonally packed and endoplasmic reticulum cisternae parallelly position to the Sertoli cell membrane (Luaces et al., 2023). The Sertoli cell tight junctions are especially critical components of the BTB as they serve to seal the paracellular space and are composed of proteins from apposing cells that interact tightly with one another (S. Wu & Cheng, 2020). These

interactions regulate the movement of small molecules and ions through the paracellular space with a gate and fence function (Xu et al., 2009). The gate function prevents the passage of water, solutes, and other large molecules between the paracellular space, whereas the fence function restricts the movement of proteins and lipids between apical and basolateral domains which generates cell polarity (Yan Cheng & Mruk, 2015). The gate and fence functions are regulated by specific proteins that interact and make up the tight junction complex.

The BTB is first formed in the testis at the peripubertal period during the initiation of the first round of spermatogenesis in response to gonadotropic stimulation (increase in circulating LH, testosterone and FSH) and the appearance of zygotene-pachytene primary spermatocytes (de Kretser et al., 2016; Fu et al., 2023). This formation begins with the emergence of the tight junctions, ectoplasmic specializations, desmosomes, and gap junctions between Sertoli cells (Mruk & Cheng, 2015). Formation of tight junctions are specifically coordinated by transcription factors that up- or down-regulate the expression of genes required for tight junction formation. Once apical-basal polarity is established, proteins required for the cytoplasmic plaque are delivered, followed by the trafficking of tight junction proteins to the basal domain which will be incorporated into the membrane of the Sertoli cell. In the developing human testis, the junctional

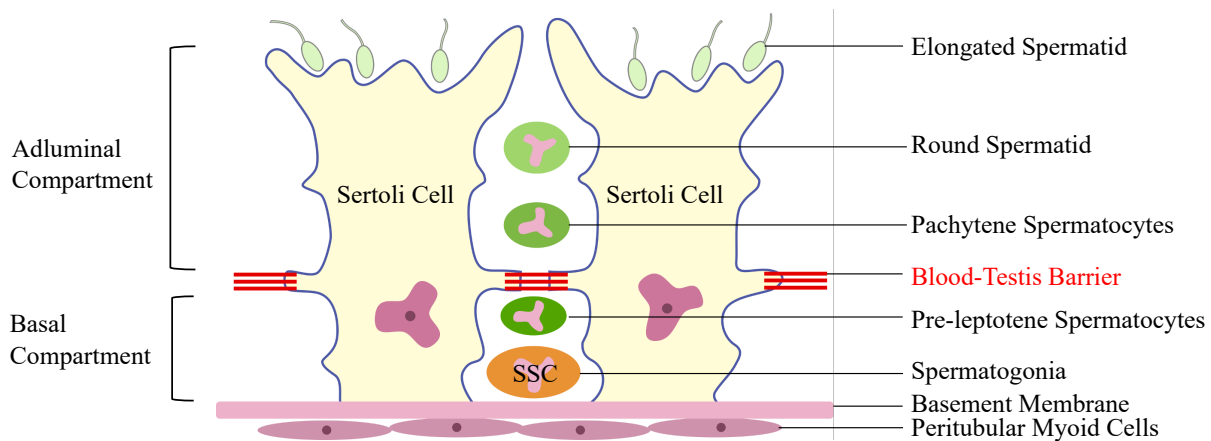


**Figure 3: The Blood-Testis Barrier organization.** The Blood-Testis Barrier is located basally between adjacent Sertoli cells. The BTB provides a divide in environment in which the basal compartment contains spermatogonia and preleptotene spermatocytes, while the adluminal compartment contains pachytene spermatocytes, round spermatids, and elongated spermatids. Adapted from Hofmann & McBeath, 2022.

specializations between Sertoli cells occur in the early phase of puberty around 11 to 13 years of age, thus establishing the basal and adluminal compartments of the seminiferous tubule (de Kretser et al., 2016). In mice, the BTB is formed between 15 and 18 days postpartum (Hogarth, 2015). The BTB was discovered and characterized in the nineteenth century when dyes injected into rodents were shown to be prevented from reaching the basement membrane of the seminiferous tubules (Chiquoine, 1964; Yan Cheng & Mruk, 2015). Additionally, the junctions were characterized by the presence of punctate tight junctions between the cell membranes of adjacent Sertoli cells (de Kretser et al., 2016).

During spermatogenesis, the SSCs that have differentiated and matured into preleptotene spermatocytes will migrate through the barrier between mouse spermatogenesis stages VII and VIII of the seminiferous epithelium cycle from the basal compartment to the adluminal compartment while the tight junction reforms basally (Hogarth, 2015). This separation by the BTB creates distinct microenvironments optimized for the different stages of germ cell development, forming equally an immunological and physical barrier (Jiang et al., 2014; Matsumoto & Bremner, 2016; Sourdain et al., 2018). Therefore, the BTB is essential in maintaining the basal stem cell niche, without which spermatogenesis would not occur (de Kretser et al., 2016; Takashima et al., 2011). However, in order to achieve successful SSC transplantation, the injected SSCs must migrate to their niche located on the basal membrane, passing through the BTB, repopulating the environment and regenerating spermatogenesis (Yan Cheng & Mruk, 2015). Therefore, while the BTB plays a crucial role in regulating spermatogenesis and providing distinct microenvironments for germ cells, this biological barrier is equally a major obstacle impeding efficient SSC engraftment following transplantation.

### **1.5 Tight Junction Proteins: Claudins**

Integral tight junction membrane proteins contributing to the function of the BTB include Occludin, junctional adhesion molecules (JAMs), and claudins (Cheng & Mruk, 2012; Lee et al., 2009; Morrow et al., 2010). Occludin was the first tight junction protein identified (Furuse et al., 1993). Occludin knockout (KO) mice are infertile; however, this protein, unlike the murine model, is undetectable in the human testis (Mok et al., 2013; Moroi et al., 1998; Morrow et al., 2010; Stammler et al., 2016). Additionally, tight junctions can be formed in the absence of Occludin (Balda et al., 1996; Wong & Gumbiner, 1997). When Occludin was removed from

various cells lines, it did not affect cell morphology, tight junction fibrils, or localization of other tight junction associated proteins (Balda et al., 1996; Wong & Gumbiner, 1997). On the other hand, claudins are found in both human and mouse BTB and are essential to the formation of tight junctions and the BTB, particularly Claudin-11 which has been studied extensively in both models (Saitou et al., 2000; Stammler et al., 2016). Claudins were first named in 1998 by Japanese researchers Mikio Furuse and Shoichiro Tsukita at Kyoto University when they isolated Claudin-1 and Claudin-2 from chicken liver tight junction membrane fractions (Furuse et al., 1998). Furuse and his colleagues demonstrated that claudins were essential and responsible for the formation and function of tight junctions (Furuse et al., 1998). Claudins are the largest family of critical tight junction proteins, predominantly contributing to the functional properties of the

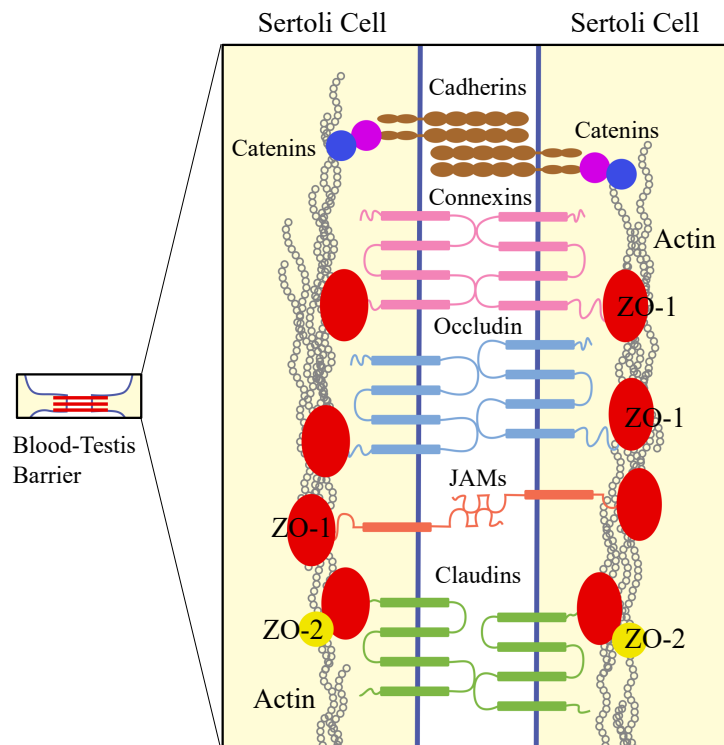


**Figure 4: Proteins in the Blood-Testis Barrier.** Tight junctions such as claudins, Occludin and JAMs are the major protein constituents of the BTB. Claudins will interact with cytoplasmic proteins such as ZO-1, linking them to the actin cytoskeleton. In addition to tight junction proteins, there are other junctional proteins in the inter-Sertoli cell junctional complex, including gap junctions such as connexins and adherens junctions such as cadherins. Adapted from Lee et al., 2009 and Cheng & Mruk, 2012.

tight junction barrier (Ding et al., 2013). Claudins will interact with scaffolding proteins such as ZO-1 (tight junction protein encoded by the *TJPI* gene in humans) among others, which belong to the cytoplasmic plaque, linking them to the actin cytoskeleton and enabling their localization to the tight junctions (Figure 4) (Aydin et al., 2020; Morrow et al., 2010). Claudins can be categorized into classical (Claudins 1–10, 14, 15, 17, and 19) or nonclassical (Claudins-11–13, -16, -18, and -20–24) types according to their sequence similarities (Mruk & Cheng, 2015). Notably, Claudin-11 is a nonclassical type claudin. Among the many proteins associated with the tight junction, the combinations of claudin family members and their interactions with the cytoplasmic components ultimately determine the properties of the tight junction (Günzel & Yu, 2013). These interactions will depict the overall paracellular electrical resistance and paracellular charge selectivity of the tight junctions (Ding et al., 2013). By linking the tight junction transmembrane protein to the actin cytoskeleton, the cytoplasmic plaque proteins will aid in regulating and modifying barrier properties, enabling coordinated responses. Moreover, the combination of claudins present will determine the properties of the paracellular barrier (Krause et al., 2008). For example, Claudins-4, -5, -8, -11, -14, and -18 are known to increase the paracellular electrical resistance while Claudins-2, -7, -10, -15, and -16 are known to increase paracellular cation permeability (Mruk & Cheng, 2015). Additionally, various researchers and studies have shown that claudins affect the maintenance of tissue shape, tension between cells during morphogenic movements, and hydrostatic pressure during lumen expansion (Bagnat et al., 2007; Behr et al., 2003; Nelson et al., 2010; Siddiqui et al., 2010; V. M. Wu et al., 2004).

Claudins are 20-27kDa tetraspan transmembrane proteins with 207 to 305 amino acids in length for which there are currently 24 members described in mammals (Lal-Nag & Morin, 2009). Claudins are structurally composed of 2 extracellular loops (EL1 and EL2) and 4 transmembrane domains, with the N-terminus and C-terminus in the cytoplasm (Figure 5) (Krause et al., 2008). The first extracellular loop consists of 49-59 amino acids whereas the second extracellular loop consists of 14-35 amino acids (Krause et al., 2008). The transmembrane domains consist of 20-30 amino acids, the N-terminal domain consists of approximately 7 amino acids and the C-terminal domain consists of between 27-65 amino acids, depending on the specific claudin (Overgaard et al., 2011; Tsukita et al., 2001).

The extracellular loops of the apposed claudins will interact with the respective loops of the adjacent claudin. The first extracellular loop is known to determine the charge selectivity of

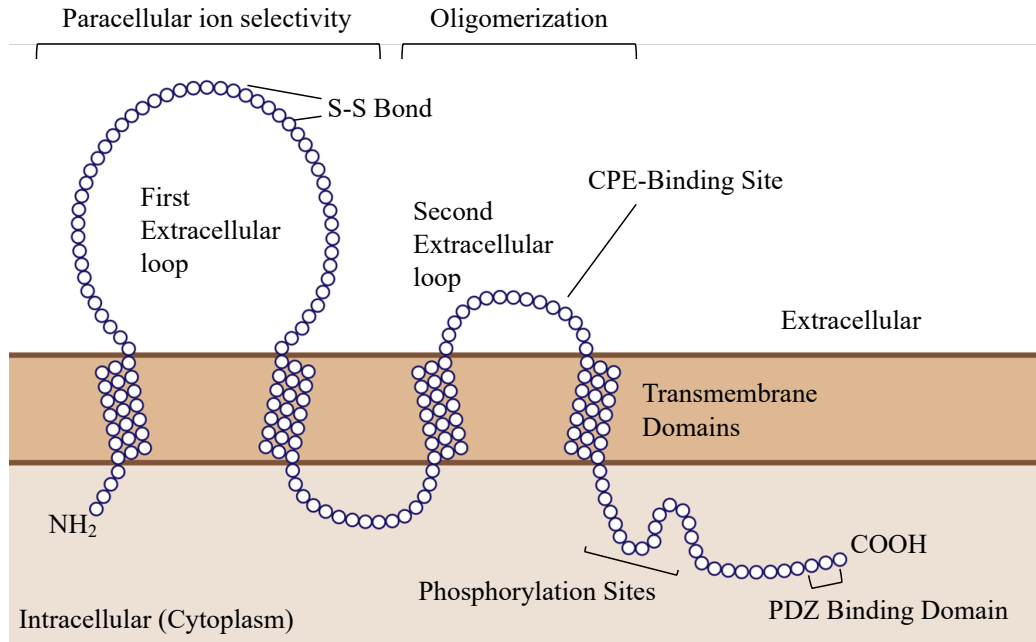


**Figure 5: Schematic representation of a claudin molecule.** Claudins are tetraspan proteins with 2 extracellular loops, 4 transmembrane domains and both the C-terminal and N-terminal ends within the cytoplasm. Adapted from Günzel & Yu, 2013.

the barrier, while the second extracellular loop contributes to the trans interaction of claudins between adjacent cells (Krause et al., 2008). The specific amino acid sequences of the first extracellular loop will affect the characteristics of the pore (Overgaard et al., 2011). Thus, various claudins will form pores that will affect the size of the molecules that can pass through the tight junction in addition to being selective, restrictive, or permissive for specific cations and anions (Meoli & Günzel, 2020). They can be classified according to their ability to promote barriers that are cation- or anion-specific, or form barriers that create a seal to prevent the passage of molecules. The EL1 has a conserved motif (W-GLW-C-C) where a cysteine disulfide bond acts to stabilize the loop (Lal-Nag & Morin, 2009; Morrow et al., 2010). The second extracellular loop will determine the tightness of the barrier as it is involved in the trans interactions with claudins in the apposing cell and cis interactions with claudins in the same cell (Krause et al., 2008). Claudin-11, which has the shortest EL2 consisting of 14 amino acids, is known to form very tight barriers such as the BTB (Morita, Sasaki, et al., 1999). The four transmembrane domains consist of many hydrophobic amino acids which participate in the cis interactions of claudins in the same cell (Günzel & Yu, 2013). They are also essential for the

proper folding of the claudin (Krause et al., 2008). Lastly, the cytoplasmic C-terminal domain interacts with scaffolding proteins that bridge the tight junction to the actin-cytoskeleton (Takahashi et al., 2005; Xu et al., 2009). Most claudins have a PDZ binding domain at their C-terminus which contribute to the binding of the scaffold machinery in the cytoplasmic plaque (English & Santin, 2013; Lui et al., 2003; Nomme et al., 2015). Thus, claudins have an essential role in the tight junctions and directly affect the barrier paracellular permeability.

## **1.6 Sertoli Cell Tight Junction Remodelling**

The mechanism by which spermatocytes move from the basal to the adluminal compartment, passing through the Sertoli cell barrier is largely unknown (de Kretser et al., 2016; Meng et al., 2005). However, various ideas have been suggested, including the involvement of claudins and transforming growth factor- $\beta$ 2 [TGF $\beta$ 2], a signalling molecule (Stanton, 2016). Researchers suggest that disruption of the adluminal tight junctions is mediated by the release of TGF $\beta$ 2 from Sertoli cells and transiting spermatocytes (de Kretser et al., 2016). As previously mentioned, movement of preleptotene spermatocytes across the BTB occurs via the new formation of tight junctions and dissolution of old tight junctions. The release of TGF $\beta$ 2 will signal the sequestration of the tight junction protein Occludin to lysosomes for disposal (de Kretser et al., 2016). Thus, testosterone and TGF $\beta$ 2 act together for germ cells to cross the barrier and continue with meiotic maturation while maintaining BTB integrity through self-mediated restructuring during the seminiferous epithelial cycle of spermatogenesis (Loveland, 2018; Meng et al., 2005). As preleptotene spermatocytes migrate across the BTB towards the adluminal compartment, tight junction disassembly ahead of the spermatocyte is coordinated with the tight junction assembly that occurs behind these germ cells such that the events are synchronized with one another (Mruk & Cheng, 2015). Testosterone will promote the reassembly of BTB proteins on the basal side of the transiting spermatocyte. In the absence of androgen receptor, there is a decrease in tight junction proteins suggesting that testosterone signaling through androgen receptor is essential for BTB remodelling and movement of germ cells across the BTB (L. B. Smith & Walker, 2014).

Additionally, it is suggested that when spermatocytes separate from the basement membrane, there is a surge in Claudin-3 localization at the basal membrane during mouse spermatogenesis stages VI to IX of the Sertoli cell which is mediated by androgen receptor

signaling (Meng et al., 2005; B. E. Smith & Braun, 2012). Disruption of androgen signaling in Sertoli cells interferes with Sertoli cell tight junction remodeling (Chakraborty et al., 2014). Claudin-3 emergence occurs in accordance with the emergence of the preleptotene spermatocytes and Sertoli cell tight junction remodeling, localizing to the BTB. This tight junction protein is absent in Sertoli cell androgen receptor knockout mice (Chakraborty et al., 2014). Claudin 3 localizes to the newly forming tight junction between the new Sertoli-Sertoli cell contacts near the basement membrane at mouse stages VIII-IX of spermatogenesis (Chakraborty et al., 2014; Chihara et al., 2010; B. E. Smith & Braun, 2012). Claudin-3 is then replaced with Claudin-11 such that spermatocytes are surrounded by Sertoli cell tight junctions (McCabe et al., 2016; B. E. Smith & Braun, 2012). Once the preleptotene spermatocytes are surrounded by tight junctions, the old tight junctions above will dissolve, releasing the spermatocytes into the adluminal compartment with a proper restructured BTB formed below, effectively separating the basal and adluminal compartment (B. E. Smith & Braun, 2012; Stammer et al., 2016). The interactions that occur at the BTB are regulated by proteins whereby claudins are known to play a major role in determining the properties of the tight junction.

### **1.7 Claudin Interactions in the Blood-Testis Barrier**

Various research studies have shown that individual claudin family members contribute uniquely to the paracellular properties of the BTB (Stammer et al., 2016). In the human testis, Claudin-11 has been most explored along with a single article on Claudins-5, -6, -7 (Manku et al., 2016) and another on Claudin-3 (Ilani et al., 2012). A study by Cornelia Fink and colleagues detected Claudin-11 at the mRNA and protein level in human seminiferous tubules (Fink et al., 2009). Claudin-11 protein was co-localized with ZO-1 in the basal compartment, corresponding to the BTB (Tarulli et al., 2013). They observed that men with testicular intraepithelial neoplasia have a significant increase in Claudin-11 expression in their testis tubules suggesting that the neoplasia is a result of disorganization and dysfunction of Claudin-11 (Fink et al., 2009; McCabe et al., 2016). Various other researchers also suggest that Claudin-11 levels are inversely correlated with spermatogenic activity in the human testes (Chiba et al., 2012; Nah et al., 2011). In another study, researchers showed that Claudin-11 expression was increased in decreased spermatogenesis whereby increased Claudin-11 immunoreactivity was observed at the inter-

Sertoli tight junctions in maturation arrest and in the cytoplasm of Sertoli cells in Sertoli cell only testes (Nah et al., 2011; Park et al., 2010).

Furthermore, de Michele and colleagues observed a transient expression of Claudin-11 in humans from 0 to 3 years of age, which was attributed to the mini-puberty phenomenon, characterized by an increase in testosterone production and a first wave of Sertoli cell maturation, along with an increase from 9 years of age onwards which is correlated with the time puberty (de Michele et al., 2018). In another study, Claudin-11 organization was examined with immunofluorescent staining across Sertoli cell-only (SCO) and meiotic arrest (MA) in human testis tubules (Haverfield et al., 2013). This study observed filamentous Claudin-11 staining pattern that was restricted to the basal aspect of the tubule in men with normal spermatogenesis and punctate Claudin-11 staining diffusely spread throughout both the basal and adluminal aspects of the tubule in tubules from MA and SCO men (Haverfield et al., 2013). Thus, many researchers have studied the role of Claudin-11 in the human testis. One article has shown that Claudin-3 is present in newly formed tight junctions; however, another discusses that Claudin-3 is only found in mice and not humans (Ilani et al., 2012; Stammler et al., 2016). Additionally, another team of researchers has shown increased expression of Claudin-6 and Claudin-7 in seminomas while Claudin-5 expression remained unchanged (Manku et al., 2016). Thus, while there are various research articles illustrating the role of Claudin-11 in human BTB, the rest of the claudin family members in the human testes are still largely unknown.

In the mouse testis, Claudin-11 is the most well-characterized claudin molecule. Additional research has also identified mRNAs for *Claudins-1, -2, -3, -4, -5, -7* and *-8* using northern blot analyses (Furuse et al., 1998; Morita, Furuse, et al., 1999; Morita, Sasaki, et al., 1999). Moreover, microarray analysis identified Claudins-10, -12 and -23 in mice testis (Singh et al., 2009). Claudin-11 is expressed in Sertoli cells during the entire cycle of the seminiferous epithelium in mice, whereas Claudin-3 is described to be strictly stage-specific and androgen-dependent (Singh et al., 2013; Stammler et al., 2016). In a study where most of the genital tract in Claudin-11 knockout mice appeared normal, the testes from these mutants were 30%–50% smaller (hypogonadism) than those of wild-type testes (Gow et al., 1999). The Claudin-11 protein is first detectable in mouse testes at postnatal day 13 and is primarily localized to the area of the BTB (Gerber et al., 2016; Morrow et al., 2010). Furthermore, Claudin-11 is an obligatory protein for tight junction formation and barrier integrity in the testis; spermatogenesis does not

proceed beyond meiosis in its absence, resulting in male sterility (Mazaud-Guittot et al., 2010; Yang et al., 2014). Claudin-11 knockout mice exhibit degeneration of the seminiferous epithelium with detachment of Sertoli cells and absence of spermatogenesis (McCabe et al., 2016). Thus, Claudin-11 knockout mice are infertile. The infertility associated with the absence of an intact BTB in the Claudin-11 knockout mouse is further evidence for the importance of the BTB in maintaining the stem cell niche.

Interestingly, Shinohara and her colleagues found that autologous SSC transplantation of Claudin-11-deficient SSCs rescued male infertility in chemically castrated Claudin-11-deficient mice, allowing development of fertile sperm from the donor cells (Kanatsu-Shinohara et al., 2020). In their article, they discuss that the removal of endogenous germ cells for recipient preparation reprogrammed claudin expression patterns in Sertoli cells, rescuing fertility in the Claudin-11-deficient mice (Kanatsu-Shinohara et al., 2020). Therefore, while various claudins can be detected in the mouse and human testis, Claudin-11 is a pivotal tight junction protein belonging to the BTB that has been well studied in both human and mouse model.

For Claudin-3, immunofluorescence analyses identified Claudin-3 expression specifically when the preleptotene and leptotene spermatocytes migrated across the mouse BTB (Morrow et al., 2010). A prolonged preleptotene stage can be observed in Claudin-3 knockout mice, supporting its role on the migration of spermatocytes; however, Claudin-3 knockout mice are fertile and have an intact BTB unlike Claudin-11 knockout mice (Komljenovic et al., 2009; Stammler et al., 2016). Additionally, Claudin-5 is expressed at stage VIII along with Claudin-3 (Meng et al., 2005). These results suggest that the interactions among these tight junction membrane protein in the mouse testis may play a role in the course of the seminiferous epithelial cycle (Hollenbach et al., 2018; Morrow et al., 2010; Wang et al., 2018). *Claudin-3* mRNA was first detected in mouse testis at postnatal day 15 and decreased during adulthood. Additionally, in another study, Claudin-1 protein was detected in mouse testes at postnatal day 3, increased at postnatal day 10 and subsequently decreased between postnatal days 16 to 30 (Gye, 2003).

Therefore, claudins are ideal candidates for targeting the BTB due to their significant role in the BTB and the maintenance of spermatogenesis. Particularly, Claudin-11 that has been well studied in human as well as mouse and known to have a critical role in tight junctions, is an ideal target. Targeting Claudin-11 to disrupt the BTB structure may improve SSC engraftment. By removing claudins from the tight junction, more SSCs will traverse the BTB and successfully

reach their niche on the basement membrane. However, while this method is promising with respect to disrupting the barrier, it is evident that proper BTB formation and structural integrity are paramount for functional spermatogenesis to occur (Mazaud-Guittot et al., 2010). Consequently, it is crucial that the disruption of the BTB is temporary and claudin expression is restored for proper BTB formation. The barrier can then be re-established upon SSC migration into the basal compartment, providing the appropriate SSC niche needed for spermatogenesis. Thus, disrupting the BTB by removing claudins from the tight junctions will allow more SSCs to reach their niche while subsequent recovery of the BTB will enable SSCs to self-renew in their microenvironment and regenerate spermatogenesis.

### **1.8 Disrupting the Blood-Testis Barrier**

*Clostridium perfringens* enterotoxin (CPE) is a single chain 319 amino acid polypeptide, associated with *C. perfringens* food poisoning in humans (Black et al., 2015; Wieckowski et al., 1994). Many studies have shown that Claudin-3 and -4 are natural receptors of CPE as it interacts with high affinity to their claudin EL2 domains. In contrast, the EL2 domains of Claudin-1, -2, -5, -10, and -11 do not interact with CPE (Black et al., 2015; Hanna & McClane, 1991; Horiguchi et al., 1987; Katahira et al., 1997; Kitadokoro et al., 2011; Sonoda et al., 1999). The individual interactions between Claudin-1, -2, -3, -4, -5, -10, and -11 with CPE were determined by dot blot assays, pull-downs, cytotoxic assays and cellular binding assays. The interaction between CPE and claudins were mapped to the EL2 through mutagenesis studies where Winkler and his colleagues found that CPE binds to a central motif (the hydrophobic turn and flanking polar residue) located in the EL2, NP(L/M)(V/L/T)(P/A) (Winkler et al., 2009). Additionally, Kimura and his colleagues showed that the negatively-charged acidic amino acids located in the C-terminal domain of CPE are attracted to the last 12 positively-charged basic amino acids of the EL2 of CPE-sensitive claudins (Kimura et al., 2010).

CPE bound to claudins can form CH-1 and CH-2 complexes (Chakrabarti et al., 2003; Robertson et al., 2007; Shrestha et al., 2016). The CH-1 complex results in a calcium influx in the cell that promotes caspase-3 mediated apoptosis and oncosis (Chakrabarti et al., 2003; Robertson et al., 2007). This complex is formed when six molecules of CPE bind to claudin receptors on the cell surface and oligomerize into a cation-selective beta-barrel pore. (Shrestha et al., 2016). On the other hand, CH-2 complexes are formed when CPE bound to claudin causes

the internalization of the complex and removal of the claudin from the tight junction (Shrestha et al., 2016). Thus, the CH-2 complex will promote the internalization of tight junction membrane proteins leading to the opening of the paracellular barrier (Shrestha et al., 2016).

The C-terminal fragment of CPE (C-CPE) contains the claudin binding domain in the last 30 amino acids and a stabilization domain but lacks the cytotoxic domain (Hanna et al., 1989, 1991; Hanna & McClane, 1991; Van Itallie et al., 2008; Kokai-Kun & McClane, 1997; Singh et al., 2000; Smedley & McClane, 2004; Veshnyakova et al., 2010). When claudins interact with CPE, the claudin protein is internalized and destroyed, resulting in the partial disruption of the tight junction barrier (Black et al., 2015). However, cellular death occurs due to the toxic N-terminal domain (Black et al., 2015; Kitadokoro et al., 2011; Kokai-Kun et al., 1999; Smedley et al., 2007; Smedley & McClane, 2004). By exposing cells solely to the C-terminal fragment of CPE, various claudin members (Claudin-3, -4, -6, -7, -8, and -14) are removed from the tight junction without cytotoxic effects (Black et al., 2015; Ebihara et al., 2007; Harada et al., 2007;

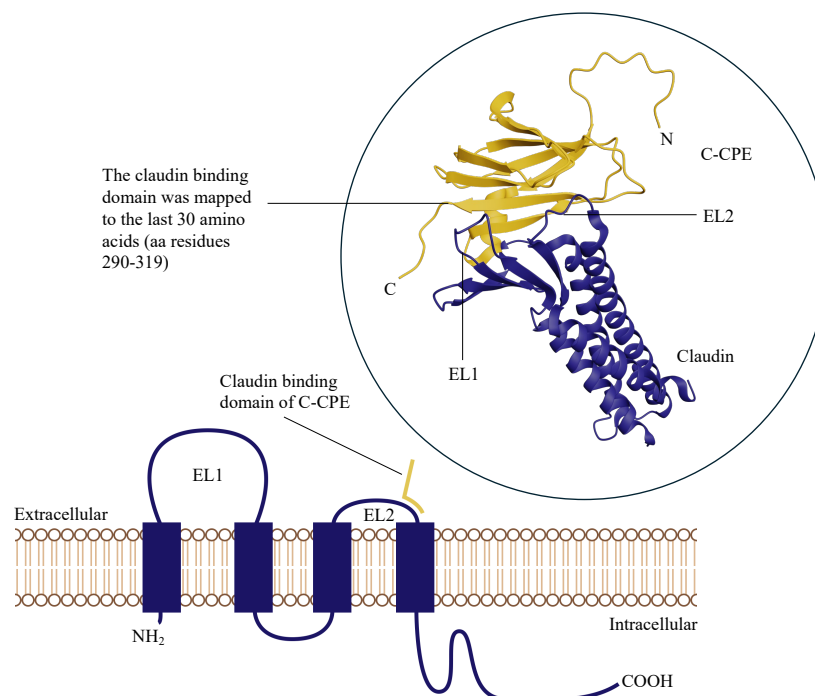


**Figure 6: Schematic representation of C-CPE interacting with a claudin molecule.** The claudin binding domain of C-CPE was mapped to the last 30 amino acids on the C-terminal domain. This claudin binding domain will interact with the second extracellular loop (EL2) of a claudin molecule. Adapted from English & Santin, 2013 and Vecchio et al., 2021a.

Van Itallie et al., 2008; Kojima et al., 2016; Kondoh et al., 2005; Takahashi et al., 2005, 2008). In a previous study, they removed the last 30 amino acids from the C-terminal domain of CPE and demonstrate that CPE could no longer bind to claudins (Van Itallie et al., 2008; Kimura et al., 2010). Thus, the claudin binding domain of C-CPE was mapped between amino acids 290 and 319 (Figure 6) (Van Itallie et al., 2008; Kimura et al., 2010).

Interestingly, the absence of the CPE N-terminal domain prevents the formation of CH-1 complexes. Thus, claudins bound to C-CPE form solely CH-2 complexes, leading to the internalization of the target claudins (Shrestha et al., 2016; Suzuki et al., 2017). Therefore, C-CPE is an ideal peptide for the removal of claudins as it is 1) not cytotoxic, 2) binds to claudins and removes them from the tight junction without affecting the localization of other claudin members, 3) does not affect gene expression such that claudins can repopulate the tight junction upon C-CPE removal, and 4) does not bind to other cell surface proteins (Takahashi et al., 2008). The Nagano lab showed that when C-CPE was co-injected with testis cells from fertile donor mice into the testes of infertile recipient mice there was improved SSC engraftment. SSC engraftment was measured by visualizing SSC colonies with lacZ staining and the kinetics of BTB disruption by C-CPE was analyzed by injecting C-CPE into busulfan-treated mice and observing the ability of biotin to cross the BTB. In control GST-injected testes biotin staining was seen only in the interstitium, but in the C-CPE-treated mice, positive biotin signals were detected in the tubule lumen as well, indicating the disruption of the BTB. BTB disruption after C-CPE injection was most evident on day 3 and restored by day 10. Therefore, C-CPE is capable of transiently disrupting the tight junction barrier.

A critical drawback to C-CPE is that it only binds to a subset of claudins, limiting its potential function to disrupt tight junctions to Claudins-3, -4, -6, -7, -8, and -14 (Kojima et al., 2016). Various researchers have attempted to overcome this challenge by modifying the sequence of C-CPE using site-directed mutagenesis which led to the development of C-CPE variants that target Claudins-1, -2, -3, -4 and -5 (Beier et al., 2019; Liao et al., 2016; Piontek et al., 2020; Protze et al., 2015; Walther et al., 2012; Winkler et al., 2009). Other studies have used peptides corresponding to the EL2 domain of Claudin-2 to block the trans-interaction amongst Claudin-2, -3, and -4 in order to increase tight junction permeability (Dithmer et al., 2017; Nasako et al., 2020; Sauer et al., 2014; Staat et al., 2015; Zwanziger et al., 2012). The blood-brain barrier and blood-nerve barrier of rats, showed increased permeability to small

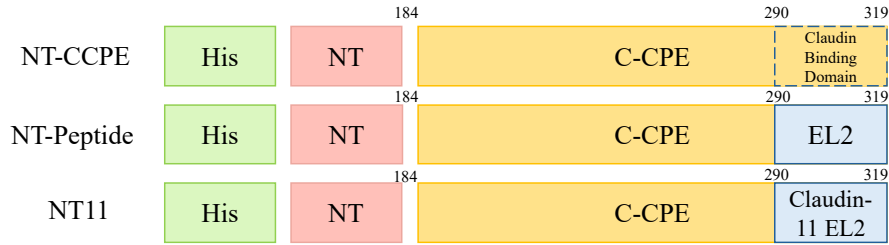


**Figure 7: Scheme of C-CPE::Claudin fusion proteins.** Peptides contain a His tag for purification and a NT tag to improve solubility. For NT11, the claudin binding domain of C-CPE (amino acid residues 290 to 319) was replaced by the EL2 of mouse Claudin-11. Adapted from Enrique Gamero-Estevez' thesis.

macromolecules when using peptides corresponding to the C-terminal region of Claudin-1 and Claudin-5 EL1 were present (Dithmer et al., 2017; Sauer et al., 2014). Additionally, monoclonal antibodies against Claudin-3 and -5 increase barrier permeability *in vitro* by blocking claudin interactions between apposing cells, (Fukasawa et al., 2015; Kato-Nakano et al., 2010; Okai et al., 2018; Tokunaga et al., 2007).

Despite significant progress, it is important to note that neither C-CPE nor these other peptides, target Claudin-11, the most crucial claudin family member in the mouse and human BTB (Dithmer et al., 2017; Sauer et al., 2014). While C-CPE has shown positive effects, it primarily interacts with other claudin members in the BTB. To overcome this challenge, a former PhD student, Enrique Gamero-Estevez, in the Ryan and Nagano labs designed a series of peptides to target individual claudin family members; one of these was NT11 which targets Claudin-11. The claudin binding sequence of C-CPE was replaced with the sequence of the EL2 of mouse Claudin-11, making the peptide target Claudin-11. The EL2 is responsible for claudin homodimerization such that this domain would enable targeting of the claudin of interest. Thus, the fusion protein is predicted to bind and remove Claudin-11 by recognizing the Claudin-11 EL2 sequence. However, the C-CPE $\Delta$ CBD::CLDN11 peptide was highly insoluble. Thus, an NT solubility tag, derived from spider silk, was added to make NT11 a water-soluble peptide (Kronqvist et al., 2017). Moreover, NT11 contains a poly-histidine (His) tag to purify the tagged protein by His-tag purification. Thus, the NT11 construct is as follows: His::NT::C-CPE $\Delta$ CBD::Cldn11EL2 (Figure 7). My project will focus on demonstrating that our peptide NT11 will disrupt the BTB in an *ex vivo* model of mouse testicular tubules by removing Claudin-

11 from the tight junction. In this manner, we hope to bring SSC transplantation closer to clinical reality with the ability of our generated peptide to transiently disrupt the BTB.

## 1.9 Summary and Hypothesis

In light of the increasing number of cancer survivors, there is a significant demand for effective fertility preservation methods, particularly among male patients facing the detrimental effects of cancer treatments on sperm production. SSCs play a pivotal role in continuously generating sperm through their self-renewal and differentiation abilities. Consequently, SSC transplantation could be used to restore fertility in male oncofertility patients. However, a critical drawback to SSC transplantation is the low efficiency of SSC engraftment due to the BTB which prevents the transplanted SSCs from reaching their stem cell niche. Thus, targeting the BTB to enhance homing to the germ cell niche is predicted to enhance SSC transplantation efficiency. This can be done by specifically targeting claudins, which play an important role in the formation and function of the BTB (Furuse et al., 1998).

Various strategies, including the use of *Clostridium perfringens* enterotoxin (CPE) and its derivatives have been explored to transiently disrupt tight junctions. CPE interacts with specific claudins, notably Claudin-3, -4 and -8, to induce their internalization or form cytotoxic complexes (Black et al., 2015). Interestingly, the C-terminal fragment of CPE (C-CPE) can be used similarly for transient disruption of tight junctions, including those in the BTB, without cytotoxic effects (Black et al., 2015; Kojima et al., 2016). By targeting claudins and promoting their internalization, C-CPE facilitates the partial disruption of tight junctions. A significant limitation of C-CPE is its specificity to a subset of claudins, excluding crucial members such as Claudin-11. To address this challenge, we designed the NT11 peptide by incorporating the Claudin-11 EL2 into C-CPE.

I hypothesize that the NT11 peptide will reversibly remove Claudin-11 in an *ex vivo* model of testicular tubules. To test this hypothesis, I established an *ex vivo* organ culture system to investigate the effect of NT11 on Claudin-11 localization to the BTB in *ex vivo* cultured testis tubules from two infertile mouse models. Additionally, I hypothesize that upon the removal of the peptide, Claudin-11 will return to the tight junctions of the testis tubules. By investigating these hypotheses, my study lays the groundwork for defining effective peptides that disrupt the mouse blood-testis barrier and encourages further investigation in the development of peptides

capable of disrupting cellular barriers. Furthermore, I hypothesize that implementing additional purification procedures in our current NT11 induction and purification protocol would optimize NT11 purity for future application in *in vivo* mice studies or *ex vivo* human tissue biopsy studies. Ultimately, my project has focused on optimizing Claudin-11 removal by anti-claudin peptide NT11 in the mouse BTB for future stem cell delivery.

## **2. Materials and Methods**

### **2.1 Animal: W/W<sup>v</sup> Mice and Busulfan-Injected 129/B6 Mice**

W/W<sup>v</sup> mice (The Jackson Laboratory, WBB6F1/J-Kit<sup>W</sup>/Kit<sup>W-v</sup>/J, 100410, Bar Harbor, ME, USA) were euthanized between 6 and 10 weeks postpartum for all experiments. Kit<sup>W</sup>/Kit<sup>W-v</sup> compound heterozygotes are viable but sterile due to germ cell deficiency. W/W<sup>v</sup> mice are the offspring of a cross between WB/ReJ Kit<sup>W</sup>/J (The Jackson Laboratory, WB/ReJ Kit<sup>W</sup>/J, 000692, Bar Harbor, ME, USA) females and C57BL/6J-Kit<sup>W-v</sup>/J (The Jackson Laboratory, C57BL/6J-Kit<sup>W-v</sup>/J, 000049 Bar Harbor, ME, USA) males. Average weight of testis for W/W<sup>v</sup> mice was 12mg.

129/B6 mice (The Jackson Laboratory, B6129SF1/J, 101043, Bar Harbor, ME, USA) were injected with 50mg/kg of busulfan (Sigma-Aldrich, B2635, Burlington, MA, USA) 2 weeks after weaning which corresponds to 5 weeks postpartum. Busulfan damages germ cells, decreases sperm motility and testis weight, and increases sperm abnormality rate. Consequently mice injected with busulfan are infertile (Jiang et al., 2022). Busulfan-treated 129/B6 mice were euthanized between 8 and 10 weeks postpartum for all experiments. 129/B6 Mice are the offspring of a cross between C57BL/6J females (B6; The Jackson Laboratory, C57BL/6J, 000664, Bar Harbor, ME, USA) and 129S1/SvImJ males (129S; The Jackson Laboratory, 129S1/SvImJ, 002448, Bar Harbor, ME, USA). Average weight of testis for busulfan-injected 129/B6 mice was 30mg.

### **2.2 Animal Protocol Ethics**

Animal Use Protocol #MUHC-7376 with McGill University and its Affiliated Hospital's Research Institutes has been granted to Dr. Makoto Nagano, Glen site of the RI-MUHC. The Animal Certificate for the Protocol "Improving colonization of spermatogonial stem cells by disrupting blood-testis barrier" is renewed every year. The latest protocol's expiration date is August 30<sup>th</sup>, 2024.

### **2.3 SSC culture medium**

The SSC culture medium is a complex mixture made in the laboratory which contains the following components: Minimum Essential Medium  $\alpha$  (Invitrogen, 12561, Carlsbad, CA, USA) with 0.2% BSA (Sigma-Aldrich, A3803, Burlington, MA, USA), 5 $\mu$ g/mL insulin (Sigma-

Aldrich, I5500, Burlington, MA, USA), 10 $\mu$ g/mL iron-saturated transferrin (Sigma-Aldrich, T1283, Burlington, MA, USA), 3 x 10<sup>-8</sup> M sodium selenite (Sigma-Aldrich, S5261, Burlington, MA, USA), 50 $\mu$ M 2-mercaptoethanol (Sigma-Aldrich, M7522, Burlington, MA, USA), 10mM HEPES pH 7.2-7.4 (Sigma-Aldrich, H0887, Burlington, MA, USA), 60 $\mu$ M putrescine (Sigma-Aldrich, P5780, Burlington, MA, USA), 2mM glutamine (Invitrogen, 25030-081, Carlsbad, CA, USA), 50 units/mL penicillin and streptomycin (Invitrogen, 15070-063, Carlsbad, CA, USA), and finally 7.6 $\mu$  eq/L free fatty acids (31mM palmitic acid (Sigma-Aldrich, P0500, Burlington, MA, USA), 2.8mM palmitoleic acid (Sigma-Aldrich, P9417, Burlington, MA, USA), 11.6mM stearic acid (Sigma-Aldrich, S4751, Burlington, MA, USA), 13.4mM oleic acid (Sigma-Aldrich, O1008, Burlington, MA, USA), 35.6mM linoleic acid (Sigma-Aldrich, L1012, Burlington, MA, USA), 5.6mM linolenic acid (Sigma-Aldrich, L2376, Burlington, MA, USA)) (Kubota et al., 2004). Final pH of the media should be between 7.2-7.4. This media was used for all *ex vivo* organ cultures performed throughout this study.

## 2.4 Air-Liquid Interface Culture System

Mouse testes were retrieved from a W/W<sup>v</sup> mouse and/ or a busulfan-treated 129/B6 mouse. When using busulfan-treated 129/B6 mice, individual testes were weighed and only those around 30mg were used. Mouse testes were immediately placed in a petri dish filled with 7mL of PBS (137mM NaCl, 2.7mM KCl, 10mM Na<sub>2</sub>HPO<sub>4</sub>, and 1.8 mM KH<sub>2</sub>PO<sub>4</sub>, adjusted to pH 7.4) where the tunica was removed without disturbing the structure of the seminiferous tubules. The

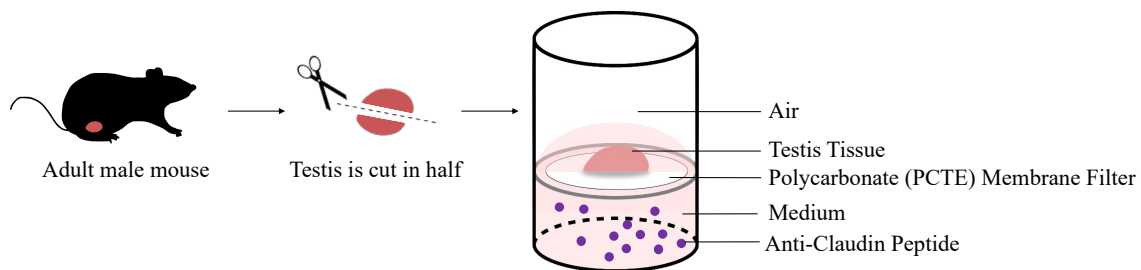


**Figure 8: Air-liquid interface *ex vivo* culture system.** Testis tissue pieces are cut in half after the removal of the tunica and placed in a single well in a 24-well plate. The testis tissue piece will float on the PCTE membrane filter in 300 $\mu$ L of SSC culture medium. The medium will contain 40 $\mu$ M of NT11 for the NT11-treated samples and the equivalent volume of PBS for the controls. A thin layer of medium covers the tissue in a dome-like shape.

testis was then cut in half in the longitudinal direction to increase surface area. The testis tissue was placed gently on a polycarbonate (PCTE) membrane filter (Disc 13mm PCTE 1.0 $\mu$ m) (Thomas Scientific, GVS Filter technology 4663F85, Swedesboro, NJ, USA) that is floating in a single well of a 24-well plate with SSC culture media (Figure 8). Medium in the well consisted of 40mM of NT11 or C-CPE in addition to the amount of SSC culture medium to make the total volume 300 $\mu$ L. The control culture contained an equivalent volume of PBS added to the media. A layer of medium from under the filter was gently pipetted over the testis tissue which was placed flat on the floating PCTE membrane filter with the cut side of the testis on the membrane filter. This layer of medium formed a dome-like shape over the tissue. Once the air-liquid interface culture system was complete; the 24-well plate containing the sample was placed in the 32°C incubator for the course of treatment, i.e. 16 or 72 hours.

For Claudin-11 restoration, the 24-well plate containing the sample was placed in the 32°C incubator for the course of treatment (Figure 9). After 16 hours, the plate was taken out for 5 minutes: Media from the well was completely drained by removing the 300 $\mu$ L with a pipette. 300 $\mu$ L of fresh SSC culture medium was then placed into the well containing the testis tissue on the PCTE membrane filter. Again, a thin layer of medium from the 300  $\mu$ L was gently pipetted

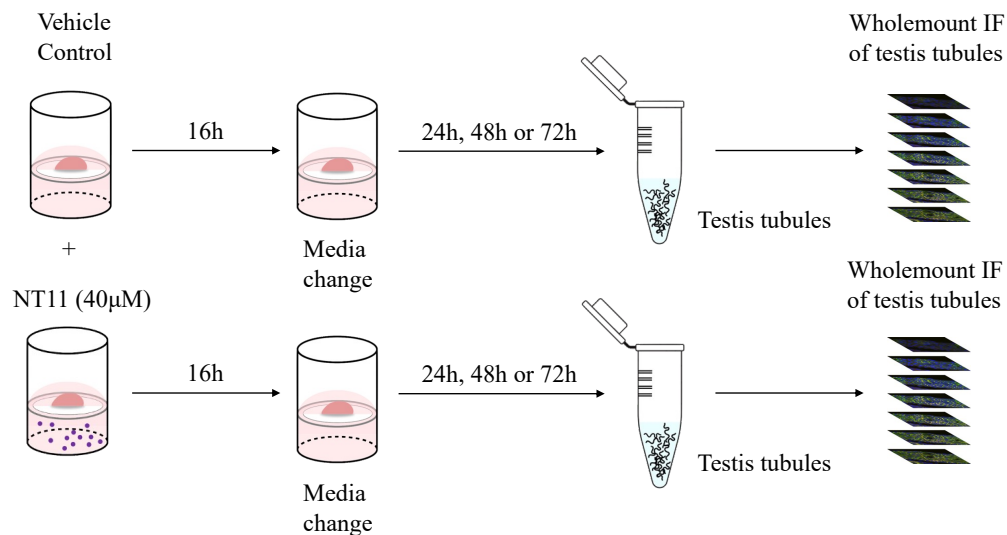


**Figure 9: Scheme for claudin recovery experiment.** Testis tissue pieces were treated with NT11 (40  $\mu$ M) or vehicle control for 16 hours, followed by a change in media to complete SSC culture medium. Tubules were collected at 24, 48, or 72 hours, fixed in Trichloroacetic acid (TCA) and subjected to whole-mount immunofluorescence.

over the tissue to form a dome-like shape. The 24-well plate was then placed into the 32°C incubator for 24 hours, 48 hours and/or 72 hours, respectively.

## **2.5 Antibodies for Immunofluorescence**

Primary antibodies used for immunofluorescence were: Claudin-11 (Invitrogen, 364500, Carlsbad, CA, USA) and ZO-1 (Invitrogen, 339100, Carlsbad, CA, USA). The Claudin-11 polyclonal antibody was raised in rabbit (IgG) using a synthetic peptide derived from the C-terminal region of human OSP/Claudin-11 (one amino acid different from mouse and rat sequences). The ZO-1 monoclonal antibody was raised mouse (IgG1) using the human recombinant ZO-1 fusion protein encompassing amino acids 334-634. In addition, secondary goat anti-rabbit (Alexa Fluor 488, Invitrogen, Carlsbad, CA, USA) and goat anti-mouse (Alexa Fluor 568, Invitrogen, Carlsbad, CA, USA), were used.

## **2.6 Whole-Mount Immunofluorescence**

After treatment was complete, testis tissue pieces were individually placed in plastic snap cap tubes containing 5mL of Hanks' Balanced Salt Solution (ThermoFisher Scientific, ICN1810054, Waltham, MA, USA) with 1mg/mL of Collagenase IV (Sigma-Aldrich, C5138, Burlington, MA, USA) for 5 minutes each in a 37°C-water bath. The tubules were digested and separated into individual strands by lightly agitating the tube back and forth. After tubules sedimented to the bottom at unit gravity (< 1 min), 15 mL of 1xPBS was added to dilute the collagenase. The supernatant was removed as much as possible without removing the tubules and PBS was added again to wash the tubules. This process of adding PBS to wash the tubules was repeated two more times for a total of three washes.

To fix the tubules, the testis that was separated into tubules in the snap cap tubes were incubated in 10% trichloroacetic acid (TCA) (ThermoFisher Scientific, BP555-500, Waltham, MA, USA) by fully submerging the tubules (1 mL) for 90 minutes at 4°C with agitation. This step was followed by an extensive wash of the tubules 3 to 4 times for 10 minutes each with PBS on a shaker at room temperature (RT). This entailed removing the TCA, adding 10mL of 1xPBS and placing the snap cap tube on the shaker for 10 minutes, followed by the sedimentation of the tubules before removing the PBS and adding another 10mL of PBS. For all these steps, the tubules were avoided with the pipette as much as possible to not lose or damage the testis

tubules. Samples were then incubated in blocking buffer (10% normal goat serum (Multicell Wisent, 053110, St. Bruno, QC, CAN) in 0.3% Triton X-100 (Sigma-Aldrich, 112298, Burlington, MA, USA) in 1xPBS) for 1 hour at RT on a shaker. Enough volume of blocking buffer was added to ensure that the testis tubules were fully submerged even while being agitated on the shaker during incubation. Following the blocking process, the supernatant was removed, and the testis tubules were incubated in primary antibody (diluted in 5% normal goat serum in 0.3% Triton X-100 in 1x PBS) at 4°C overnight on a shaker, enough to ensure that the tubules were submerged in the solution during agitation. For Claudin-11 primary antibody (Invitrogen, 364500, Carlsbad, CA, USA), a dilution of 1:50 was used and for ZO-1 primary antibody (Invitrogen, 339100, Carlsbad, CA, USA) a dilution of 1:200 was used.

Following the overnight primary antibody incubation, samples were washed 4 times with 10mL of 1xPBS for 10 minutes each at RT on a shaker. This process was repeated three more times where the tubules would sediment to the bottom, followed by the removal of the supernatant and addition of 10mL of PBS to wash the tubules. Samples were then incubated in secondary antibody (diluted Alexa Fluor-conjugated secondary antibodies (1:500) in 0.3% Triton X-100 in 1x PBS) along with DAPI (Invitrogen, Carlsbad, California, USA) for 1 hour at RT. After incubation was complete, tubules were washed three to four times with PBS for 10 minutes at RT on a shaker. Once the tubules sedimented to the bottom after being taken off the shaker, the supernatant was removed, and PBS was added. After the washes, the seminiferous tubules were transferred to glass microscope slides. This transfer process was done by removing most of the supernatant from the tubes and pouring the contents (200µL of PBS with tubules) directly onto the slides without going over the edges. This method was chosen as the least number of tubules would be lost. Forceps were then used to gently disperse the tubules along with Kimwipes® to remove all the excess PBS from the slide. A single drop of FluorSave reagent (EMD Millipore, 34789, Massachusetts, USA) was added over the tubules followed by a 1.5mm coverslip. The testis tubules were next visualized with a microscope.

## **2.7 Confocal Imaging**

Wholemout immunofluorescent testis tubules were visualized with the Zeiss LSM780 laser scanning confocal microscope and Z-stack images were acquired to visualize the 3D tubular structure of the testis tubules. Images were acquired in grayscale and the colours green,

red and blue were added above to the corresponding individual signals. For all the images taken throughout this project, the green channel represents the claudin signals, the red channel represents the ZO-1 signals, and the blue channel represents the DAPI. Brightness and contrast of channels were determined with the control samples and treated samples were imaged with the same settings, per experiment. This enabled comparison in intensity and not only protein localization pattern between Claudin-11 and ZO-1 on individual testis tubules. The Master gain, digital offset, and digital gain in conjunction with laser power, were adjusted to set the threshold of detection by adjusting the sensitivity of the detector, the background/ noise and signal intensities (Shihan et al., 2021).

Images with the 20x objective (Objective Plan-Apochromat 20x/0.8 M27) were taken with 1024x1024 pixels (386.4510 $\mu$ m x 386.4510 $\mu$ m), a depth around 40 $\mu$ m, and with a resolution of 2.6498 pixels per micron. Images with the 63X objective (Objective Plan-Apochromat 63x/1.4 Oil DIC M27) were taken with 1024x1024 pixels (134.9511 $\mu$ m x 134.9511 $\mu$ m), a depth around 10 $\mu$ m, and with a resolution of 7.5879 pixels per micron. The slice before ZO-1 signals can be seen (all background) was selected as the first stack and the last slice of the Z-stack was selected to be the slide when ZO-1 appears punctate on each side of the tubule. In this manner, the Z-stack captures from the top of the tubule to the middle of the lumen

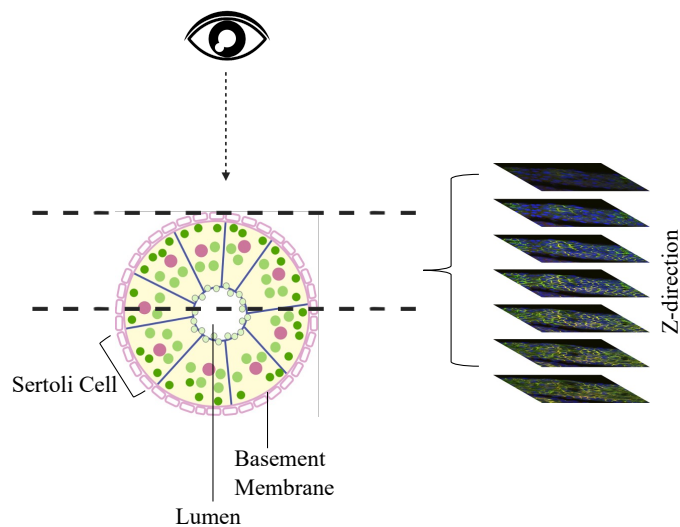


**Figure 10: Confocal imaging of mice testis tubules.** A cross section of a testicular tubule with the dotted lines denoting the first and last Z-stack of a single image using 20x and 63x objectives.

(Figure 10). The distance between each Z-stack was  $2\mu\text{m}$  for the 20x objective and  $0.69\mu\text{m}$  for the 63x objective. Approximately 20 Z-stacks were taken per tubule using the 20x objective and 15 Z-stacks when the 63x objective was used. 10 different testis tubules were imaged per slide and condition by navigating different fields of view with 5 images taken using the 20x objective and another 5 images taken using the 63x oil immersion objective. The tubules chosen for imaging were selected based on tissue integrity and dispersion on the glass slide. Damaged tubules were not imaged. Additionally, only tubules that could be singled out with a complete empty background were imaged. These two conditions limited the tubules that could be imaged and prevented bias against testis tubule selection based on protein localization pattern or intensity.

## 2.8 ImageJ Analysis of Confocal Images

Colocalization of Claudin-11 with ZO-1 was determined using Pearson's correlation coefficient analysis of Maximum Intensity Projections (MIPs) of testis tubule images obtained using the 63x objective with the using FIJI/Image J (version 2.9.0/1.53t, ImageJ2, National Institutes of Health, Bethesda, MD, USA) and their colocalization tool. MIPs were created using the Z-stack with the highest intensity of ZO-1 as well as the stack immediately before and the stack immediately after. This method allowed us to visualise solely the Sertoli cells, excluding the myoid cells. To assess the signals (colocalization and intensity) at the membrane, the image

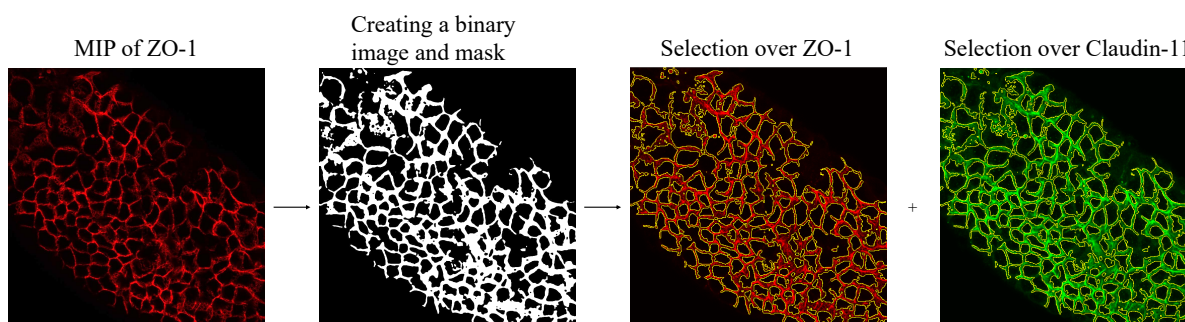


**Figure 11: Creating an ROI using ZO-1 signal at the membrane.** Using the MIP of ZO-1 that contains the Z-stack with highest intensity of ZO-1 taken along with the previous and subsequent stack, an ROI is created by selecting auto-threshold with Huang 2 and filtering for the median at 4.0 pixels. Using this ROI, Coloc 2 (colocalization) is assessed within the area of the selection (yellow outline) for ZO-1 (red) and Claudin-11 (green).

was first converted to 8-bit. An ROI was drawn using the MIP of ZO-1 (channel 1) by making the image into a binary image, converting it to a mask and creating a selection. Huang 2 was used from the auto-threshold selection. The ROI selection was further refined by filtering for the median at 4.0 pixels. “Adjust” → “Auto Threshold” → “Huang2” → “Process” → “Make binary” → “Convert to Mask” → “Process” → “Filter” → “Median, 4 pixels” → “Edit” → “Selection” → “Create Selection” → “Add to ROI” (Figure 11). After creation of the ROI for each individual image, Coloc 2 was selected and colocalization was compared using channel 1 (ZO-1) and channel 2 (Claudin-11) along with the ROI/mask. Costes was selected from the threshold regression and PSF was set to 3 pixels with no Costes randomization. The value for Pearson’s correlation coefficient with no threshold was then taken and plotted using Excel. Additionally, the integrated sum intensity ratios were analyzed for Claudin-11/ ZO-1 amongst treatment conditions. The integrated sum intensity values were taken from the Coloc 2 output, made into a ratio by dividing Claudin-11 over ZO-1 and plotted.

## **2.9 Statistical Analysis of Images**

Statistical analyses were performed using Excel (version 16.83, Microsoft Office 365, Redmond, WA, USA) and Graph-Pad PRISM (version 8.02, GraphPad Software, Inc., California, USA). A two tailed t-test, ANOVA one-way factor test and Tukey-Kramer Post Hoc test analyses were used to analyze the effects of treatment. Differences were considered significant when  $p < 0.05$ . A two tailed t-test was chosen to compare the values between the controls and NT11 treated samples, critically assessing if the mean is significantly greater than one and/ or if the mean significantly less than other. Additionally, using Excel, the standard deviation, standard deviation of Mean (SEM) and 95% Confidence Interval were calculated for each condition in each experiment. An ANOVA one-way factor tested was used to compare the multiple values generated from the control, 24 hours, 48 hours, and 72 hours for the Claudin-11 restoration experiments. This analysis of variance compared the means of 4 independent groups to determine whether there is statistical evidence that the associated population means are significantly different. The Tukey-Kramer Post Hoc test then tested the null hypothesis of no difference between the means for all pairs of groups. These statistical analysis methods provided a measure to quantify the significance in Pearson’s correlation coefficients and Integrated Sum

Intensities between control and NT11 treated testis tubules at 16 hours, 72 hours, and the chosen restoration intervals (24 hours, 48 hours, and 72 hours after 16 hours of NT11 treatment).

## 2.10 Plasmid Generation

NT11 (His::*NT*::C-CPE::*Cldn11EL2*) was generated by Dr. Enrique Gamero-Estevez. Briefly, the cDNA clone encoding the C-CPE $\Delta$ CBD::*Cldn11EL2* fusion protein was generated by replacing the nucleotide sequence encoding C-CPE's claudin binding domain (amino acids 290- 319) with the nucleotide sequence encoding the EL2 domain of Claudin-11 (*SSHREITIVSFGYSLY*). Two serines were added as a linker. Sequences encoding a His tag and the Spidroin protein (NT) solubility domain (Kronqvist et al., 2022) were added to the 5' end of the cDNA construct to encode the final fusion protein His::*NT*::C-CPE $\Delta$ CBD::*Cldn11EL2*. We refer to this polypeptide as NT11 and it was used for all experiments described in this thesis.

## 2.11 Protein Induction

First, 340ng of cDNA expression vector for NT11 was added to 200 $\mu$ L of *E. coli* BL21 (DE3) pLysS Competent Cells (Promega, L1191, Madison, WI, USA) in a 15mL plastic snap cap tube and left on ice for 30 minutes. The tube was heat-shocked in a 42°C-water bath for 45 seconds and then 500 $\mu$ L of Lysogeny broth/Luria-Bertani (LB) (10g/L Tryptone, 10g/L NaCl, 5g/L Yeast Extract, ddH<sub>2</sub>O) was added to the tube and the tube was placed in a 37°C shaker for one hour. The mixture was plated on LB agar plates containing 50 $\mu$ g/mL kanamycin sulfate (ThermoFisher Scientific, BP906-5, Waltham, MA, USA) and 34 $\mu$ g/mL chloramphenicol (Sigma-Aldrich, C3175, Burlington, MA, USA). The plate was incubated at 37°C overnight. Individual colonies were used to inoculate 5mL of LB media containing 50 $\mu$ g/mL of kanamycin and 34 $\mu$ g/mL of chloramphenicol. and incubated overnight at 37°C with shaking (250rpm).

4mL of the overnight culture was used to inoculate 400mL of LB media containing 50 $\mu$ g/mL of kanamycin and 34 $\mu$ g/mL of chloramphenicol in a 2L Erlenmeyer flask. The cultures were grown at 37°C with shaking (250 rpm) until they reached an optical density (OD) 600nm of 0.4-0.6. A 1mL "uninduced" aliquot was centrifuged and the bacterial cell pellet was stored at -20°C. Protein expression was induced by adding IPTG (Isopropyl  $\beta$ -D-1-thiogalactopyranoside) (ThermoFisher Scientific, BP1755-10, Waltham, MA, USA) to a final concentration of 0.2mM. The culture was then incubated overnight at RT on a shaker at 250rpm. Following the overnight

induction, 500µl aliquots of the “induced” culture were centrifuged and the pellets stored at -20°C. The remaining culture was centrifuged at 5000g (J6-HC, Rotor JS-4.2, 4200rpm) for 30 minutes 4°C. The pellets were then transferred from the 250mL plastic centrifuge bottles to 50mL conical tubes and 800mL of bacterial culture pellets were pooled together (2 x 400mL bacterial cultures). Each pellet was weighed, noted, and labelled. Finally, pellets were stored at -80°C until protein purification.

## 2.12 Studier Method for Auto-Induction of Protein Expression

This protocol describes the production of recombinant proteins in bacteria originally developed by F. W. Studier (Studier, 2005, 2014, 2018). Transformation of the cDNA expression vector for NT11 into *E. coli* BL21 (DE3) pLysS Competent Cells was done in the same manner as described above. The mixture containing 500µL of LB with the *E. coli* BL21 cells and cDNA expression vector for NT11 was plated on a LB + 1% glucose agar plate containing 100µg/mL kanamycin sulfate and 34µg/mL chloramphenicol. Once plated, the plate was left to incubate at 37°C overnight.

Individual colonies were used to inoculate 50mL of ZYP-0.8G non inducing media (46.5mL of ZY, 50µL of 1M MgSO<sub>4</sub> (1mM) (ThermoFisher Scientific, M63, Waltham, MA, USA), 1ml of 40% glucose (0.8%), 2.5mL of 20xNPS (1x)) with 100µg/mL of kanamycin, and 34µg/mL of chloramphenicol. ZY is composed of 10g of Bacto™ Tryptone (ThermoFisher Scientific, 211705, Waltham, MA, USA), 5g yeast extract (Sigma-Aldrich, Y1625, Burlington, MA, USA) and 925mL of ddH<sub>2</sub>O. 20xNPS is composed of 0.5M (NH<sub>4</sub>)<sub>2</sub>SO<sub>4</sub> (ThermoFisher Scientific, 446450250, Waltham, MA, USA), 1M KH<sub>2</sub>PO<sub>4</sub> (Sigma-Aldrich, P5379, Burlington, MA, USA), and 1M of Na<sub>2</sub>HPO<sub>4</sub> (Sigma-Aldrich, S9390, Burlington, MA, USA) added in sequence until all was dissolved. 24.65g of MgSO<sub>4</sub>•7H<sub>2</sub>O was dissolved and filled to 100mL to make 1M MgSO<sub>4</sub>. 40% glucose was made with 40g of Dextrose Anhydrous (ThermoFisher Scientific, BP350-1, Waltham, MA, USA) and 74mL of ddH<sub>2</sub>O by adding the glucose slowly into the stirring water and left to stir for 1 hour until all was dissolved. The flask was then placed into a 37°C shaking incubator overnight at 300rpm.

OD<sub>600</sub> of the overnight ZYP-0.8G non inducing media culture was noted. After the overnight culture, the 50mL overnight ZYP-0.8G non inducing media culture was used to inoculate 500mL of ZYP-5052 auto-inducing media (464mL of ZY, 500µL of 1M MgSO<sub>4</sub>

(1mM), 10mL of 50x5052 (1x), 200 $\mu$ L of 1000x trace metal mixture, 25mL of 20xNPS (1x), 100 $\mu$ g/mL of kanamycin sulfate, and 34 $\mu$ g/mL of chloramphenicol) in a 2L baffled flask. OD<sub>600</sub> of hour 0 was taken directly after putting the overnight starter culture. The ZYP-5052 culture was then placed into a 37°C-shaking incubator at 300rpm and OD<sub>600</sub> was noted every hour for 12 hours, taken along with 1mL aliquots, before moving the culture into a RT shaking incubator at 300rpm overnight. 100mL of 50x5052 is composed of 25g of glycerol (ThermoFisher Scientific, PI17904, Waltham, MA, USA), 73mL of ddH<sub>2</sub>O, 2.5g of glucose, and 10g of  $\alpha$ -lactose (Sigma-Aldrich, L3625, Burlington, MA, USA) which were added in sequence and stirred for 2 hours until dissolved. 1000x trace metal mixture is composed of the following listed in Table 1 which were added to 36mL of ddH<sub>2</sub>O. All metals were made into individual stock solutions and autoclaved except for FeCl<sub>3</sub>•6H<sub>2</sub>O which was dissolved in 0.1M concentrated HCl (Sigma-Aldrich, 320331, Burlington, MA, USA).

OD<sub>600</sub> of the overnight ZYP-5052 auto-inducing media culture was noted. OD<sub>600</sub> was taken every hour until hour 26. The cultures were then poured into 250mL plastic centrifuge bottles and centrifuged at 5000g (J6-HC, Rotor JS-4.2, 4200rpm) for 30 minutes, collected in the same manner as described above. Each 1ml aliquot taken from every hour was then run on an SDS-PAGE gel to confirm induction. Finally, these pellets were stored at -80°C until the next step of protein purification.

<b>1000x Trace Metal Mixture</b>	
<b>Trace Elements</b>	<b>Final Concentrations</b>
<b>FeCl<sub>3</sub>•6H<sub>2</sub>O</b> (Sigma-Aldrich, F2877, Burlington, MA, USA)	50mM
<b>CaCl<sub>2</sub>•2H<sub>2</sub>O</b> (Sigma-Aldrich, C3881, Burlington, MA, USA)	20mM
<b>MnCl<sub>2</sub>•4H<sub>2</sub>O</b> (Sigma-Aldrich, M3634, Burlington, MA, USA)	10mM
<b>ZnSO<sub>4</sub>•7H<sub>2</sub>O</b> (Sigma-Aldrich, Z4750, Burlington, MA, USA)	10mM
<b>CoCl<sub>2</sub>•6H<sub>2</sub>O</b> (Sigma-Aldrich, C8661, Burlington, MA, USA)	2mM
<b>CuCl<sub>2</sub>•2H<sub>2</sub>O</b> (Sigma-Aldrich, C6641, Burlington, MA, USA)	2mM
<b>NiCl<sub>2</sub>•6H<sub>2</sub>O</b> (Sigma-Aldrich, N5756, Burlington, MA, USA)	2mM
<b>Na<sub>2</sub>MoO<sub>4</sub>•2H<sub>2</sub>O</b> (Sigma-Aldrich, M1003, Burlington, MA, USA)	2mM
<b>Na<sub>2</sub>SeO<sub>3</sub>•5H<sub>2</sub>O</b> (Sigma-Aldrich, S5261, Burlington, MA, USA)	2mM
<b>H<sub>3</sub>BO<sub>3</sub></b> (Sigma-Aldrich, B6768, Burlington, MA, USA)	2mM

**Table 1: 1000x trace elements.** Table listing the final concentrations of the metals required to make 1000x trace metal mixture for auto-induction media. Stock solutions of the metals were prepared except for FeCl<sub>3</sub> which was dissolved in 50 ml of 100x diluted concentrated HCl.

### 2.13 Protein Purification

The previously centrifuged bacterial cell pellets were resuspended in 10mL of resuspension buffer (50mM Tris pH7.5 (ThermoFisher Scientific, BP153, Waltham, MA, USA), 150mM NaCl (ThermoFisher Scientific, S271, Waltham, MA, USA), 10mM imidazole pH 7.5 (Sigma-Aldrich, I5513, Burlington, MA, USA)) per 1g of pellet. Protease inhibitors (1.45nM Pepstatin A (ThermoFisher Scientific, 78436, Waltham, MA, USA), 2.1nM Leupeptin (ThermoFisher Scientific, 78435, Waltham, MA, USA), 0.15nM Aprotinin (ThermoFisher Scientific, 78432, Waltham, MA, USA), and 0.57mM PMSF (ThermoFisher Scientific, 36978, Waltham, MA, USA)) were added to the 10mL of resuspension buffer per 1g of bacterial cell pellet. After resuspension, 500 $\mu$ L of lysozyme (10mg/mL ddH<sub>2</sub>O) (Sigma-Aldrich, 62971, Burlington, MA, USA) for 10mL of resuspension buffer was added and left on ice for 20 minutes. Next, 10% sodium deoxycholate and NaCl were added to a final concentration of 0.2% and 0.5M, respectively. This was placed on ice for another 5 minutes for cells to lyse.

The lysate was sonicated (Sonics Vibra-Cell VC 50 Ultrasonic Homogenizer, 19308C, Sonics & Materials Inc. Danbury, CT, USA) in the 4°C room (20 times for 30 seconds each at 45° amplitude) with a small probe (CV 18 Generator Probe) in an ice bucket. A 10 $\mu$ L aliquot was taken from the lysate, labelled “before centrifuge” and stored at -20°C. The lysate was then transferred to a 30mL centrifuge round bottom tube and centrifuged at 15000g (J2-HS, rotor JA-17, 11500rpm) for 30 min at 4°C, twice. A 10 $\mu$ L aliquot was taken from the supernatant, labelled “after centrifuge” and stored at -20°C. Another aliquot was taken from the pellet, labelled “pellet” and stored at -20°C. The resulting supernatant containing the His-tagged fusion protein was then pipetted to an appropriate size conical tube and incubated at 4°C overnight rocking with Ni-NTA agarose beads (Qiagen, 30210, Germantown, MD, USA) (80 $\mu$ L of 50% Ni-NTA slurry per 400mL of bacterial culture) that were swelled in resuspension buffer.

Following the overnight incubation, the Ni-NTA agarose beads were collected with a low-speed centrifuge at 270g (Sigma 4-15C, rotor 312/J 11156). A 10 $\mu$ L aliquot was taken from the supernatant and labelled “unbound” and stored at -20°C. Additionally, another 10 $\mu$ L aliquot was taken from the beads and labelled “bound” and stored at -20°C. The supernatant was then discarded, and the beads were washed in 10mL of wash buffer (50mM Tris pH7.5, 0.5M NaCl and 15mM imidazole) 4 times. 10mL of wash buffer was pipetted with the beads, centrifuged at 270g (Sigma 4-15C, rotor 312/J 11156) and then discarded while keeping the beads. A 100 $\mu$ L

aliquot was taken of the wash buffer after a wash, labelled “wash” and stored at  $-20^{\circ}\text{C}$ . The washed beads were then transferred to a column and washed further until the eluant was free of protein as assessed by a standard Bradford assay, pipetting 5mL of wash buffer into the column and collecting  $2\mu\text{L}$  fractions for the Bradford assay.

Once there was no longer any protein being washed away, 1 bed volume of elution buffer (50mM Tris pH7.5, 150mM NaCl and 300mM imidazole) was added to the column with the beads, eluted into microcentrifuge tubes and repeated until approximately 10 fractions were collected. A  $10\mu\text{L}$  aliquot was taken from the beads, labelled “beads”, and stored at  $-20^{\circ}\text{C}$ . A Bradford protein assay was used to identify the eluted fractions containing purified recombinant protein which were then pooled together. The pooled fractions were then dialyzed against PBS. The pooled fractions were inserted into a dialysis cassette with a 3kDa molecular weight cut off (MWCO) using a syringe. The cassette, along with a sponge, was placed into a beaker with 2L of PBS spinning gently for 2 hours at  $4^{\circ}\text{C}$ . The cassette was then transferred into a different beaker

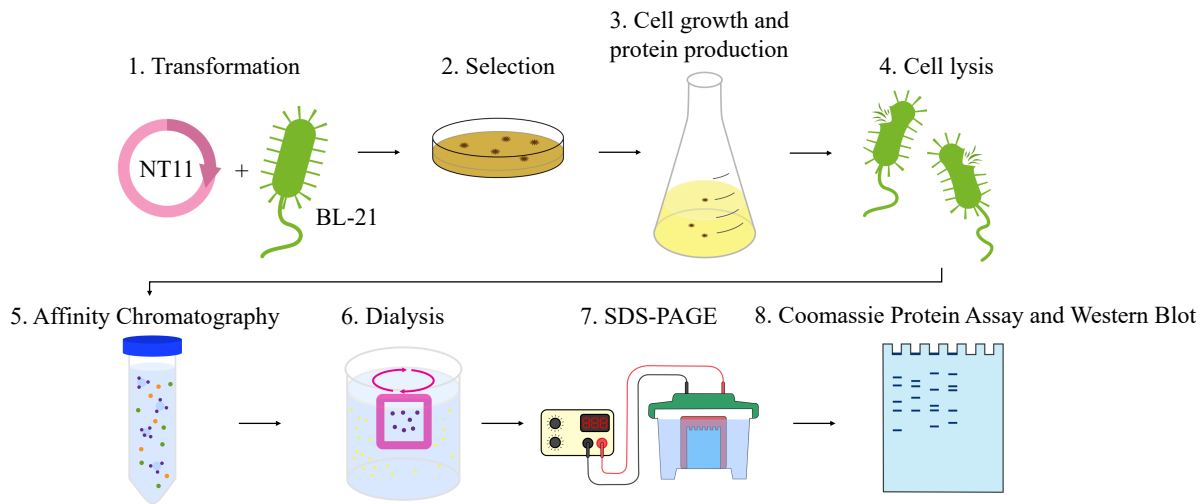


**Figure 12: Scheme of NT11 induction and purification.** Starting with transformation, the bacterial colonies (selected with Kanamycin and Chloramphenicol) are used to inoculate bacterial cultures and induced (with IPTG or allolactose from auto induction media) to express NT11. The cultures are centrifuged, and the pellet is resuspended in resuspension buffer, sonicated and centrifuged. The supernatant is incubated with Ni-NTA beads, washed with wash buffer and eluted. The eluate containing the NT11 peptide is placed in a dialysis cassette and stored in aliquots before performing a Coomassie protein assay or western blot. Adapted from Gomes et al., 2022.

with 4L of PBS and spun gently overnight at 4°C and transferred again into a different beaker with 2L of PBS for another 2 hours at 4°C the next day. Finally, the purified recombinant protein was collected, and volume and concentration were recorded. Aliquots were stored at -80°C. Figure 12 illustrates the steps for protein induction and purification.

#### **2.14 Size Exclusion Chromatography**

A 30cm column with Sephadex G-75 (Sigma-Aldrich, G10050-10G, Burlington, MA, USA) was prepared. Sephadex G-75, with an 80kDa limit, allows smaller molecules to interact with the pores, while those exceeding 80kDa do not. The gel filtration resin was swelled with PBS and 480µL of His-tag purified NT11 12.7µg/µL was pipetted into the column. Subsequently, 26 fractions of 1mL (column's bed volume) were collected in microcentrifuge tubes labelled 1 to 26. Detection of protein was done with a standard Bradford assay. 2µL aliquots were taken from each 1mL fraction and fractions containing protein were collected and further purified with a second round of His-tag purification. The collected fractions were separated into two pools and incubated overnight with Ni-NTA agarose beads. The beads were then treated in the same manner as described above for protein purification. After dialysis, the concentration and volumes were recorded for both pools of SEC fractions, respectively.

#### **2.15 Amicon Ultra Centrifugal Filters**

Amicon<sup>®</sup> Ultra Centrifugal Filters (Sigma-Aldrich, Burlington, MA, USA) were used for protein purification by separating eluted protein by size and/ or as a tool to concentrate protein. For protein purification, a single fraction collected from the SEC was pipetted into a 50kDa MWCO Amicon ultra-15 centrifugal filter (Sigma-Aldrich, UFC9050, Burlington, MA, USA) and centrifuged for 45 minutes at 4000g (J6-HC, Rotor JS-4.2, 3800rpm) in a swinging bucket rotor. In a separate experiment, the eluted protein after dialysis was pipetted directly into a 50kDa MWCO Amicon ultra-15 centrifugal filter and centrifuged for 45 minutes at 4000g (J6-HC, Rotor JS-4.2, 3800rpm). The eluted product in the filtrate collection tube was then collected by recording the volume and measuring the concentration while the remaining un-eluted product in the filter chamber was discarded. Alternatively, 10kDa Amicon ultra-4 centrifugal filters (Sigma-Aldrich, UFC8010, Burlington, MA, USA) and/ or 3kDa Amicon ultra-4 centrifugal filters (Sigma-Aldrich, UFC8003, Burlington, MA, USA) were used to concentrate protein after

dialysis. If the concentration measured by the spectrophotometer (Amersham Biosciences UltroSpec 1100 *pro* UV/ Visible, 80-2112-00/01/02/03, 79000) was below  $1\mu\text{g}/\mu\text{L}$ , the eluted protein was placed in the centrifugal filters, centrifuged for 30 minutes at 4000g (J6-HC, Rotor JS-4.2, 3800rpm) in a swinging bucket rotor. The protein was then recovered from the filter chamber whereby the volume and concentration would be recorded.

## 2.16 Solubility Test

To test the solubility of our protein peptide, various different buffers including 10% glycerol (ThermoFisher Scientific, PI17904, Waltham, MA, USA), 1% Triton X-100 (Biorad Laboratories, 1610407, Hercules, CA, USA) and 10% DMSO (Sigma-Aldrich, D5879-1L, Burlington, MA, USA) were tested in our resuspension buffer (50mM Tris pH7.5, 150mM NaCl, 10mM imidazole pH 7.5) with 0.2mg/mL of lysozyme (10mg/mL ddH<sub>2</sub>O). NT11 non-induced and induced pellets were either resuspended in 200 $\mu\text{L}$  of 10% glycerol, 1% Triton X-100 and/ or 10% DMSO in our resuspension buffer with 0.2mg/mL of lysozyme. The microcentrifuge tubes containing the lysed pellets were then placed on a Glas-Col Tube Rotator (The LabWorld Group, 14628, Hudson, MA, USA) for 30 minutes at RT. If the cells were lysed after 30 minutes, they were sonicated for 1 second (Sonics Vibra-Cell VC 50 Ultrasonic Homogenizer, 19308C, Sonics & Materials Inc. Danbury, CT, USA). The lysed cells were then centrifuged for 20 mins at 4°C (Eppendorf 5415D Microfuge Centrifuge, Standard Rotor F-45-24-11, 13200rpm). The supernatant was separated from the pellet. In the microcentrifuge tubes containing the supernatant (soluble fraction), 50 $\mu\text{L}$  of 5x loading dye was added and in the microcentrifuge tubes containing the pellet (insoluble fraction) 250 $\mu\text{L}$  of 1x loading dye was added. These samples were then visualized by western blot analysis and Coomassie protein assays.

## 2.17 Antibodies for Western Blot

Primary antibody used for Western Blot was Anti-His-Tag (DSHB, N144/14, Iowa City, IA, US) and *Clostridium perfringens* enterotoxin A antibody (Biorad Laboratories, 2120-0130G, Hercules, CA, USA). The Anti-His-Tag monoclonal antibody was raised in mouse (IgG1) using a hexahistidine (6xHis) fusion protein amino acids 720-804, variable portion of cytoplasmic C-terminus, of mouse ProtocadherinGammaA3. The *Clostridium perfringens* enterotoxin A polyclonal antibody was raised in rabbit using purified enterotoxin A from *C. perfringens*. In

addition, Goat Anti-Rabbit-HRT Conjugated (Cell Signaling, 70748, Danvers, Massachusetts, USA) and Goat Peroxidase-Conjugated Anti-Mouse IgG Antibody (Jackson ImmunoResearch, 115-035-146, West Grove, Pennsylvania, USA) were used.

## **2.18 Western Blot Analysis and Coomassie Protein Assay**

Western blot analyses and Coomassie protein assays were used to visualize the protein from induction and purification steps leading up to the collected purified recombinant protein. Aliquots were taken and labelled at each step: “uninduced, induced, before centrifuge, after centrifuge, pellet, unbound, bound, wash, beads, purified protein”. LD is composed of 0.5M Tris (pH 6.8), Glycerol, 10% SDS, 0.5% Bromophenol Blue (Sigma-Aldrich, B0126, Burlington, MA, USA), and ddH<sub>2</sub>O to which 5% of  $\beta$ -mercaptoethanol (Sigma-Aldrich, M6250, Burlington, MA, USA) is added. For the uninduced, 25 $\mu$ L of ddH<sub>2</sub>O and 25 $\mu$ L of 2x Loading Dye (LD) were added, resuspending the pellet. For the induced, 100 $\mu$ L of ddH<sub>2</sub>O and 100 $\mu$ L of 2x LD were added, resuspending the pellet. For the 10 $\mu$ L aliquoted samples, 90 $\mu$ L of ddH<sub>2</sub>O were added along with 100 $\mu$ L of 2x LD. For 100 $\mu$ L aliquoted samples, 100 $\mu$ L of 2x LD was added. For the purified protein, protein concentration was measured using a standard Bradford Assay and appropriate amounts of ddH<sub>2</sub>O and 5x LD were added to 10 $\mu$ g of protein for a total volume of 25 $\mu$ L. All samples were denatured at 95°C for 5 minutes prior to loading.

To run the SDS-PAGE gels (15% separating gel and 4% stacking gel (4x separating buffer pH 8.8 or 4x stacking buffer pH 6.8, Acrylamide 30%, Temed, 10% APS and ddH<sub>2</sub>O)) 15 or 10 well 1.5mm SDS-PAGE gels were placed in the gel electrophoresis tank. 1x running buffer was added to the gel electrophoresis tank and 25 $\mu$ L of each sample were loaded along with the protein ladder (Precision Plus Protein Dual Color Standards, Biorad Laboratories, 1610374, Hercules, CA, US). 2 SDS-PAGE gels were run at 35mA (constant amps) per gel per experiment which was later visualised with Coomassie blue and western blotting, respectively.

For a Coomassie protein assay, the SDS-PAGE gel was placed in a container filled with Coomassie Brilliant Blue R-250 Stain Solution (MeOH, Glacial Acetic Acid, ddH<sub>2</sub>O and 1g/L Coomassie R250 (Biorad Laboratories, 1610400, Hercules, CA, USA). The container was placed on a shaker for 30 minutes at RT. The Coomassie Brilliant Blue R-250 staining solution was then discarded and de-staining solution (MeOH, Glacial Acetic Acid, and ddH<sub>2</sub>O) was added. De-staining solution was exchanged every 20 minutes for 2 hours. De-staining solution was then

discarded and exchanged for ddH<sub>2</sub>O and left shaking overnight. The gel was imaged using Amersham imager 600 (GE Healthcare, Little Chalfont, United Kingdom).

For Western blot analysis, the SDS-PAGE gel was placed into a gel holder cassette with foam pads and filter paper. A 0.45µm Amersham™ Hybond® P Western blotting polyvinylidene difluoride (PVDF) membrane (Sigma-Aldrich, GE10600121, Burlington, MA, USA) was cut and soaked in methanol for 30 minutes prior to assembling the cassette. The cassette was then soaked in cold transfer buffer (1x transfer buffer, MeOH and ddH<sub>2</sub>O) and placed in the buffer tank. The transfer was run for 90 minutes at 100V (constant voltage). After the protein transferred from the SDS-PAGE gel to the PVDF membrane (confirmed by ladder), the PVDF membrane was washed with TBST (Tris-HCl 10 mM pH 7.4, NaCl 150 mM, and 0.1% tween 20) for 5 minutes, repeated 3 times. After 3 washes, the membrane was blocked in blocking buffer (5% non-fat dry milk in TBST) for 1 hour at RT. Next, the blocking buffer was discarded, and the membrane was incubated overnight at 4°C on a rocker with a primary antibody in TBST: Anti-His (1:400) or Anti-CPE (1:10000). Following overnight primary antibody incubation, the membrane was washed 3 times in TBST for 10 minutes each on a shaker at RT. The membrane was then incubated with goat anti mouse peroxidase conjugated (1:5000) or goat anti-rabbit-HRT conjugated (1:5000) in TBST on a shaker for 1 hour at RT. The membrane was then washed 3 times in TBST for 10 minutes each on a shaker at RT. Finally, the membrane was revealed using Clarity Western ECL substrate (Biorad Laboratories, 1705061, Hercules, CA, USA), and imaged using Amersham imager 600 (GE Healthcare, Little Chalfont, United Kingdom).

### 3. Results

#### 3.1 Aim 1: Claudin-11 Removal from the Blood-Testis Barrier by NT11

##### 3.1.1 Establishing an *Ex Vivo* Organ Culture System to Investigate Peptide Effects

First, it was necessary to establish an *ex vivo* organ culture system that would enable the investigation of our peptide on testis tissue over several days. This *ex vivo* culture system would provide the groundwork to transition from an *ex vivo* mouse model to an *ex vivo* human model for future clinical applications. Several rounds of optimization were required to establish an *ex vivo* culture system that supported survival of testis tubules and visualization of NT11 effects on Claudin-11 in mouse BTB. Claudin-11 is expressed around the Sertoli cells in a hexagonal pattern at the membrane, overlapping with ZO-1 (Figure 13). When treating the testis tubules with NT11, I expect to visualize delocalization of Claudin-11 from the tight junction.

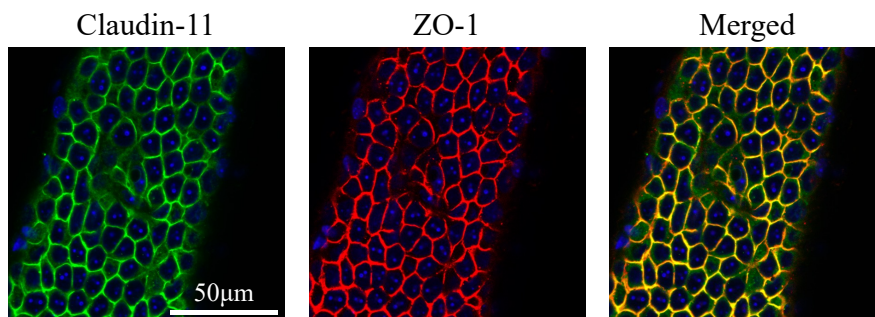


**Figure 13: Claudin-11 protein localization pattern in W/Wv mice testis tubules.**

Immunofluorescent wholemount staining of a W/Wv mouse uncultured testis tubule. The hexagonal pattern shows that Claudin-11 (green) is co-localized with the tight junction adaptor protein ZO-1 (red) in the BTB at the cell membrane. Scale bar = 50µm.

It was previously shown by Baumholtz et al., 2017 that 5 hours was sufficient to see the effects of C-CPE on claudin localization in chick embryos. Therefore, 5 hours was chosen as the initial treatment time point to observe the effects of NT11 and C-CPE on Claudin-11 and Claudin-8 in the BTB of mouse testis tubules. To culture B6 mouse (The Jackson Laboratory, C57BL/6J, 000664, Bar Harbor, ME, USA) whole testis tissue *ex vivo* the tunica albuginea was removed, and several cuts were made to the whole testis before submerging the tissue in 1mL of SSC culture media with PBS (untreated control), or in PBS containing 40µM NT11, 40µM C-

CPE, or 40 $\mu$ M NT11 and 40 $\mu$ M C-CPE. Immunofluorescence analysis revealed that there was no effect on Claudin-11 or Claudin-8 localization after 5 hours of culture with NT11 or C-CPE (Figure 14). Therefore, to determine if a longer incubation time was needed for NT11 or C-CPE to act on the claudins in the BTB of the testis, I analyzed tubules at 10 hours of treatment. However, no effects on localization of Claudin-11 or Claudin-8 were observed after 10 hours of culture (Figure 14). When comparing the results between the control, NT11, and NT11+C-CPE treatment, Claudin-11 was expressed around the Sertoli cells in the hexagonal pattern, overlapping with ZO-1 across all conditions.

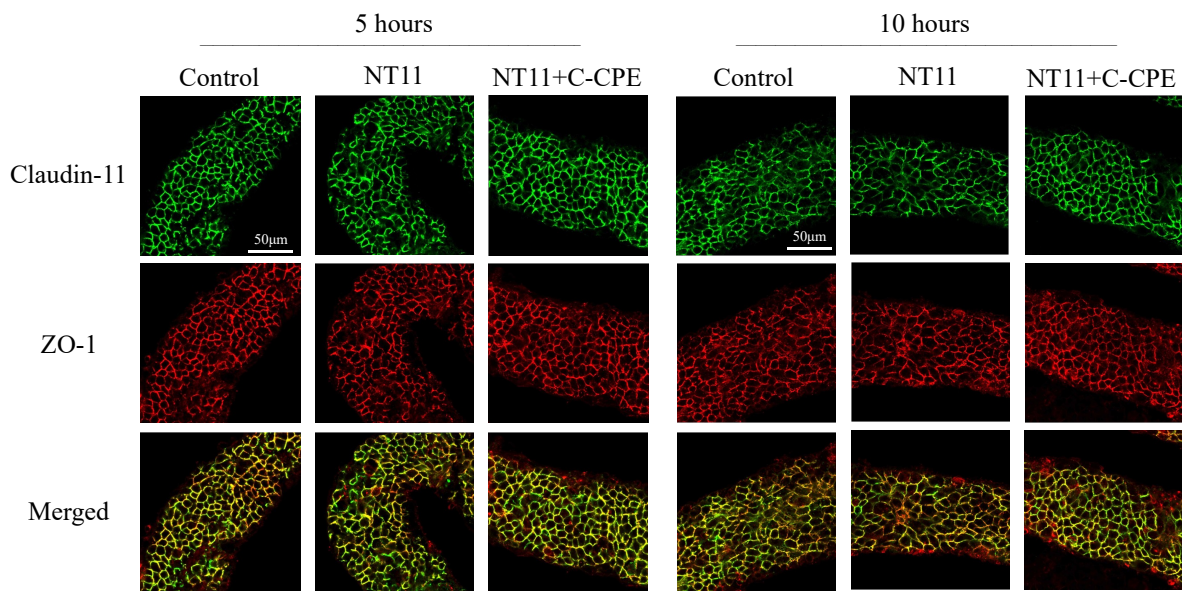


**Figure 14: NT11 treatment had no effect on localization of Claudin-11 at 5 hours and 10 hours in a submerged whole testis *ex vivo* culture system.** Claudin-11 (green) and ZO-1 (red) immunofluorescent wholemount staining of B6 mice testis tubules after 5 and 10-hours of 40 $\mu$ M NT11 or 40 $\mu$ M NT11 + 40 $\mu$ M C-CPE treatment. Scale bar = 50 $\mu$ m.

One possibility is that NT11 and C-CPE were not able to reach the tight junctions of the individual testis tubules when the whole testis was submerged in the media due to the minimal manipulation of the testis before culturing. To overcome this challenge and increase the surface area for the peptide to enter the testis tubules, the testis was digested with Collagenase IV before submerging the sample in the media containing NT11 and C-CPE. The 5-hour and 10-hour treatment submerged testes tubules experiments with NT11 and NT11+C-CPE were repeated; however, there was still no effect on the localization of Claudin-11 and Claudin-8 following

treatment. Based on these data, longer treatment times including, 24h, 48h, and 72h cultures were tested.

Prior to increasing the duration of treatment, the mouse model that was used for these studies was changed. IF analysis of testis tubules with anti-Claudin-11 antibodies revealed some variation in Claudin-11 staining and differences in the cellular shapes observed along the length of individual tubules from fertile B6 mice (Figure 15). The different stages in spermatogenesis affected the protein localization pattern of Claudin-11 along the tubule such that we could not identify whether the difference was a result of NT11 and/or C-CPE or merely a different stage in spermatogenesis at the specific region of the tubule. Therefore, I transitioned to the use of W/W<sup>v</sup> (Yuan et al., 2015) and busulfan-treated 129/B6 mice (Tang et al., 2012) which do not have germ cells, consequently no variation in claudin localization associated with different stages of spermatogenesis. Therefore, these mouse models allowed us to more easily visualize and compare the staining patterns of Claudin-11 between the control and treated testes. Additionally, the absence in germ cells in these mouse models could increase the ability of NT11 to access the Claudin-11 from the BTB between the Sertoli cells.

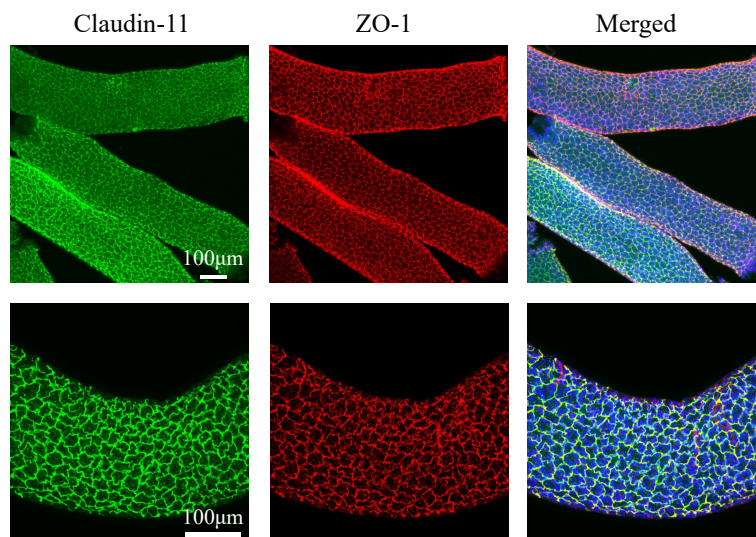


**Figure 15: Variation in Claudin-11 protein localization pattern in B6 mice testis tubules.** Claudin-11 (green), ZO-1 (red), and DAPI (blue) immunofluorescent wholemount staining of B6 mice testis tubules. Variations in Claudin-11 localization can be observed along the testis tubules in addition to different cellular shapes. Scale bar = 100µm.

Initial culture of the testis from these two infertile mouse models showed that the integrity of the tissue was greatly affected by the preparation and culture system I was using. Therefore, we developed our air-liquid interface *ex vivo* culture system using W/Wv testis and busulfan-treated 129/B6 testis which provided a more standardized comparison of signaling patterns across the tubule between the control and NT11 treated samples. In this method, I cut the testis in half and gently placed the testis tissue in 300 $\mu$ L of SSC culture media on a PCTE membrane filter. A thin layer of SSC culture media containing the anti-claudin peptide was pipetted over the tissue to form a dome-like shape. This increased the surface area for NT11 to reach the BTB, maximizing the peptide's accessibility, while minimizing disruption and maintaining tissue integrity for the 24h, 48h, and 72h cultures. Integrating these changes, I was able to establish an *ex vivo* organ culture system, which has allowed us to visualize the effects of NT11 on mouse testis tubules. These adaptations enabled us to refine our experimental approach, leading to a more robust assessment of NT11's effect on Claudin-11 in the BTB of W/Wv and Busulfan treated 129/B6 mouse. All future experiments were carried out using the air-liquid interface culture system whereby a thin film of medium would cover the surface of the testis tissue fragment on a semipermeable membrane.

### **3.1.2 Decrease in Claudin-11 Localization After 16- and 72-hour NT11 Treatments**

Upon establishing the air-liquid interface culture system, I compared the localization of Claudin-11 in W/Wv mutant mice testes tissue pieces cultured with 20 $\mu$ M and 40 $\mu$ M of NT11 independently to a control testis culture in SSC culture media and PBS. A more significant decrease in Claudin-11 signal intensity was observed in testis cultured with 40 $\mu$ M of NT11. Therefore, all future NT11-treated samples were carried out with 40 $\mu$ M of NT11.

After treating the tubules for 16 hours *ex vivo*, I observed a decrease in Claudin-11 signal intensity in NT11-treated W/Wv testis tubules in comparison to control testis tubules in SSC culture media and PBS, The ZO-1 signal intensity, which remained unchanged across conditions, was used to compare relative levels of Claudin-11 localization between the control and NT11-treated conditions. For each experimental replicate, 10 testis tubules were imaged from each condition and representative images are shown in Figure 16. There was a decrease in Claudin-11 signal intensity in the NT11-treated testis tubules compared to control tubules. This can be observed in my laser scanning confocal microscope images throughout the Z-stacks taken from

the top of the tubule to the midline of the lumen. When W/W<sup>v</sup> mutant mice testis tubules were treated with 40μM NT11 for 72 hours, I observed a similar decrease in Claudin-11 signal intensity compared to the control testis tubules. This experiment was replicated two times, each time using one W/W<sup>v</sup> mutant mouse. Thus, using an air-liquid interface culture system, I was able to observe a decrease in Claudin-11 localization across W/W<sup>v</sup> testis tubules in NT11 treated samples over 16 hours and 72 hours. The decrease in Claudin-11 intensity between the 16-hour and 72-hour time points did not differ.

Next, I cultured busulfan-treated 129/B6 mice testes with 40μM of NT11 for 16 hours and 72 hours, respectively. The busulfan-injected 129/B6 mice served as my induced infertile mouse model. When treated for 16 hours, I observed a decrease in Claudin-11 signal intensity in NT11-treated testis tubules in comparison to control testis tubules. A similar decrease was observed when W/W<sup>v</sup> testis tubules were treated with NT11 for 72 hours. For both experiments, ZO-1 signal intensity remained unchanged across conditions and results were compared by examining the merged Claudin-11 and ZO-1 stacks between the control and NT11-treated conditions. Furthermore, like the results observed in the W/W<sup>v</sup> mice testis tubules, the decrease in Claudin-11 signal intensity can be observed in the images taken with the 20x (Figure 17A) and 63x (Figure 17B) objectives. Both objectives were chosen to image in order to observe the Claudin-11 protein localization pattern across the entirety of the tubule in addition to a higher magnification section which would provide higher definition/resolution.

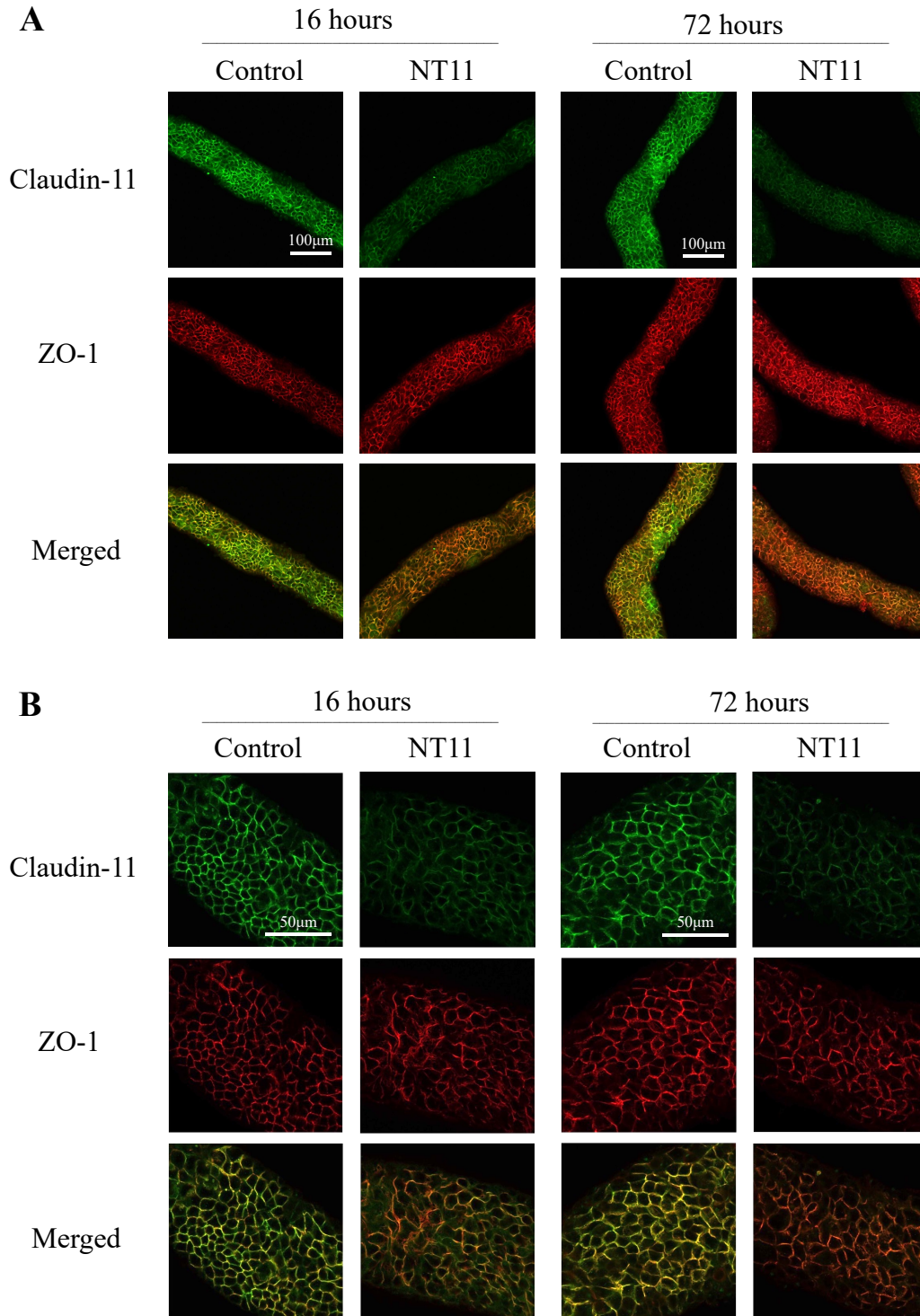


**Figure 16: NT11 treatment decreased localization of Claudin-11 at the BTB in W/W<sup>v</sup> testis tubules.** **A.** Claudin-11 (green) and ZO-1 (red) immunofluorescent wholemount staining of W/W<sup>v</sup> mutant mice testis tubules after 16- and 72-hours of 40 $\mu$ M NT11 treatment. Scale bar = 100 $\mu$ m. **B.** Higher magnification images of different testis tubules. Scale bar = 50 $\mu$ m.

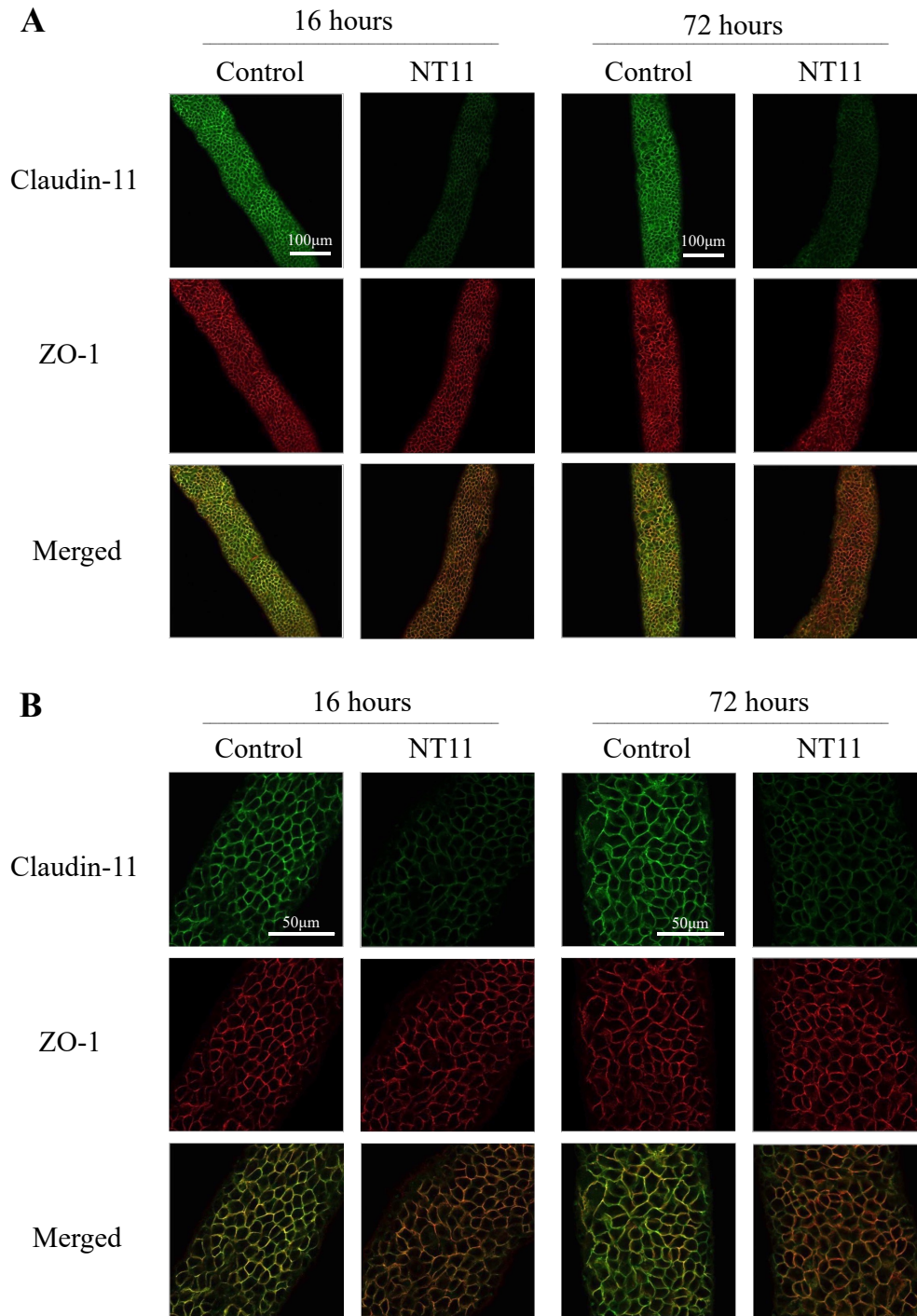


**Figure 17: NT11 treatment decreased localization of Claudin-11 at the BTB in 129/B6 busulfan-treated testis tubules. A.** Claudin-11 (green) and ZO-1 (red) immunofluorescent wholemount staining of 129/B6 busulfan-treated mice testis tubules after 16- and 72-hours of 40 $\mu$ M NT11 treatment. Scale bar = 100 $\mu$ m. **B.** Higher magnification images of different testis tubules. Scale bar = 50 $\mu$ m.

### 3.1.3 Removal of NT11 Allows Claudin-11 to Repopulate the BTB

The BTB is essential for spermatogenesis, particularly for spermatogonia and preleptotene spermatocytes, as it acts as an immunological barrier and provides the microenvironment necessary for the completion of meiosis. To test the reversible manner in which NT11 disrupts the BTB, I treated W/W<sup>v</sup> mutant mice testes with 40 $\mu$ M of NT11 for 16 hours and then removed the NT11 media and replaced it with complete SSC culture media and allowed the tubules to recover prior to collecting the tubules for IF wholemout staining. Control tubules from W/W<sup>v</sup> mutant mice testes were covered by a thin layer of PBS + vehicle on a semipermeable membrane for 16 hours followed by an exchange in media to complete SSC culture media. A small sample of testis tissue was taken at the 16-hour treatment time point to verify the effect of NT11 on the testis tubules. As observed previously there was a decrease in Claudin-11 signal intensity compared to the untreated control (Figure 18).

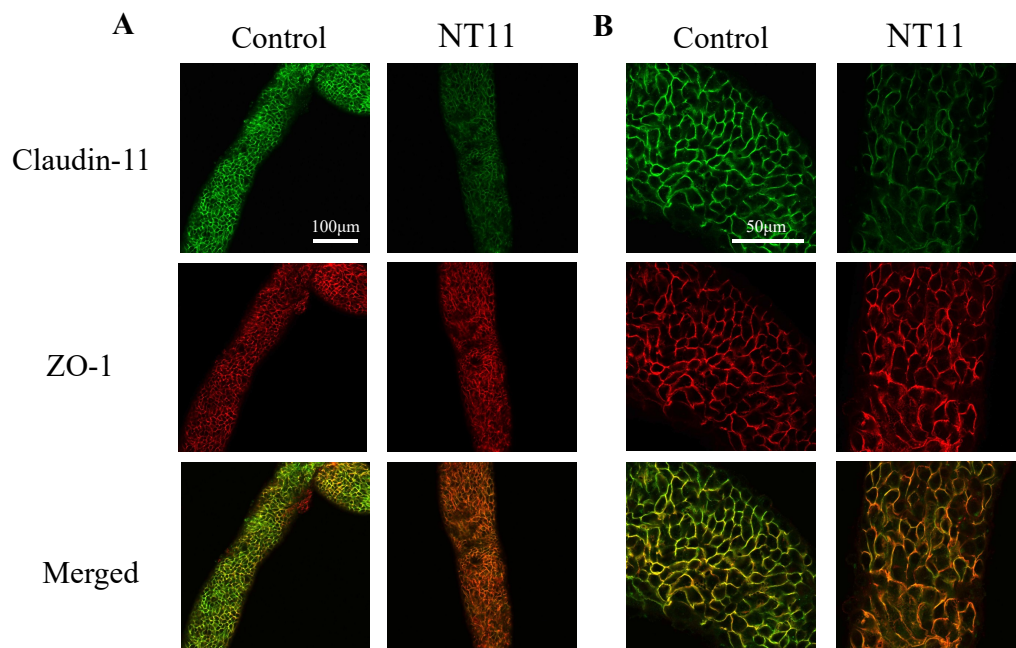


**Figure 18: Decrease in Claudin-11 localization at the BTB after 16-hour NT11 treatment before removing the peptide from the media. A.** Claudin-11 (green) and ZO-1 (red) immunofluorescent wholemount staining of W/W<sup>v</sup> mice testis tubules after 16 hours of 40 $\mu$ M NT11 treatment before removing NT11 for 24, 48, and 72hours of additional culture. Scale bar = 100 $\mu$ m. **B.** Higher magnification images of different testis tubules. Scale bar = 50 $\mu$ m.

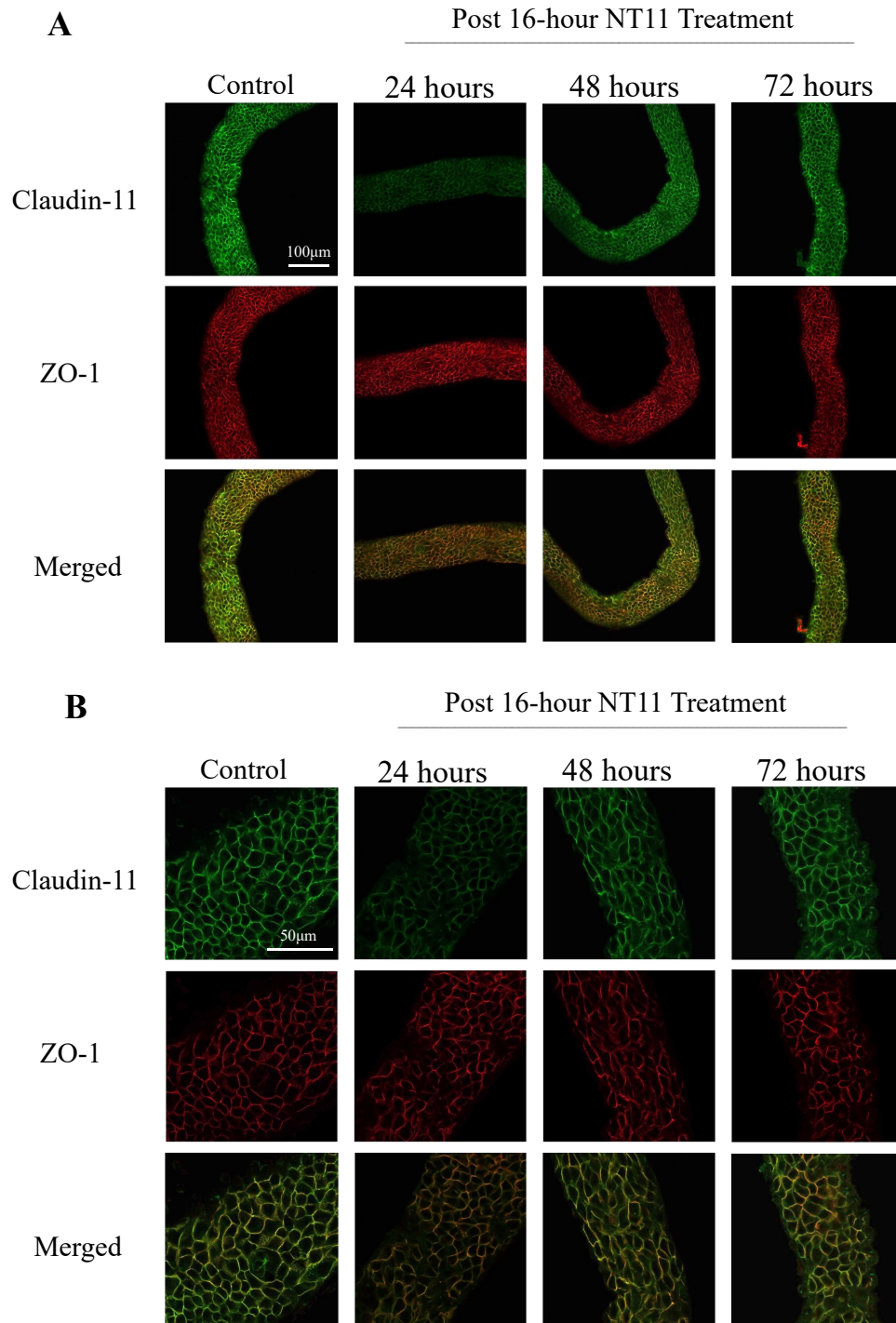


**Figure 19: Recovery of Claudin-11 to the BTB following treatment with NT11.** Claudin-11 (green) and ZO-1 (red) immunofluorescent wholemount staining of W/Wv mutant mice testis tubules cultured in control media, in media with 40 $\mu$ M NT11, and 24, 48, and 72 hours after NT11 treatment. Scale bar = 100 $\mu$ m. **B.** Higher magnification images of different W/Wv testis tubules from the same culture conditions described in A. Scale bar = 50 $\mu$ m.

We observed that the Claudin-11 signal intensity in W/Wv mutant mice testes tubules treated with NT11 for 16 hours with NT11 and allowed to recover for 72 hours was similar to that of the control testis tubules (Figure 19). Thus, to determine when Claudin-11 was restored within the BTB, two shorter periods of recovery were added: 24 hours and 48 hours. After 24 hours of recovery, the overall Claudin-11 signal intensity remained significantly lower compared to the control and was similar to the signal intensity observed after 16 hours of NT11 treatment (Figure 19). However, there was more variation in the level of Claudin-11 between tubules (Figure 20). After 48 hours of recovery, the Claudin-11 signal intensity was increased relative to immediately following treatment or 24 hours of recovery but still not as strong as in control tubules or those that have recovered for 72 hours (Figure 19). There was still considerable variability in Claudin-11 signal intensity from one tubule to another such that some had more intense Claudin-11 staining like the 72-hour time point whereas some were lower like the 24-hour time point (Figure 20). These data support that it takes approximately 72 hours for Claudin-

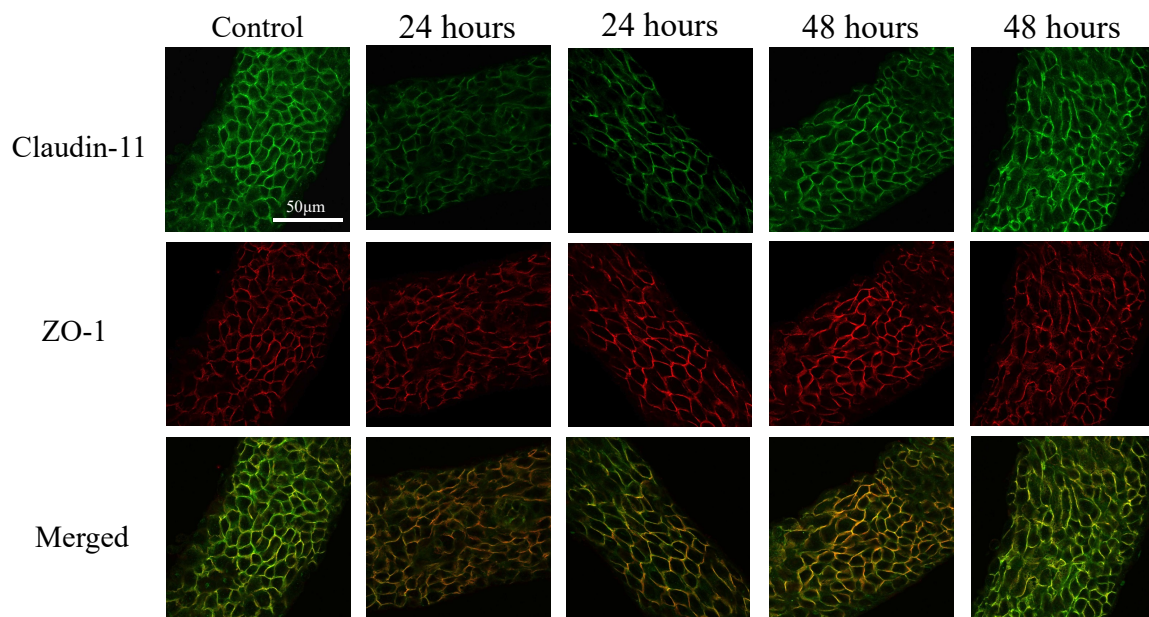


**Figure 20: Variation in Claudin-11 localization across tubules of the same recovery time points.** Claudin-11 (green) localization varied across immunofluorescent wholemount staining of W/Wv mutant mice testis tubules cultured with 40µM of NT11 after 24 and 48 hours of recovery. Various tubules had increased Claudin-11 localization after 24hours than others. Similarly, at 48 hours, Claudin-11 had varying levels of Claudin-11 localization between tubules. Scale bar = 50µm.

11 to fully repopulate tight junctions in the BTB following NT11 treatment. The recovery experiment was repeated two additional times, and the results were reproducible.

### 3.1.4 Pearson's Correlation Coefficient Supports Claudin-11 Delocalization from the Sertoli Cell Tight Junctions

To quantify the localization of Claudin-11 to the BTB I compared its colocalization with the tight junction cytoplasmic adaptor protein ZO-1 using Pearson's correlation coefficient. Pearson's correlation coefficient considers both signal intensity and localization of the two proteins being examined. Pearson's correlation coefficient was analyzed on Maximum Intensity Projections (MIPs) obtained from combining the Z-stack with the highest intensity of ZO-1 plus the Z-stack immediately above and the one immediately below. Each individual point represents a technical replicate from 3 biological replicates performed for each experiment. It is hypothesized that Claudin-11 is delocalized from the membrane when targeted by NT11, similarly to the effects of C-CPE on Claudin-3 or -4; therefore, colocalization was analyzed

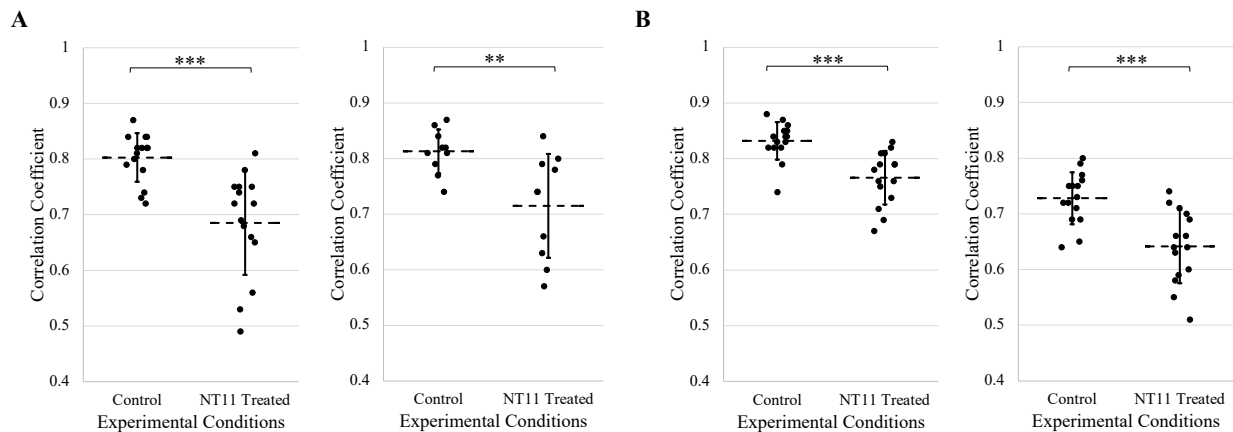


**Figure 21: Claudin-11 colocalization with ZO-1 in W/Wv and 129/B6 busulfan-treated testis tubules after 16 and 72-hour NT11 treatments.** **A.** Pearson's correlation coefficients for Claudin-11 and ZO-1 in W/Wv mice testis tubules treated with NT11 for 16 hours (left) or 72 hours (right). The mean and SD are shown. Statistical significance was evaluated using a two tailed t test. \*\*  $p \leq 0.01$ ; \*\*\*  $p \leq 0.001$  **B.** Pearson's correlation coefficients for Claudin-11 and ZO-1 in 129/B6 busulfan-treated mice testis tubules treated with NT11 for 16 hours (left) or 72 hours (right). The mean and SD are shown. Statistical significance was evaluated using a two tailed t test. \*\*\*  $p \leq 0.001$

(Baumholtz et al., 2017). This method of analysis also serves as an internal control and provides confirmation that Claudin-11 signal intensity is being reduced/ delocalized from the tight junction and that it is not merely an artifact of confocal imaging.

There was a statistically significant difference in the co-localization (mean Pearson's R colocalization value) of Claudin-11 with ZO-1 between control W/Wv testis tubules and those treated with NT11 for 16 hours (Control: 0.80, SD = 0.04, NT11: 0.69, SD = 0.09;  $p = 2.8 \times 10^{-4}$ ) which was calculated using a two tailed t test (Figure 21A). Similarly, there was a statistically significant difference in mean Pearson's R colocalization value of Claudin-11 with ZO-1 between control W/Wv testis tubules and those treated with NT11 for 72 hours (Control: 0.81, SD = 0.04, NT11: 0.72, SD = 0.09;  $p = 9.8 \times 10^{-3}$ ).

Furthermore, there was a statistically significant difference in mean Pearson's R colocalization value of Claudin-11 with ZO-1 between control busulfan-treated 129/B6 mice

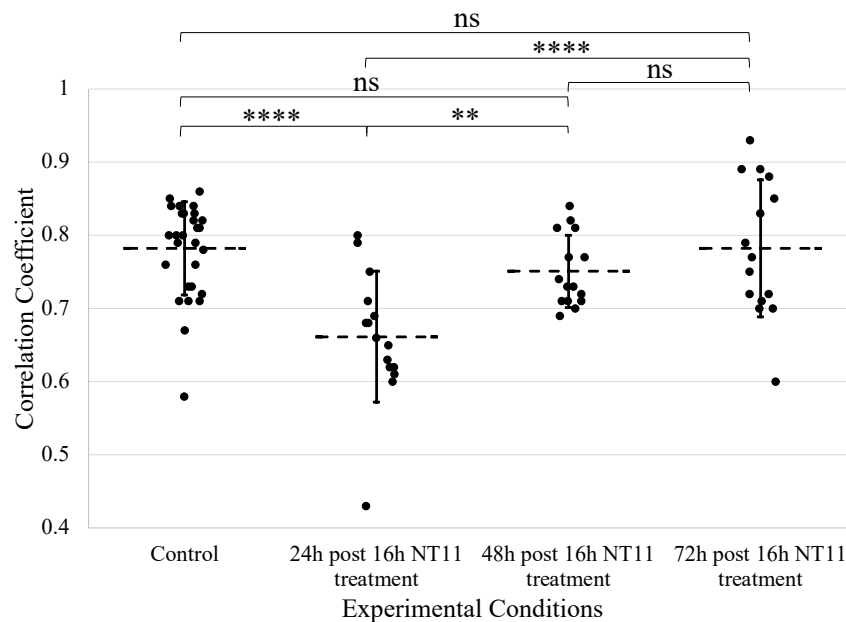


**Figure 22: Claudin-11 colocalization with ZO-1 in W/Wv testis after 24, 48 and 72 hours post 16-hour NT11 treatment.** Pearson's correlation coefficients for Claudin-11 and ZO-1 in W/Wv mice testis tubules treated with NT11 for 16 hours followed by 24h, 48h, and 72h in culture after NT11 was removed. The mean and SD are shown. Statistical significance was evaluated using an ANOVA one-way factor test and Tukey-Kramer Post Hoc test. ns  $p > 0.05$ ; \*\*  $p \leq 0.01$ ; \*\*\*\*  $p \leq 0.0001$

testis tubules and those treated with NT11 for 16 hours (Control: 0.83, SD = 0.03, NT11: 0.77, SD = 0.05;  $p = 2.1 \times 10^{-4}$ ) (Figure 21B). Similarly, there was a statistically significant difference in mean Pearson's R colocalization value of Claudin-11 with ZO-1 between control busulfan-treated 129/B6 mice testis tubules and those treated with NT11 for 72 hours (Control: 0.73, SD = 0.05, NT11: 0.64, SD = 0.07;  $p = 3.3 \times 10^{-4}$ ). Together, this data shows that Claudin-11 delocalized from the BTB when treated with NT11.

Finally, an ANOVA one-way factor test and Tukey-Kramer Post Hoc test was used to examine the statistical significance of Pearson's correlation coefficient for Claudin-11 and ZO-1 amongst the control, 24 hours post 16-hour NT11 treatment, 48 hours post 16-hour NT11 treatment, and 72 hours post 16-hour NT11 treatment conditions from the Claudin-11 restoration experiments (Figure 22). There was a statistically significant difference in mean Pearson's R colocalization value of Claudin-11 with ZO-1 between the control vs 24 hours, 24 hours vs 48 hours, and 24 hours vs 72 hours ( $p$  value =  $1.0 \times 10^{-4}$ ,  $7.8 \times 10^{-3}$ , and  $2.0 \times 10^{-4}$ , respectively) but not for 48 hours vs 72 hours, control vs 48 hours, and control vs 72 hours ( $p$  value = 0.65, 0.51, and 0.99, respectively) (Control: 0.78, SD = 0.06, 24 hours: 0.66, SD = 0.09, 48 hours: 0.75, SD = 0.05, 72 hours: 0.78, SD = 0.09).

### **3.1.5 Measuring Integrated Sum Intensities to Quantify Relative Amount of Claudin-11 at the BTB**

In addition to Pearson's correlation coefficient, I compared the integrated sum intensities of Claudin-11 over ZO-1 for each condition. The integrated sum intensity is the sum of the pixel intensity over all the pixels in the selection, more specifically, the signals located at the blood-testis barrier of the testis tubules which was selected using an ROI. Notably, ZO-1 pixels were used to create this selection from MIPs, which consist of the Z-stack with the highest intensity of ZO-1 and the stacks immediately above and below. This method was chosen as a secondary measure of analysis as I observed a strong decrease in signal intensity specifically for Claudin-11 at the BTB in the imaged testis tubules.

Analysis of the W/Wv testis tubules treated with NT11 for 16 hours revealed a statistically significant difference in the integrated sum intensity value of Claudin-11/ZO-1 between the control and NT11-treated tubules (Control: 1.0, SD = 0.22, NT11: 0.78, SD = 0.25;  $p = 0.01$ ) (Figure 23A). For the W/Wv testis tubules treated with NT11 for 72 hours, there was

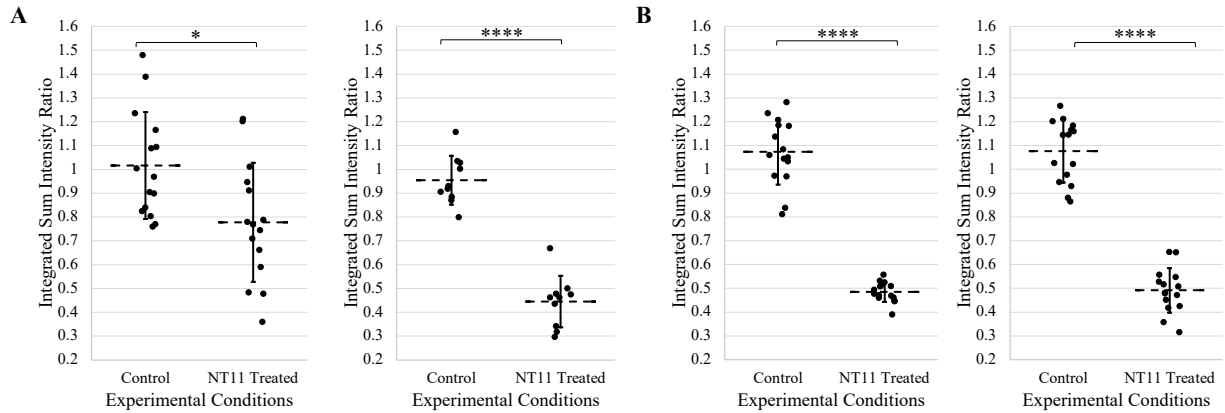


**Figure 23: Integrated sum intensity of Claudin-11 over ZO-1 in W/Wv and 129/B6**

**busulfan-treated testis tubules after 16 and 72-hour NT11 treatments.** Integrated Sum

Intensities **A.** Integrated sum intensities of Claudin-11/ ZO-1 in W/Wv mice testis tubules treated with NT11 for 16 hours (left) or 72 hours (right). The mean and SD are shown.

Statistical significance was evaluated using a two tailed t test. \*  $p \leq 0.05$ ; \*\*\*\*  $p \leq 0.0001$  **B.**

Integrated sum intensities for Claudin-11 and ZO-1 in 129/B6 busulfan-treated mice testis tubules treated with NT11 for 16 hours (left) or 72 hours (right). The mean and SD are shown.

Statistical significance was evaluated using a two tailed t test. \*\*\*\*  $p \leq 0.0001$

also a statistically significant difference in the integrated sum intensity value of Claudin-11/ZO-1 between control mice testis tubules and those treated with NT11 (Control: 0.95, SD = 0.10, NT11: 0.44, SD = 0.11;  $p = 2.7 \times 10^{-9}$ ).

Additionally, there was a statistically significant difference in the integrated sum intensity values of Claudin-11/ZO-1 between the control busulfan-treated 129/B6 mice and NT11-treated tubules (Control: 1.1, SD = 0.14, NT11: 0.48, SD = 0.04;  $p = 1.8 \times 10^{-11}$ ) (Figure 23B). Similarly, there was a statistically significant difference in the integrated sum intensity value of Claudin-11/ZO-1 between control busulfan-treated 129/B6 mice testis tubules and those treated with NT11 (Control: 1.1, SD = 0.13, NT11: 0.49, SD = 0.09;  $p = 2.1 \times 10^{-13}$ ). This data provided a relative measure of the amount of Claudin-11 present at the BTB after being treated with NT11, further confirming its removal from the tight junction of the testis tubules.

Lastly, an ANOVA one-way factor test and Tukey-Kramer Post Hoc test was used to examine the statistical significance of the integrated sum intensities of Claudin-11/ZO-1 amongst the control, 24 hours post 16-hour NT11 treatment, 48 hours post 16-hour NT11 treatment, and

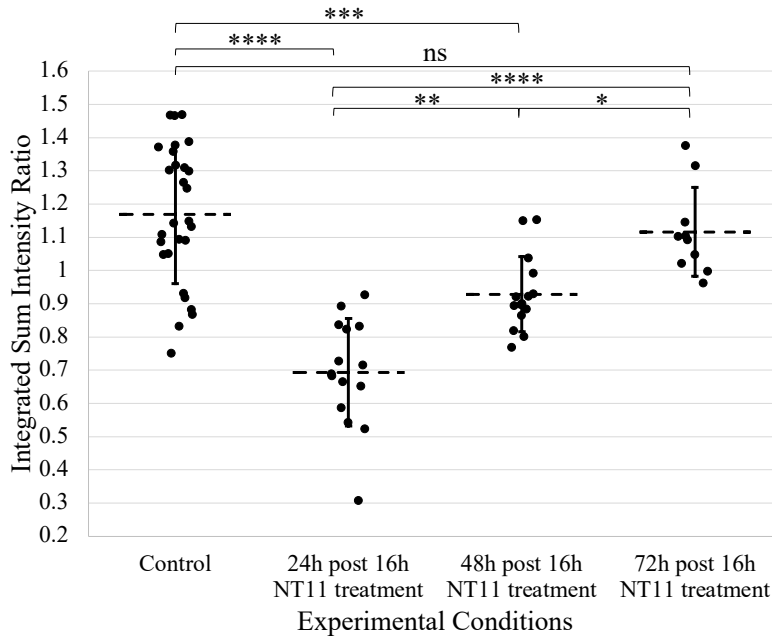


**Figure 24: Integrated sum intensity of Claudin-11 over ZO-1 in W/Wv testis tubules after 24, 48, 72 hours post 16-hour NT11 treatment.** Integrated Sum Intensities of Claudin-11/ ZO-1 in W/Wv mice testis tubules treated with NT11 for 16 hours followed by 24h, 48h, and 72h in culture after NT11 was removed. The mean and SD are shown. Statistical significance was evaluated using an ANOVA one-way factor test and Tukey-Kramer Post Hoc test. ns  $p > 0.05$ ; \*  $p \leq 0.05$ ; \*\*  $p \leq 0.01$ ; \*\*\*  $p \leq 0.001$ ; \*\*\*\*  $p \leq 0.0001$

72 hours post 16-hour NT11 treatment conditions from the Claudin-11 recovery experiment (Figure 24). There was a statistically significant difference in the integrated sum intensity value of Claudin-11/ZO-1 between the control vs 24 hours, control vs 48 hours, 24 hours vs 48 hours, 24 hours vs 72 hours, and 48 hours vs 72 hours ( $p$  value =  $1.0 \times 10^{-4}$ ,  $3.0 \times 10^{-3}$ ,  $2.0 \times 10^{-3}$ ,  $1.0 \times 10^{-4}$  and 0.04, respectively) but not for the control vs 72 hours ( $p$  value = 0.84) (Control: 1.2, SD = 0.21, 24 hours: 0.69, SD = 0.16, 48 hours: 0.93, SD = 0.11, 72 hours: 1.1, SD = 0.13). This data indicates that the amount of Claudin-11 present at the BTB is similar to that of the control after 72 hours in culture from the time of removal of NT11.

### 3.1.6 Summary of Results from Aim 1

After testing multiple culture conditions, we determined that the air-liquid interface culture system was the best approach to maintain healthy and viable testis tubules *ex vivo* in

order to test our peptides. These data demonstrated that NT11 removes Claudin-11 from mouse BTB after 16 hours of treatment and that the tubules remain viable despite being depleted of Claudin-11 after 72 hours in NT11-containing media. The significant decrease in Claudin-11 signal intensity at the BTB in NT11-treated tubules was observed in both W/Wv and busulfan-treated 129/B6 mouse testis tubules. I also observed that upon removal of the NT11 peptide, Claudin-11 was gradually restored to the BTB in W/Wv testis tubules between 24 and 72 hours in complete SSC culture media.

Quantification of the immunofluorescence data using Pearson's correlation coefficient of Claudin-11 and ZO-1 showed a significant decrease in Claudin-11's colocalization with ZO-1 following NT11 treatment in both W/Wv as well as Busulfan-treated 129/B6 mouse testis tubules after 16- and 72-hour NT11 treatments ( $p < 0.05$ ). This data revealed that Claudin-11 is delocalized from the BTB when treated with NT11. Additionally, Pearson's correlation coefficient of Claudin-11 and ZO-1 over 24, 48, 72 hours post 16-hour NT11 treatment were statistically significant between the control vs 24 hours, 24 vs 48 hours, and 24 hours vs 72 hours ( $p < 0.05$ ). However, 48 hours vs 72 hours, control vs 48 hours, and control vs 72 were non-significant ( $p > 0.05$ ). This data demonstrated that Claudin-11 localized to the BTB at 48 hours and continued to increase at 72 hours.

Finally, comparison of the integrated sum intensities of Claudin-11 over ZO-1 for all experiments revealed a statically significant difference between the control and NT11-treated samples in both W/Wv and Busulfan treated 129/B6 mouse testis tubules after 16- and 72-hour NT11 treatments ( $p < 0.05$ ). Thus, the amount of Claudin-11 present at the BTB was significantly lower. After the removal of NT11, the integrated sum intensity of Claudin-11 over ZO-1 was statistically significant between the control vs 24 hours, control vs 48 hours, 24 hours vs 48 hours, 24 vs 72 hours, and 48 hours vs 72 hours ( $p < 0.05$ ). The control vs 72 hours was non-significant, indicating that the relative amount of Claudin-11 returned to that of the control after 72 hours post 16-hour NT11 treatment. Thus, this data demonstrated that in the presence of NT11, Claudin-11 is removed from the BTB, and its withdrawal allows Claudin-11 to repopulate the tight junctions.

## 3.2 Aim 2: Optimizing NT11 Purification

### 3.2.1 Assessing Purity of NT11 Protein Preparations

The protein purification technique used to isolate bacterially expressed NT11 from the bacterial cell extract is affinity chromatography by His-tag purification. This method involves a single step immobilized metal affinity chromatography (IMAC), which is a specialized form of affinity chromatography that separates proteins based on their affinity for metal ions immobilized to a solid chelating resin (Bornhorst & Falke, 2000). Ni-NTA Agarose, a nickel-charged affinity resin, is used for purifying recombinant proteins containing a polyhistidine sequence. Specifically, the nickel<sup>2+</sup> ion coupled to Nitrilotriacetic acid (NTA) interacts with the polyhistidine tag from our NT11, facilitating the isolation of NT11 through this protein purification process. However, His-tag purification is known to have common IMAC contaminants due to competitive binding by endogenous host proteins. These contaminants include DnaK (70 kDa), GlnS (67 kDa), AceE (100 kDa), EF-Tu (43 kDa), ArnA (74 kDa), CRP (24kDa), and SlyD (21kDa) (Samuelson, 2016).

During the initial stages of generating and purifying NT11, Dr. Enrique Gamero-Estevéz obtained extremely low yields due to the fact that the protein was highly insoluble. To increase the yield and solubility of the NT11, several modifications were made to the bacterial culture and protein induction conditions along with the addition of a His tag and Spidroin protein (NT) solubility tag (Kronqvist et al., 2022), resulting in the protein purification described above in the methods. Figure 25A is an SDS-PAGE gel stained with Coomassie Brilliant Blue R-250 and a western blot probed with a Mouse anti His antibody showing the different steps in the NT11 induction and purification process leading up to the final product (Figure 25A lane 2 to lane 11). Figure 25B shows the different preparations of NT11 generated by Dr. Enrique Gamero-Estevéz and Sayaka Hansen. The protocol described above was used to generate the NT11 used in all the experiments shown in Figure 25B (NT11 1.36ug/μL, NT11 3.1ug/μL, and NT11 2.7ug/μL (Figure 25B lanes 3, 6, and 7, respectively)) by Sayaka Hansen. Our peptide has a molecular weight of 29.8kDa as seen on the western blot. However, our final product contains many bacterial contaminants as demonstrated in the equivalent column on the Coomassie-stained gel (example, comparing Figure 25B lane 7 on the western blot with lane 7 on the Coomassie-stained gel). The size of the protein recognized by the antibody does not align with the major bands stained with Coomassie blue (29.8kDa vs 24kDa). Therefore, in order to purify NT11, I

explored various methods of purification in addition to the affinity chromatography by His-tag purification currently employed in our purification protocol.

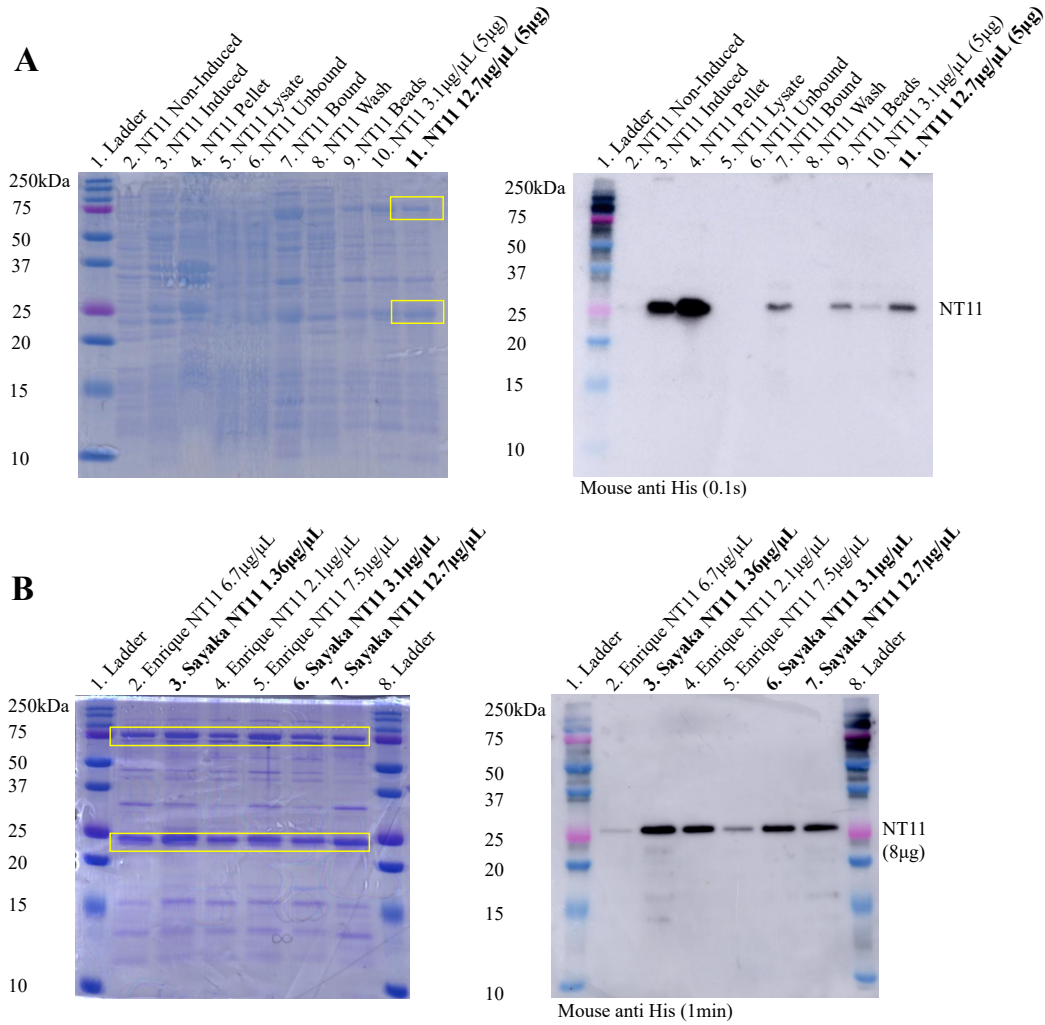


**Figure 25: Assessing NT11 purification and comparing purified NT11s.** **A.** Each lane is an aliquot taken from a step in the induction and purification process of NT11 12.7µg/µL. Bacterial contaminants of concern are outlined with yellow boxes in the final product after His-purification. The Coomassie-stained gel and western blot contain the same samples and were run simultaneously. **B.** Purified NT11s generated by Dr. Enrique Gamero-Estevez and Sayaka Hansen. 8µg of total protein was loaded in each lane. Similarly, bacterial contaminants of concern are outlined with yellow boxes in the final product on the SDS-PAGE gel stained with Coomassie blue.

### **3.2.2 Incorporation of Size Exclusion Chromatography and Amicon Centrifugal Filters to Improve Purity of NT11**

Initially, our hypothesis for further purifying NT11 was to isolate it based on size following His-tag purification. In an attempt to isolate NT11 from its contaminants, primarily those around 80 kDa and 24 kDa, I explored Size Exclusion Chromatography (SEC) and the use of Amicon Centrifugal Filters. When I introduced 480ul of His-tagged purified NT11 12.7ug/ $\mu$ L (6.069mg of total protein) into the SEC Sephadex G-75 column, protein had visibly eluted from Fractions 8 to 14 (Figure 26A lanes 9, 10, 11, 12, 13, 14, and 18) but with very little separation as observed in Figure 26A. The bacterial protein contaminant around 80kDa predominantly eluted in Fraction 8 (Figure 26A lane 9) in addition to NT11 which began eluting from Fraction 8 (Figure 26A lane 9) until Fraction 14 (Figure 26A lane 18) along with the contaminant at 24kDa (Figure 26A). To enhance purity, a second round of His-tag purification was conducted on pooled fractions 9 to 11 (Figure 26A lanes 10, 11, and 12) and Fractions 12 to 14 (Figure 26A lanes 13, 14, and 18) with steps shown in Figure 26B. Total protein concentration for pooled Fractions 9 to 11 and pooled Fractions 12 to 14 were measured at 1.7ug/ $\mu$ L (Figure 26B lane 8) and 0.37ug/ $\mu$ L (Figure 26B lane 17), respectively. However, upon visualizing with a western blot (Figure 26D lanes 5 and 6), NT11 was only minimally detected in pooled Fractions 9 to 11 (Figure 26D lane 5) and not at all in pooled Fractions 12 to 14 (Figure 26D lane 6). Thus, size exclusion chromatography with Sephadex G-75 did not effectively isolate NT11 from the bacterial contaminants.

Next, I tested Amicon Ultra Centrifugal Filters which can also be used to separate molecules of different sizes. Using a 50kDa MWCO Amicon filter, I attempted to separate NT11 from its contaminant around 80kDa. I processed Fraction 8 (Figure 26A lane 9) from our SEC for 45 minutes in a 15mL conical Amicon centrifugal filter at 3800 rpm (4000 RCF) in a swinging bucket rotor. I expected that NT11 would be eluted from the 50KDa Amicon filter, however, NT11 was retained as shown by the western blot in Figure 26C lane 4 along with the various bacterial contaminants. Therefore, the Amicon Ultra Centrifugal Filter (Figure 26D lane 7) nor SEC improved the purity of our NT11 peptide (Figure 26D lanes 5 and 6). Based on these data I next decided to focus on the buffers that are used throughout the NT11 purification process to prevent non-specific binding of bacterial contaminants to the Ni-NTA Agarose beads: resuspension/ lysis buffer, wash buffer, and elution buffer.

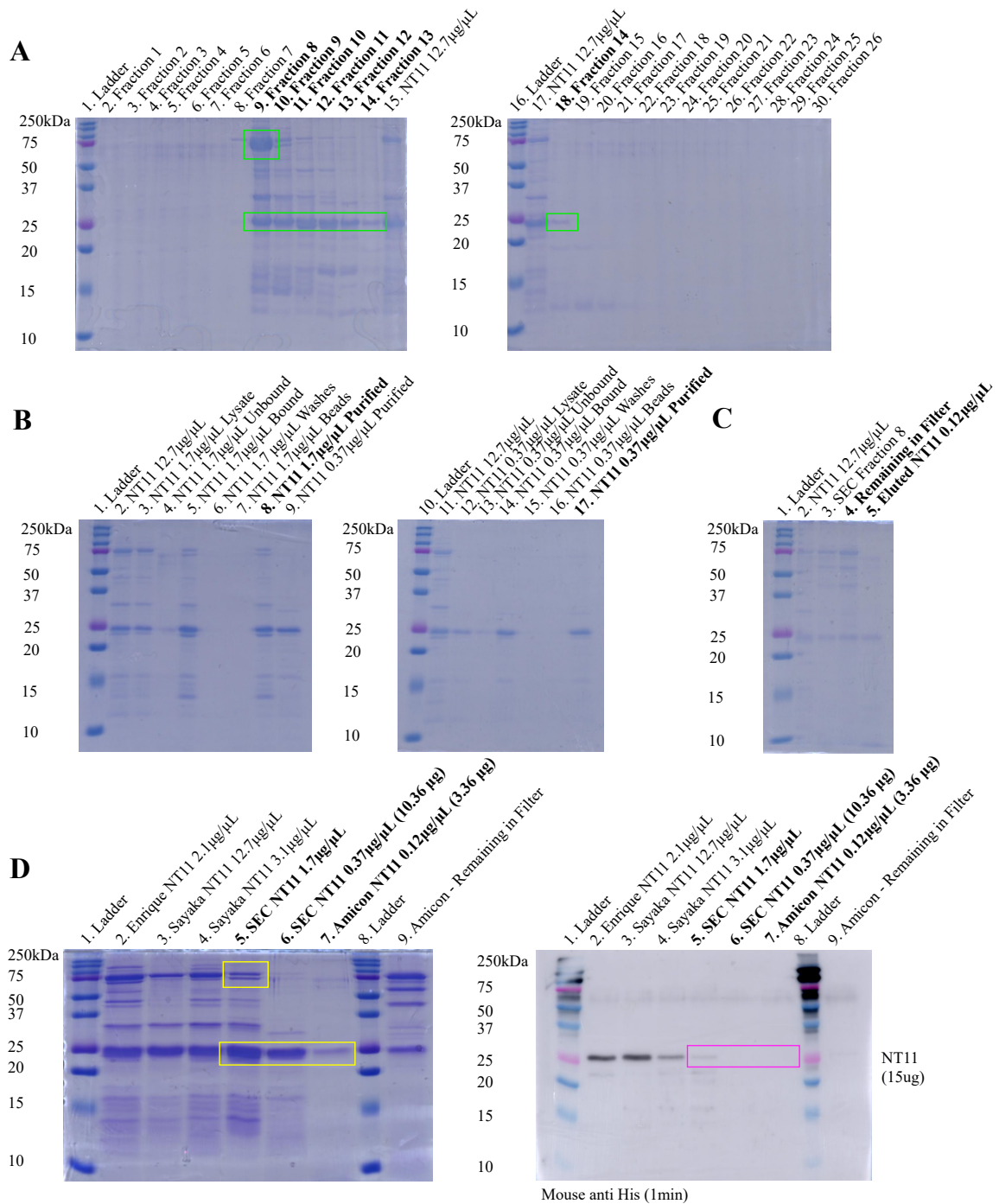


**Figure 26: Analysis of NT11 purity after Size Exclusion Chromatography and Amicon Centrifugal Filters.** **A.** SDS-PAGE gel stained with Coomassie blue of SEC with 480ul of NT11 12.7µg/µL. The bacterial contaminant at 80kDa eluted mostly at fraction 8 while NT11 and the remaining contaminants continued to elute until fraction 14. Each fraction is 1ml. The green boxes show the eluted protein from the SEC. **B.** SDS-PAGE gel stained with Coomassie

blue of second His-tag purification steps after SEC with fractions 9 to 11 (NT11 1.7 $\mu$ g/ $\mu$ L) and fractions 12 to 14 (NT11 0.37  $\mu$ g/ $\mu$ L). **C.** SDS-PAGE gel stained with Coomassie blue of SEC fraction 8 that was purified using an Amicon ultra-15 centrifugal filter with a 50kDa MWCO. **D.** SDS-PAGE gel stained with Coomassie blue and western blot of generated products from SEC and Amicon Centrifugal Filter. 15 $\mu$ g of total protein was loaded in each lane. The yellow boxes outlined on the Coomassie-stained gel are the bacterial contaminants. The pink box outlined on the western blot shows that there is no NT11 in the SEC nor Amicon centrifugal filter products.

### 3.2.3 Adjustment of Binding Buffers to Modify Non-Specific Interactions with Ni-NTA Agarose Beads and Improve Elution

Another known method for improving the purity of His-tag purified recombinant proteins is increasing imidazole concentrations in the resuspension/lysis, wash and elution buffers (Bornhorst & Falke, 2000). Increasing the concentration of imidazole can also help with elution to prevent the protein from remaining on the beads. Additionally, adding 20 mM  $\beta$ -mercaptoethanol ( $\beta$ -ME) to the resuspension/ lysis buffer can help reduce disulfide bonds that may have formed between contaminating proteins and the 6xHis-tagged protein (QIAGEN, 2003). Furthermore, increasing NaCl concentrations will give buffers sufficient ionic strength to prevent nonspecific interactions between proteins and the Ni-NTA matrix. The buffer recipe used for all NT11 purifications along with the modified buffers can be found in Table 2. The purification process was compared using an 800mL bacterial culture of NT11 using both buffers

<b>Original and modified buffers for NT11 purification</b>						
	<b>Original Buffers</b>			<b>Modified Buffers</b>		
	<b>Resuspension Buffer</b>	<b>Wash Buffer</b>	<b>Elution Buffer</b>	<b>Resuspension Buffer</b>	<b>Wash Buffer</b>	<b>Elution Buffer</b>
Tris HCl pH 7.5	50mM	50mM	50mM	50mM	50mM	50mM
NaCl	150mM	500mM	150mM	500mM	500mM	500mM
Imidazole	10mM	15mM	300mM	10mM	60mM	500mM
B-Mercapto-ethanol	-	-	-	20mM	-	-

**Table 2: Original and modified buffers for NT11 purification.** The quantities of Tris HCl, NaCl, Imidazole, and  $\beta$ -mercaptoethanol used in the original buffers compared to the modified buffers for NT11 purification. Buffers were modified with the goal of increasing the purity of the final NT11 product.

independently. However, when comparing the final products visualized by a Western blot (Figure 27A lane 12 and Figure 27B lane 12) and Coomassie protein assay (Figure 27A lane 12 and Figure 27B lane 12), the increased imidazole buffers hindered the final yield of NT11 and did not improve the purity of NT11. In both products, the contaminants around 80kDa and

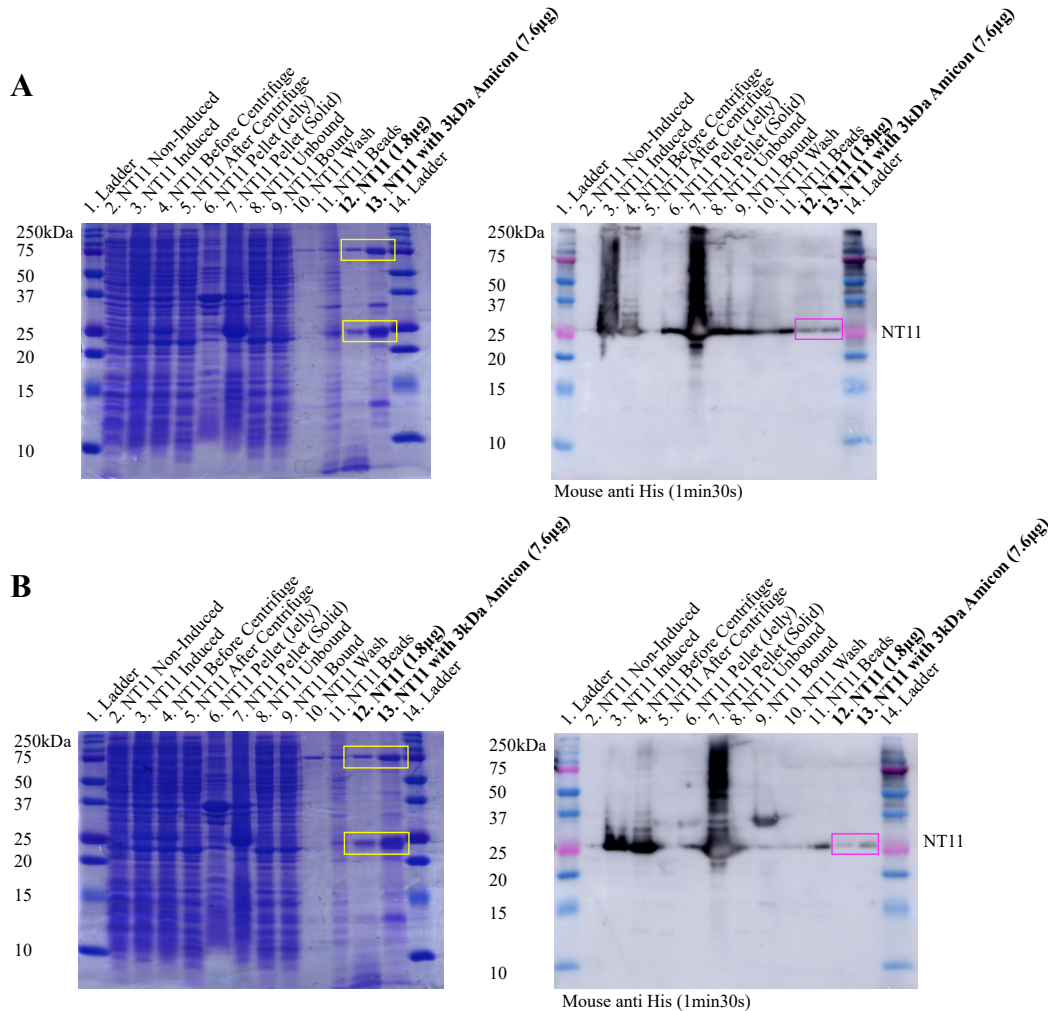


**Figure 27: Comparing buffers with different additives for NT11 purification. A.** SDS-PAGE gel stained with Coomassie blue and western blot of NT11 purification steps using original buffers. The yellow boxes on the Coomassie-stained gel outlines the contaminants and the pink box on the western blot outlines the obtained NT11. **B.** SDS-PAGE gel stained with Coomassie blue and western lot of NT11 purification steps using buffers with additional imidazole, NaCl, and  $\beta$ -mercaptoethanol in the resuspension buffer, wash buffer and elution buffer. Similarly, the yellow and pink box outline the contaminants and NT11, respectively.

24kDa remained (western blot and Coomassie-stained gel in Figure 27A lane 13 and Figure 27B lane 13). Additionally, much less NT11 was obtained in the final purified protein using the increased imidazole buffers compared to the buffers with the original recipe (Figure 27A Coomassie-stained gel lanes 12 and 13 compared to Figure 27B Coomassie-stained gel lanes 12 and 13). As a result, increasing imidazole and NaCl concentrations in addition to adding  $\beta$ -mercaptoethanol did not further purify our NT11 compared to our original protocol. Thus, I reverted to using our original buffers and proceeded to focus on possible non-specific interactions with the Ni-NTA agarose beads.

### 3.2.4 Exploring Column Purification to Prevent Non-Specific Interactions with Ni-NTA Agarose Beads

In the standard purification protocol, the lysate was incubated with the Ni-NTA agarose beads overnight to facilitate binding. This extended period of incubation and/or excess beads

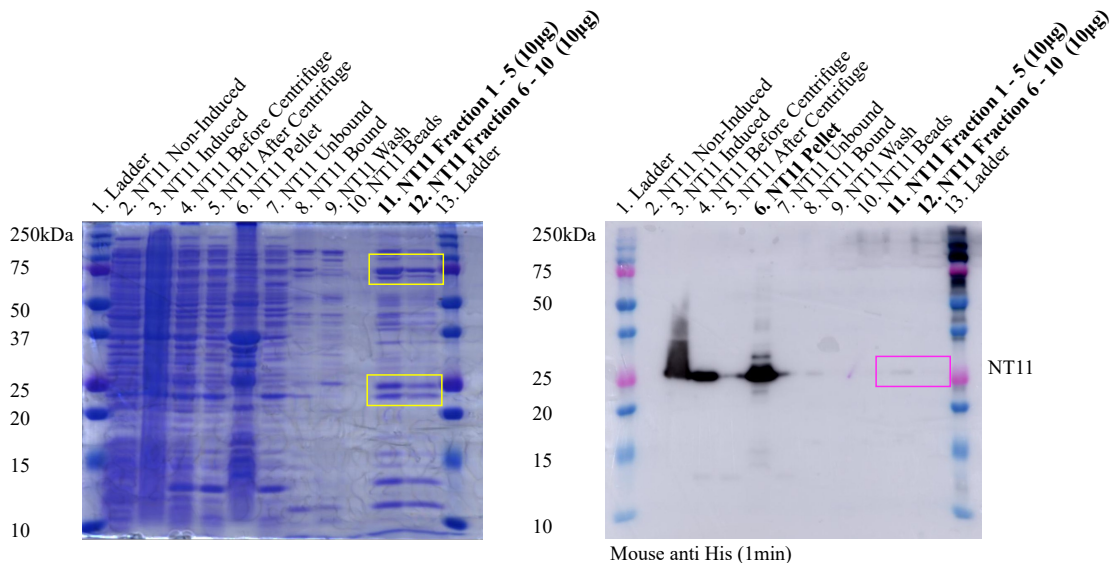


**Figure 28: Assessing NT11 purity after column purification.** SDS-PAGE gel stained with Coomassie blue and western blot of NT11 purification steps using a column purification method instead of the batch purification method. More contaminants can be observed in the yellow boxes on the Coomassie-stained gel compared to previous gels. The pink box outlines the NT11 recovered in Fractions 1- 5 and 6-10 which were pooled. Protein yields listed in Table 3.

	NT11 Non-Induced	NT11 Induced	Before Centrifuge	After Centrifuge	Pellet	Unbound	Bound	Wash	Beads	NT11 Fraction 1-5	NT11 Fraction 6-10
Sample Volume/ Total Volume	1mL/ 400mL	500µL/ 399mL	10µL/ 100mL	10µL/ 100mL	-	10µL/ 100mL	10µL of 2mL 50% Ni-NTA (1mL)	100µL/ 30mL	10µL of 2mL 50% Ni-NTA (1mL)	3.90µL/ 6.50mL	12.8µL/ 6.90mL
Volume on Gel (25µL)	25µL water, 25µL 2X LD	100µL water, 100µL 2X LD	10µL sample, 90µL water, 100µL 2X LD	10µL sample, 90µL water, 100µL 2X LD	500µL water, 500µL 2X LD	10µL sample, 90µL water, 100µL 2X LD	10µL sample, 90µL water, 100µL 2X LD	100µL sample, 100µL 2X LD	10µL sample, 90µL water, 100µL 2X LD	3.9µL sample, 16.1µL water, 5µL 5X LD	12.8µL sample, 7.2µL water, 5µL 5X LD
Percent of Total Protein	0.125%	0.016%	1.25x10 <sup>-3</sup> %	1.25x10 <sup>-3</sup> %	-	1.25x10 <sup>-3</sup> %	6.25x10 <sup>-4</sup> %	0.021%	6.25x10 <sup>-4</sup> %	0.060%	0.186%
Protein Concentration	-	-	-	-	-	-	-	-	-	2.56µg/µL	0.780µg/µL
Total Protein on Gel	-	-	-	-	-	-	-	-	-	10µg	10µg
Relative Amount to Starting Culture	100%	12.8%	10.0%	10.0%	-	10.0%	0.500%	16.8%	0.500%	48.0%	149%

**Table 3: Yield table for total protein loaded on Coomassie-stained denaturing polyacrylamide gel and western blot on assessing NT11 purity after column purification.**

10ug of total protein was loaded on the gels for NT11 Fractions 1 -5 and 6 – 10. The amount of total protein loaded per well was quantified based on the percent of total protein in the starting culture (if 0.125% were to be considered as 100%). This suggests that very little amount of soluble NT11 was recovered using the column purification method.

could contribute to non-specific interactions with the Ni-NTA agarose beads. Therefore, a column purification approach was tested rather than the batch purification method. Briefly, the lysate was added to a column containing a 2mL bed volume of Ni-NTA agarose beads. The column was washed with 200 mL of wash buffer (50mM Tris pH7.5, 0.5M NaCl and 15mM imidazole) and NT11 was eluted with elution buffer (50mM Tris pH7.5, 150mM NaCl and 300mM imidazole) whereby 15, 1mL fractions were collected. However, this did not eliminate the contaminants, including the prominent bands at 80kDa and 24kDa, that co-eluted with NT11 (Figure 28 Coomassie-stained gel lanes 11 and 12). Moreover, I collected much less NT11 and more bacterial contaminants in our final product compared to previous NT11 purification preps as suggested by the Coomassie-stained gel (Figure 28 lanes 11 and 12) and western blot (Figure 28 lanes 11 and 12). This could suggest that it might be important to significantly reduce the number of beads used. Additionally, this could suggest that the contaminants are strongly bound

to NT11 rather than non-specifically binding to the Ni-NTA agarose beads. Alternatively, the contaminants could be binding to the Ni-NTA agarose beads due to the extremely low yield of soluble NT11. Based on these data, I next focused on our method of sonication in order to increase the amount of soluble protein. As demonstrated in the western blot in Figure 28 lane 6, NT11 has largely remained in the pellet throughout all purification preps of our protein thus far.

### **3.2.5 Optimizing Sonication Methods to Extract NT11 from the Pellet**

We observed that often our protein lysate remained viscous after initial sonication and required numerous additional rounds of sonication, without increasing the yield of NT11 in the soluble fraction. Therefore, instead of using the Sonics Vibra-Cell VC 50 Ultrasonic Homogenizer (19308C, Sonics & Materials Inc. Danbury, CT, USA) in the 4°C room (20 times for 30 seconds each at 45° amplitude) with a small probe (CV 18 Generator Probe), I used the Branson 450 Digital Sonifier (B450, Branson Ultrasonics™, Danbury, CT, USA) at RT (3 minutes ON for 1 second ON and 3s OFF at 30° amplitude) with a Step ½” tapped-end disruptor horn (101-147-037R, Branson Ultrasonics™, Danbury, CT, USA). With this alternative sonication machine, I was able to achieve a total protein yield of 27.5mg per 1L of bacterial culture compared to our average yield of 3mg per 1L of bacterial culture that has been acquired with our current NT11 protocol. However, a very important factor to note is that while the alternative sonication machine was able to more soluble protein from the supernatant, NT11 predominantly remained in the pellet, regardless of the sonication machine and protocol modifications I have made. Proteins that remain in the pellet after sonication of the lysate are often insoluble proteins. Therefore, I next focused on methods of improving protein solubility in order to increase the amount of soluble NT11 in the supernatant.

### **3.2.6 Lowering Induction Temperatures and Incorporating Various Detergents/ Additives to Increase Protein Solubility**

When the claudin binding sequence of C-CPE was replaced with the sequence of the second extracellular loop (EL2) of mouse Claudin-11 to create NT11, our protein peptide became highly insoluble. An NT solubility tag which is the N-terminal domain of Spidroin protein was added by Dr. Enrique Gamero-Estevez as a measure to improve NT11’s solubility. While this did improve the yield of soluble NT11, large quantities of bacterial culture were

needed to obtain sufficient quantities of purified NT11 for use in biological systems. To enhance the yield of NT11, I altered induction temperatures and modified the buffer components in an attempt to improve NT11's solubility and decrease the amount of protein that remained in the insoluble pellet after centrifugation.

Several reports suggest that using a lower induction temperature between 16°C and 20°C can improve solubility of bacterially-expressed proteins (Farshdari et al., 2020; Niiranen et al., 2007; Peti & Page, 2007; San-Miguel et al., 2013; Vera et al., 2007). Some even suggest that performing the induction step between 6°C and 10°C further improves solubility (J. M. Song et al., 2012). Therefore, to improve solubility of NT11, the incubation temperature was reduced to 16°C following the addition of 0.2mM IPTG at an  $OD_{600} = 0.450$ . However, comparison of the soluble (Figure 29A lanes 6, 8, 10, and 12) and insoluble (Figure 29A lanes 7, 9, 11, and 13) fractions on a Coomassie-stained denaturing polyacrylamide gel and by western blot analysis revealed that the lower induction temperature did not improve the solubility of NT11 (Figure 29A lanes 6, 8, 10, and 12).

The addition of various detergents and additives to the lysis buffer is also known to increase the solubility of a protein. More specifically, glycerol, Triton X-100 and DMSO are known to increase solubility of insoluble proteins when lysing the bacterial cell pellets. Therefore, I conducted a solubility test by adding either 10% glycerol, 1% Triton X-100 and/ or 10% DMSO in the resuspension buffer with 0.2mg/mL of lysozyme. When comparing the soluble (Figure 29A lanes 6, 8, 10, and 12) and insoluble fractions (Figure 29A lanes 7, 9, 11, and 13) on a Coomassie-stained denaturing polyacrylamide gel and by western blot, it seems that 10% glycerol and 1% Triton did slightly improve the solubility of NT11 (Figure 29A lane 10), as there appeared to be increased NT11 in the soluble fraction (Figure 29A lane 10) as compared to the soluble fraction that was resuspended solely with resuspension buffer and lysozyme (Figure 29A lane 6). However, the majority of NT11 remained in the insoluble pellet fraction (Figure 29A lanes 7, 9, 11, and 13). Another team of researchers suggested that adding glycylglycine in the range of 100 mM to 1 M enhanced solubility of insoluble proteins recovered from inclusion bodies (Ghosh et al., 2004). However, adding 300 mM glycylglycine did not improve NT11 solubility (Figure 29B lanes 6, 8, and 10 compared to Figure 29B lanes 7, 9, and 11). Therefore, these data suggest that NT11's solubility could not be increased or improved through the manipulation of induction conditions or buffer additives. Consequently, I shifted my focus

towards improving NT11 induction with the goal of producing larger quantities to obtain more fractions of the minimal soluble NT11.

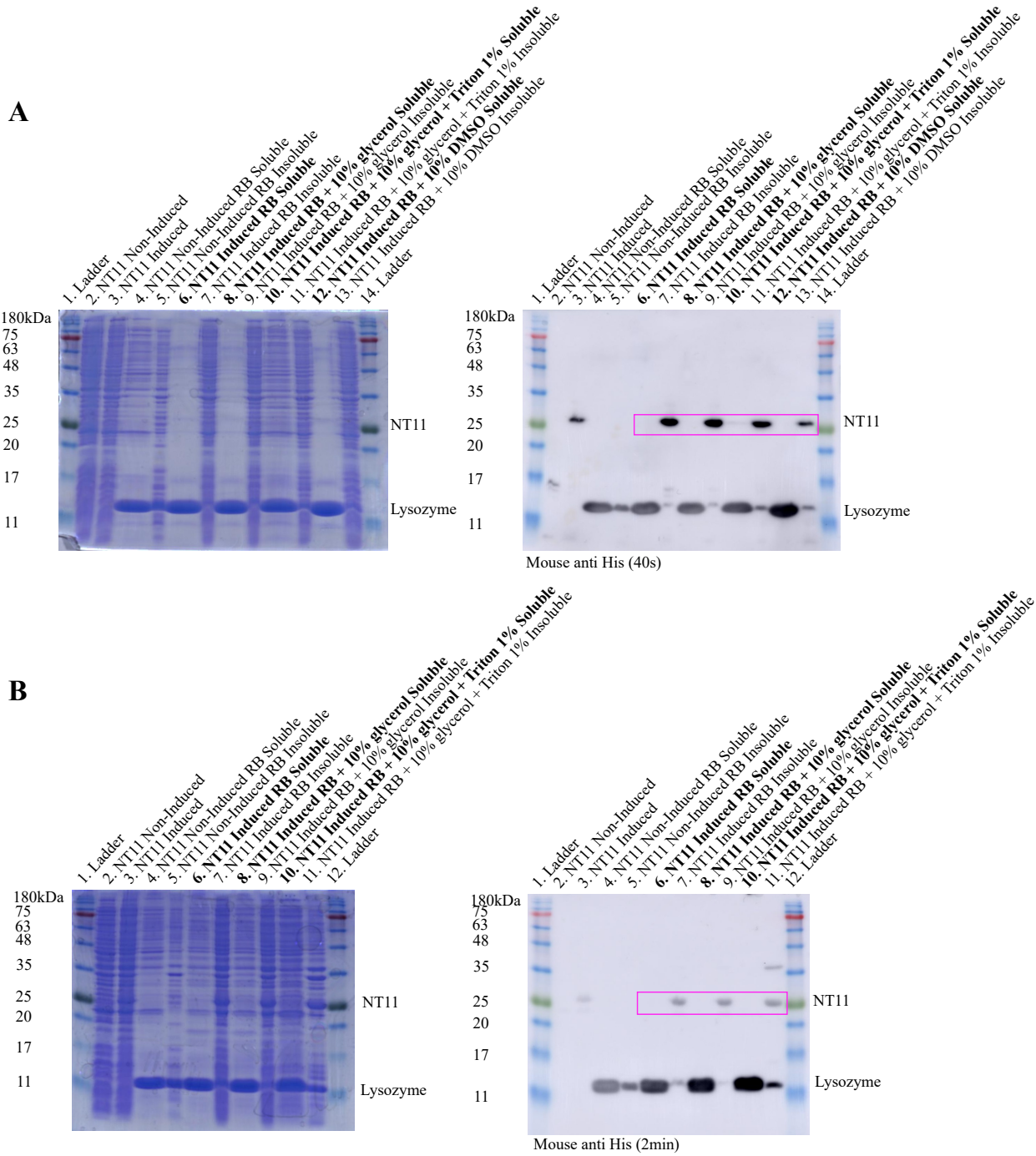


**Figure 29: Solubility test on NT11 induced at lower temperature or with additives, resuspended with various detergents. A. SDS-PAGE gel stained with Coomassie blue and**

western blot of solubility test for NT11 that was induced at 16°C. NT11 pellets are treated with either 10% glycerol, 1% Triton X-100 or 10% DMSO in resuspension buffer with 0.2mg/mL of lysozyme before spinning down and collecting soluble and insoluble fractions. The pink box outlines NT11 or no NT11 in each sample. **B.** SDS-PAGE gel stained with Coomassie blue and western blot of NT11 induced with 300mM of glycyglycine. Similarly, NT11 pellets are treated with either 10% glycerol, 1% Triton X-100 or 10% DMSO in resuspension buffer with 0.2mg/mL of lysozyme before spinning down and collecting soluble and insoluble fractions. Similarly, the pink box outlines NT11 or no NT11 in each sample.

### **3.2.7 Adjustments to Culture Conditions to Improve Induction of NT11**

Although NT11 is highly insoluble, I have been able to recover some soluble NT11 by greatly increasing the amount of induced bacterial culture at the start of the purification process. As an alternate approach I decided to determine if improving the induction conditions would yield more soluble protein at the end of the protocol. Several changes were made to the culture conditions. First, the bacterial culture media was changed from LB to the richer TB that is known to produce a higher yield of recombinant protein. TB includes glycerol as an energy source with more tryptone and yeast extract, leading to faster growth and higher yield of bacteria per volume. I also used a baffled Erlenmeyer flasks, which improves aeration leading to improved bacterial growth. The NT11 induction yield was compared between the standard cultured conditions (400mL LB culture in 2L Erlenmeyer flask induced with 0.2mM IPTG at  $OD_{600} = 0.450$ ) and “modified” conditions (1L TB culture in 2L baffled Erlenmeyer flask induced with 0.2mM IPTG at  $OD_{600} = 0.850$ ). No improvement in the induction of NT11 was observed.

Next, I tested different if varying the amount of IPTG used for protein induction would affect the yield of NT11. 50mL TB bacterial cultures were induced at room temperature with 0.2mM, 0.4mM, 0.8mM, 1.0mM IPTG at an  $OD_{600}$  of 0.450, respectively. Samples were taken at 3 hours and 16 hours after induction. The samples were analyzed by Coomassie staining and western blot analysis of a denaturing polyacrylamide gel (Figure 30A). Induction with 0.8 (Figure 30A western blot lane 6) and 1.0mM IPTG (Figure 30A western blot lane 7) generated the most NT11 at 3 hours and 0.6mM IPTG (Figure 30A western blot lane 11) generated the most NT11 16 hours post-induction at RT (Figure 30A). A previous report suggests that adding 3% ethanol to the media when inoculating the culture can help with induction (Chhetri et al.,

2015). This was tested by adding 3% ethanol to a 50mL LB bacterial culture when inoculating and inducing at RT with 0.2mM IPTG at an OD<sub>600</sub> of 0.450. However, when comparing the amount of NT11 induced with 0.2mM IPTG in the absence of 3% ethanol 16 hours post-induction (Figure 30A western blot lane 9) with that of the 0.2mM IPTG in the presence of 3% ethanol 16 hours post-induction (Figure 30A western blot lane 15), the 3% ethanol in culture media did not improve NT11 induction (Figure 30A).

Lastly, to improve NT11 protein induction and solubility, ZYP auto-induction media was used (Studier, 2005). For this experiment, 50mL of an overnight bacterial culture in ZYP 0.8G which was used to inoculate 500mL of ZYP-5052. At hour 0, the bacterial culture had an OD<sub>600</sub> of 0.5 and after 26 hours, the final OD<sub>600</sub> was measured to be 14.60. This produced a 6.95g bacterial cell pellet. Additionally, the maximum induced pellet weight for a 1ml aliquot at 26 hours was 0.03g. Thus, using auto-induction media, I was able to reach a much higher OD compared to LB or TB media. Comparison of NT11 induction at every hour and at 26 hours, revealed significantly more NT11 protein expression compared to LB or TB bacterial cultures in which IPTG was used to induce protein expression (Figure 30B western blot lane 11). However, NT11 induction using auto-induction media optimized protein induction, NT11 solubility did not improve. A solubility test using 10% glycerol and 1% Triton in resuspension buffer with 0.2mg/mL of lysozyme was done on hours 0, 4, 8, 12, 22, and 26, whereby no NT11 could be detected in the soluble fractions (Figure 30C western blot lane 6, 8, 10, and 12). Therefore, I was able to improve NT11 induction but not solubility despite various methods explored.

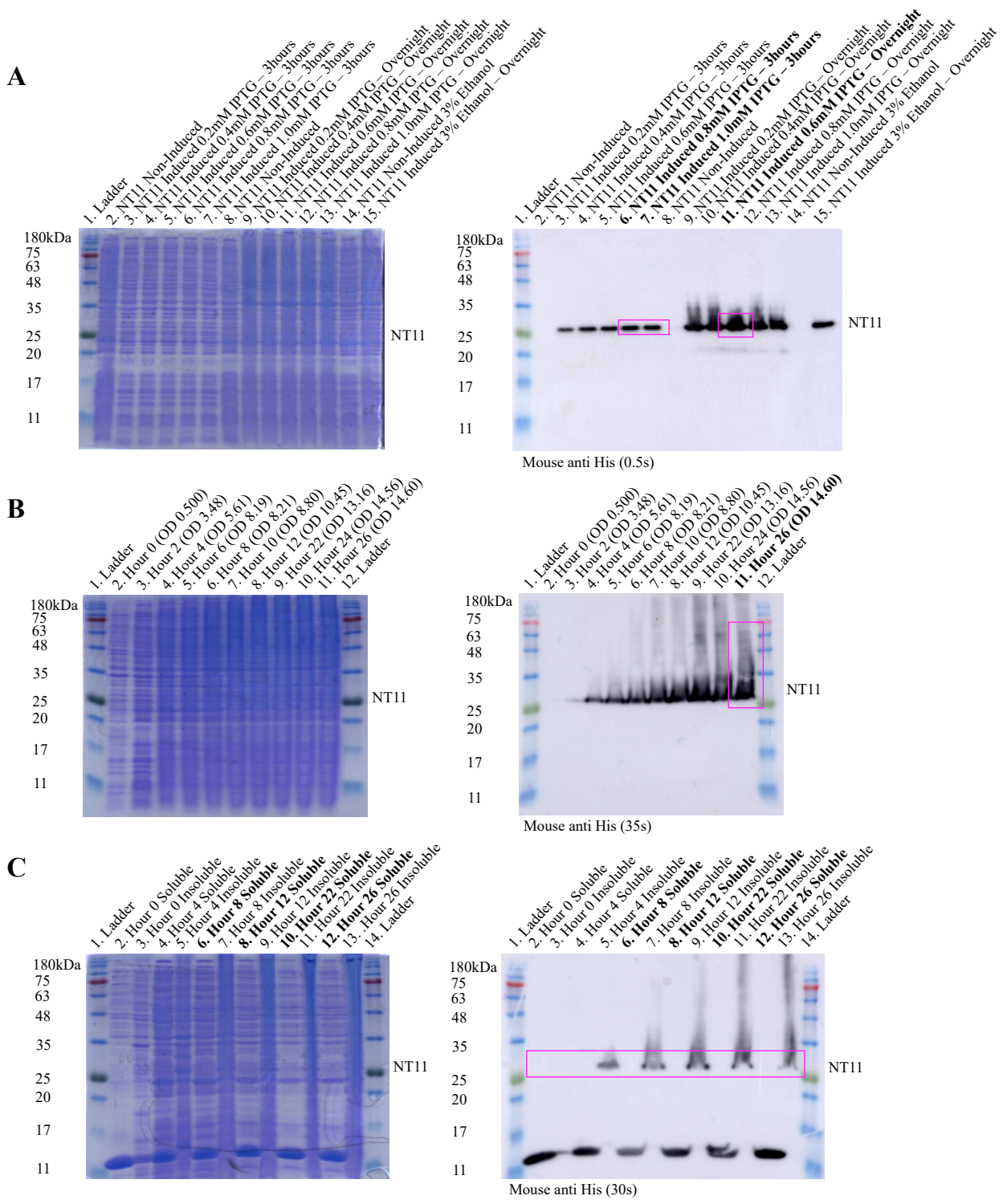


**Figure 30: Assessing NT11 induction and soluble fractions from testing IPTG concentrations and auto-induction media. A.** SDS-PAGE gel stained with Coomassie blue and western blot of NT11 induced at different IPTG concentrations and induction at 0.2mM IPTG

with 3% ethanol at the time of inoculation. The pink boxes outline the concentrations that generated the most NT11. **B.** SDS-PAGE gel stained with Coomassie blue and western blot of NT11 induced with auto induction media with each lane containing samples from different time points, beginning at the time of inoculation until hour 26. The pink box outlines the sample containing the most amount of induced NT11. **C.** SDS-PAGE gel stained with Coomassie blue and western blot of solubility test on NT11 that was induced with auto induction media using 10% glycerol and 1% Triton in resuspension buffer with 0.2mg/mL of lysozyme. The pink box outlines NT11 or no NT11 in each sample.

### **3.2.8 Summary of Results from Aim 2**

The goal of this aim was to optimize purity, solubility and induction of NT11. In order to enhance purity, many different techniques were employed: size exclusion chromatography, using Amicon Ultra Centrifugal Filters, adjusting buffer components and the duration of incubation of the supernatant and Ni-NTA agarose beads. For size exclusion chromatography with Sephadex G-75, the bacterial contaminants eluted along with NT11, and I was not able to recover our protein after a second round of his-tag purification. Similarly, using the 50kDa MWCO Amicon filter did not separate the 29.8 kDa NT11 from the 80kDa or 24kDa bacterial contaminant. Finally, the buffers used during the purification process were adjusted by increasing imidazole and NaCl concentrations in addition to adding  $\beta$ -mercaptoethanol ( $\beta$ -ME) to the resuspension buffer. However, these adjustments decreased the yield of NT11 and did not improve the purity of the NT11 peptide. Finally, duration for which the supernatant and Ni-NTA agarose beads were in contact was adjusted by introducing the supernatant to a column containing the beads and allowing it to flow through rather than incubating the beads overnight with supernatant. This also did not improve the purity of NT11 as the contaminants at 80kDa and 24kDa remained. None of these modifications improved the purity of NT11 over the initial protocol.

Several attempts were made to optimize the yield of NT11 by improving its solubility and increasing its induction. Although using the Branson 450 Digital Sonifier with a Step ½” tapped-end disruptor horn led to a dramatic increase in total protein yield, NT11 predominantly remained in the pellet. Next, to improve NT11’s solubility the induction temperature was decreased, and several modifications were made to the resuspension buffer for lysis. However, Coomassie staining and western blot analysis of the soluble and insoluble fractions showed that

the lower temperature did not improve solubility of NT11. Further attempts to improve solubility by adding either 10% glycerol, 1% Triton X-100 and/or 10% DMSO to the resuspension buffer with 0.2mg/mL of lysozyme showed that although 10% glycerol and 1% Triton increased NT11 in the soluble fraction, the majority of NT11 remained in the insoluble fraction. Finally, addition of 300 mM glycylglycine to LB media did not improve NT11 solubility.

The last approach used to increase the overall amount of protein produced was to grow the bacterial cultures in 1L TB baffled Erlenmeyer flasks and induce with 0.2mM IPTG at an OD<sub>600</sub> of 0.850 rather than the standard growth and induction conditions of 800mL LB in Erlenmeyer flask and induction with 0.2mM IPTG an OD<sub>600</sub> of 0.450. However, this did not improve NT11 induction yield. Addition of 3% ethanol also did not improve NT11 induction. Conversely, IPTG induction with 0.8mM and 1.0mM IPTG generated the most NT11 after 3hours and 0.6mM IPTG generated the most NT11 after 16 hours of induction compared to the original 16 hour, 0.2mM IPTG. Additionally, although auto-induction media ZYP-5052 significantly increased NT11 induction yield compared to LB or TB bacterial cultures, NT11 solubility did not improve. Ultimately, I was able to considerably improve NT11 induction but not solubility. Various strategies to improve NT11 purity, solubility, and induction were explored, none of which led to a substantial improvement in the production of soluble NT11. Data from these experiments will contribute towards refining the current NT11 purification and induction protocol for the future productions of this recombinant protein.

## 4. Discussion

### 4.1 NT11 Mediated Claudin-11 Removal and Recovery in the Blood-Testis Barrier

Throughout my studies, I demonstrated that Claudin-11 localization was significantly decreased at the BTB in NT11 treated samples compared to control samples in both W/Wv and busulfan-treated 129/B6 mouse testis tubules cultured *ex vivo* in an air-liquid interface culture. Analysis of my data showed that NT11 takes approximately 16 hours to remove Claudin-11 from the BTB. Additionally, I demonstrated that NT11 will target removal of Claudin-11 from the BTB in a genetically infertile mouse model (W/Wv) as well as in a mouse model of induced infertility (busulfan-treated 129/B6 mice). These observations were further supported by statistical significance when comparing Pearson's correlation coefficient and integrated sum intensities in control vs NT11-treated testis tubules. Together, these data reaffirm that in the presence of NT11, Claudin-11 delocalized from the Sertoli cell tight junctions.

For future application of our peptide, it is important to know that NT11 removed Claudin-11 within 16 hours as it suggests that the NT11 injection procedure to allow more SSCs to migrate across the BTB during SSC transplantation may be more effective in a two-step injection. In mice, SSCs require approximately 7 days to colonize the stem cell niche after SSC transplantation (Brinster & Zimmermann, 1994; Kadam et al., 2018; Nagano, 2003; Zhao et al., 2021). Thus, the timing of the NT11 injection would be crucial to coordinate with the injection of the SSCs in order to effectively disrupt the BTB at the time point where SSCs would be migrating across this barrier to reach their niche on the basement membrane. This would require the injection of NT11 and SSCs to occur at 2 different time points. This information will be important in planning a treatment regime in order to maximize the percentage of SSCs that will regenerate spermatogenesis post transplantation with an injection directly in the rete testis.

Following the removal of Claudin-11 from the BTB, there was a gradual restoration of Claudin-11 to the BTB in W/Wv mouse between 24 and 72 hours after NT11 treatment. My data suggest that at 24 hours after the removal of NT11 from the media, Sertoli cells have recognized the depletion of Claudin-11 and have initiated cell signaling mechanisms to restore protein levels. Consequently, by 48 hours, Claudin-11 begins replenishing the tight junctions, and this process continues gradually up to 72 hours. Pearson's correlation coefficient and integrated sum intensities analyses demonstrated that the most significant difference was observed between 24 hours and 48 hours, during which the majority of Claudin-11 recovered to the tight junction. By

48 hours after NT11 removal of NT11 from the media, the localization and intensity of Claudin-11 was approaching the levels observed in the control. Then, Claudin-11 localization slightly increased at 72 hours, similar to that of the control, indicating that Claudin-11 had returned to its original state. Most notably, these data suggest that NT11 was able to disrupt that BTB in a reversible manner such that Claudin-11 repopulated the tight junctions upon NT11 removal.

The BTB provides a separation which creates distinct microenvironments optimized for the different stages of germ cell development (Matsumoto & Bremner, 2016; Sourdain et al., 2018). Thus, an intact BTB is essential to maintain the basal stem cell niche (de Kretser et al., 2016; Takashima et al., 2011) and the process of spermatogenesis (Mazaud-Guittot et al., 2010). Consequently, the discovery that the NT11 peptide disrupted Claudin-11 localization to the BTB in a reversible manner supports further evaluation of this peptide in SSC transplantation because the BTB can be re-established upon SSC migration into the basal compartment, providing the appropriate SSC niche needed for spermatogenesis. This peptide could effectively be used to transiently disrupt the BTB and improve SSC transplantation.

Therefore, the broader implications of these results suggest that NT11 could be used in context of patients who are looking to restore their fertility post cancer treatment. In these cases, SSCs can be collected before therapy, stored frozen and transplanted back to the patient in the rete testis along with a timing-focused NT11 injection that will transiently disrupt the BTB. NT11 will act to temporarily disrupt the tight junctions, allowing more SSCs to engraft and appropriately reach their niche on the basement membrane. By validating the effects of NT11, my research establishes a foundation for defining effective peptides that disrupt the mouse BTB and encourages further investigation in the development of peptides with the ability to disrupt cellular barriers for potential use in drug delivery. However, moving forward, it will be important to optimize NT11 purity, solubility, and induction.

## **4.2 Optimization of NT11 Purification, Solubility and Induction**

Protein purification is an intricate process that requires the optimization of a series of steps designed to isolate the protein of interest. In the original design of NT11, Dr. Enrique Gamero-Estevez optimized the purification protocol with a focus on detergents and incorporation of a NT solubility tag to the fusion peptide. He explored various strategies such as incorporating different lysis buffers (Octyl-glucoside and CHAPS) with varying Sarkosyl concentrations,

denaturing purification with 8M urea, and adding Thioredoxin (TRX) to the C-terminal domain creating C-CPEACBD::Cldn11EL2::TRX::His but ultimately found that His::NT::C-CPEACBD::Cldn11EL2 generated the highest yield of soluble protein using the current NT11 protocol. However, despite these modifications the yield of soluble His-tagged NT11 was still low and contains several bacterial contaminants, including large amounts of 80kDa and 24kDa proteins. Attempts to remove these contaminants and increase the yield of soluble NT11 using size exclusion chromatography, Amicon Ultra Centrifugal Filters, adjusting buffer composition, or modifying protein induction and/or culture conditions were unsuccessful.

Although our SEC did not improve NT11 purification, changing the gel from a Dextran gel to a Polyacrylamide gel could be beneficial for future exploration. Bio-Gel P-30 and Bio-Gel P-60 have an upper limit of 40kDa and 60kDa, respectively. These polyacrylamide gels could potentially separate the contaminants from NT11 with the aid of pump that delivers the supernatant through the column at a controlled flow rate. In our experiments, the supernatant containing our protein was eluted by the force of gravity which could have contributed to the over diffusion of proteins across the pores caused by the slow flow rate (Ó'Fágáin et al., 2016). A pump could resolve this issue and provide an efficient manner to separate NT11 from its contaminant at 80kDa if used with Bio-Gel P-30 or Bio-Gel P-60. Additionally, when I adjusted our buffer composition or used a column purification method, these manipulations decreased the yield of NT11 and did not improve purity. These results suggest that the contaminants at 80kDa and 24kDa are either bound to NT11 directly or the extremely low NT11 yield leads to the accumulations of proteins bound to the Ni-NTA agarose beads. These contaminants could be common IMAC contaminants or chaperons bound to regions where the polypeptide chain is exposed/ unfolded (Morales et al., 2019). Therefore, future experiments identifying these contaminants would enable us to better identify measures of purification that will separate our protein of interest from its surrounding contaminants.

To address NT11's insolubility, I reduced induction temperatures, incorporated various additives into the resuspension buffer for lysis, and induced NT11 using auto-induction media. In performing solubility tests, 10% glycerol and 1% Triton were able to increase the amount of NT11 in the soluble fractions; nonetheless, the majority of NT11 remained in the pellet. These results suggest that while glycerol and Triton X-100 were able to decrease protein aggregation and disrupt hydrophobic interactions, NT11 is still largely insoluble. Results from our

glycylglycine-mediated enhanced solubilization experiment likely suggest that there are already chaperones that are currently helping the protein folding of NT11; thus, the addition of glycylglycine did not further promote this activity. When the sequence of the claudin binding domain of C-CPE (amino acids 290 – 319) was replaced with the EL2 sequence of mouse Claudin-11 to create NT11, the fusion peptide became highly insoluble. NT-CCPE was generated as a control to compare solubility, whereby NT-CCPE was highly soluble. Thus, the specific change that made our peptide insoluble is the sequence replacement of the claudin binding domain with the Claudin-11 EL2.

There are many reasons a protein could be insoluble, including misfolding and aggregation, hydrophobicity, overexpression, toxicity, inclusion body formation and non-optimal cellular environments (Bhatwa et al., 2021; Carratalá et al., 2021; Kramer et al., 2012; Pace et al., 2004; Sadeghian-Rizi et al., 2019; Sørensen & Mortensen, 2005; Trimpin & Brizzard, 2009; Vihinen, 2020; Wingfield, 2015). Misfolding and aggregation can occur due to incorrect folding environment, lack of chaperones, or inherent structural instability which can lead to the formation of insoluble aggregates (Bhatwa et al., 2021; Trimpin & Brizzard, 2009). Moreover, proteins with hydrophobic regions can aggregate and form insoluble structures. However, when comparing the specific amino acids from the claudin binding sequence of C-CPE (42.86% hydrophobic amino acids) to the EL2 of mouse Claudin-11 sequence (35.71% hydrophobic amino acids), the replaced sequence is in fact less hydrophobic (Table 4).

Comparing hydrophobicity of amino acids from exchanged sequences		
	Hydrophobic	Hydrophilic
C-CPE claudin binding domain from NT-CCPE	LDAGQYVLVMKANSSYSGNYPYILFQKF	
Mouse Claudin-11 EL2 from NT11	HREITIVSFGYSLY	

**Table 4: Comparing hydrophobicity of amino acids from exchanged sequences.** Amino acid sequences of the C-CPE claudin binding domain from NT-C-CPE and the second extracellular loop (EL2) of mouse Claudin-11.

Another cause for protein insolubility is overexpression of a protein which can overwhelm the cellular processes responsible for folding and solubility, resulting in the accumulation of insoluble aggregates. Proteins that are overexpressed or misfolded will become insoluble and inactive protein aggregates, forming inclusion bodies (Carratalá et al., 2021;

Palmer & Wingfield, 2012; Wingfield et al., 2014). However, as shown on the Coomassie-stained SDS-PAGE gels, NT11 induction is rather minimal; thus, suggesting that overexpression is likely not the cause for its insolubility. On the other hand, some proteins are inherently toxic to the host, triggering stress responses that lead to insoluble aggregate formation. In the case of NT11, our transformed *E. coli* BL21 (DE3) cells grow in a healthy and stable manner; thus, it is likely not toxic for the host and not the cause for its insolubility. Last but not least, pH, temperature, salt concentration and denaturing agents can affect protein solubility and stability (Pelegri & Gasparetto, 2005). In the case of NT11, the peptide's insolubility was caused by replacing the sequence of the claudin binding domain of C-CPE with the sequence of the EL2 of mouse Claudin-11. Therefore, this sudden change in solubility suggests that the claudin binding domain plays a crucial role in the solubility of C-CPE as suggested by other researchers (Van Itallie et al., 2008).

Various hypotheses for NT11's insolubility can be made by understanding the structure of C-CPE and the relevance of the claudin binding domain. Van Itallie and colleagues did a structural analysis on a smaller fragment of C-CPE containing amino acid residues 194-319 (Van Itallie et al., 2008). C-CPE (aa 194-319) forms a nine-strand  $\beta$  sandwich with a short helical element between strands  $\beta$ 1 and  $\beta$ 2 (Kitadokoro et al., 2011) (Figure 31). Adjacent strands within each sheet have antiparallel orientations except for the parallel alignment of strands  $\beta$ 1 and  $\beta$ 3 (Van Itallie et al., 2008). The claudin-binding region corresponds to the  $\beta$ 8 and  $\beta$ 9 strands, each positioned in the center of the opposing  $\beta$  sheets (Figure 31). Notably, Van Itallie highlights that given the central position of strands  $\beta$ 8 and  $\beta$ 9, the manipulation of these strands may severely destabilize the overall structure of this protein (Van Itallie et al., 2008). When creating NT11, the sequence that corresponds to strand  $\beta$ 8 and  $\beta$ 9 were replaced with the sequence EL2 of mouse Claudin-11 (Table 5).

Construct	Amino Acid Sequence
<b>Legend</b>	<ul style="list-style-type: none"> <li>• His Tag</li> <li>• Restriction site NdeI (CATATG)</li> <li>• N-Terminal domain of Spidroin Protein (Solubility tag)</li> <li>• Linker including restriction site Age I (ACCGGT)</li> <li>• Cleavage site (TEV)</li> <li>• C-CPE185-290</li> <li>• Mouse Claudin-11 EL2</li> <li>• <u><math>\beta</math>-sheet 8</u></li> <li>• <u><math>\beta</math>-sheet 9</u></li> </ul>
<b>C-CPE</b>	MSTDIEKEILDAAATERLNLTDALNSNPAGNLYDWRSSN SYPWTQKLNHLTITATGQKYRILASKIVDFNIYSNNFNLL VKLEQSLGDGVKDHVVDISLDAGQYVLVMKANSSYSGN YPYSILFQKFGVLVPR
<b>C-CPE Claudin Binding Domain</b>	LDAGQYVLVMKANSSYSGNYPYSILFQKFGVLVPR
<b>NT-CCPE</b>	MGHHHHHHMSHTTPWTNPGLAENFMNSFMQGLSSMPGF TASQLDKMSTIAQSMVQSIQSLAAQGRTSPNDLQALNMA FASSMAEIAASEEGGSLSTKTSSIASAMSNAFLQTTGVVN QPFINEITQLVSMFAQAGMNDVSAGTGENLYFQGRCVLTV PSTDIEKEILDAAATERLNLTDALNSNPAGNLYDWRSSNS YPWTQKLNHLTITATGQKYRILASKIVDFNIYSNNFNLLV KLEQSLGDGVKDHVVDISLDAGQYVLVMKANSSYSGNY PYSILFQKF
<b>NT-CCPE Truncated</b>	MGHHHHHHMSHTTPWTNPGLAENFMNSFMQGLSSMPGF TASQLDKMSTIAQSMVQSIQSLAAQGRTSPNDLQALNMA FASSMAEIAASEEGGSLSTKTSSIASAMSNAFLQTTGVVN QPFINEITQLVSMFAQAGMNDVSAGTGENLYFQGRCVLTV PSTDIEKEILDAAATERLNLTDALNSNPAGNLYDWRSSNS YPWTQKLNHLTITATGQKYRILASKIVDFNIYSNNFNLLV KLEQSLGDGVKDHVVDIS
<b>Mouse Claudin-11 EL2</b>	CAHREITIVSFGYSLY
<b>NT11</b>	MGHHHHHHMSHTTPWTNPGLAENFMNSFMQGLSSMPGF TASQLDKMSTIAQSMVQSIQSLAAQGRTSPNDLQALNMA FASSMAEIAASEEGGSLSTKTSSIASAMSNAFLQTTGVVN QPFINEITQLVSMFAQAGMNDVSAGTGENLYFQGRCVLTV PSTDIEKEILDAAATERLNLTDALNSNPAGNLYDWRSSNS YPWTQKLNHLTITATGQKYRILASKIVDFNIYSNNFNLLV KLEQSLGDGVKDHVVDISSHREITIVSFGYSLY

**Table 5: Amino acid sequences of different constructs and domains.** NT11 was created by adding the mouse Claudin-11 EL2 sequence, replacing the claudin binding domain of C-CPE which correspond to  $\beta$  sheets 8 and 9.

As a result, it is possible that manipulating these strands specifically destabilized the C-CPE portion of NT11, rendering NT11 a highly insoluble protein that is likely to be trapped in inclusion bodies. Various methods have been proposed in research to extract proteins from inclusion bodies, including denaturing purification using guanidine HCl (Wingfield et al., 2014). Notably, a protein folded from insoluble inclusion bodies will have the same structural and conformational integrity as the same protein directly purified from soluble extracts (Anfinsen, 1973; Palmer & Wingfield, 2012; Tsumoto et al., 2003). However, when Dr. Enrique Gamero-Estevez performed denaturing purification with urea, he found that the protein precipitated upon dialysis and changing the dialysis buffer did not prevent precipitation nor increase the recovery of folded soluble protein. In Studier's method of induction using auto-induction media, the slow production and natural conversion of  $\alpha$ -lactose to allolactose, promotes protein folding and solubility (Studier, 2005). However, NT11's solubility did not improve, further attesting to the peptide's instability likely caused by the manipulation of  $\beta$ 8 and  $\beta$ 9 centre strands.

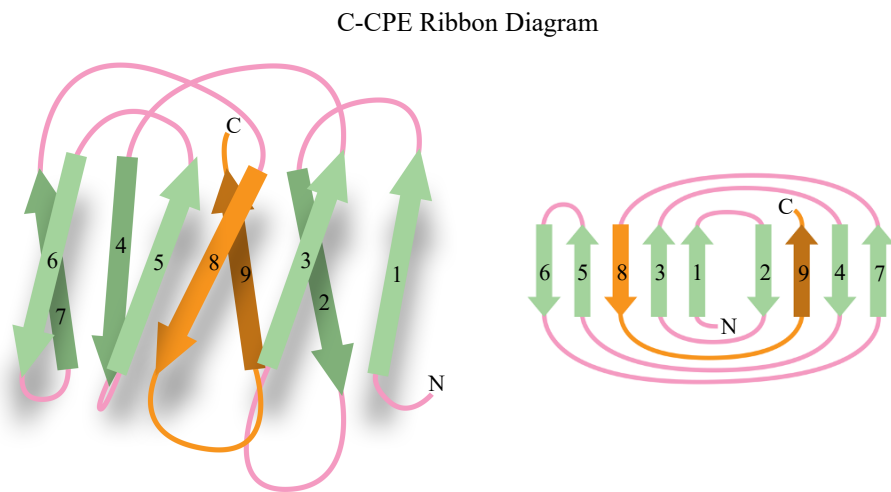


**Figure 31: Structural composition of C-CPE.** C-CPE (aa residues 194-319) forms a nine-strand  $\beta$  sandwich. The binding site for claudin is within the last 30 residues at the COOH-terminal (orange arrows and loop) that includes strands  $\beta$ 8 and  $\beta$ 9.  $\beta$  sheets 8 and 9 have a central position in the nine-strand  $\beta$  sandwich structure. Adapted from Van Itallie et al., 2008.

In summary, many challenges were faced during the optimization of NT11 purification, solubility, and induction. Despite attempts to optimize various purification methods, including

size exclusion chromatography and Amicon centrifugal filters, I was not able to isolate NT11 from the bacterial contaminants. Additional strategies, such as adjusting buffers and contact duration, were explored, but the contaminants remained together with NT11 which posed a significant challenge. The insolubility of NT11 further complicated the purification process, leading to further investigations in solubility and induction conditions. However, despite efforts to improve solubility including reduced induction temperatures, various buffer additives, adding glycylglycine and previous denaturing purification and addition of Thioredoxin (TRX), NT11 remained largely insoluble. NT11 became insoluble when the claudin binding domain of C-CPE was replaced with the EL2 sequence of mouse Claudin-11. The manipulation of the  $\beta$ 8 and  $\beta$ 9 centre strands likely caused NT11 to become unstable. Therefore, it will be important investigate potential methods of increasing NT11 stability to increase solubility. Finally, induction conditions were optimized by changing IPTG concentrations and using auto-induction media to improve the yield and recovery of our protein. My study contributes towards refining the current NT11 purification protocol and more generally, the troubleshooting of protein purification, induction, and solubility of insoluble proteins.

### **4.3 Limitations of Study**

My study successfully demonstrates the effects of NT11 on Claudin-11 protein localization within the BTB. However, there are some limitations that still need to be addressed. Firstly, the *ex vivo* nature of our experiments may not fully replicate the *in vivo* microenvironment and physiological conditions experienced by the testis tubules. Thus, although I have observed positive effects in our *ex vivo* culture of testis tissue, NT11's effects on Claudin-11 may be different in an *in vivo* setting. Thus, future experiments would include mouse *in vivo* studies to investigate the effects of NT11 locally injected into the rete testis on mouse BTB. In my study, I evaluated the effects of NT11 up to 72 hours post a 16-hour NT11 treatment; however, there could potentially be long-term consequences of BTB disruption. Therefore, conducting a longitudinal study over an extended period of time to observe the changes experienced in the testis tubules following NT11 treatment would be interesting. This could be a longitudinal study on mouse testis for the duration of a single cycle of spermatogenesis (34.5 days) post NT11 injection. This would provide information if there were any long-term consequences of BTB disruption. Furthermore, while I assessed the effects of NT11 by

evaluating Claudin-11 localization, it would also be valuable to perform functional assays, such as trans-epithelial electrical resistance (TEER) measurements, to assess the impact of NT11 on BTB integrity. This data would suggest whether Claudin-11 removal is sufficient for BTB disruption. Additionally, another limitation of the study is that I solely quantified NT11's effect on Claudin-11; therefore, it is important to investigate if NT11 has any potentially undesirable effects on other crucial proteins in the BTB. This could be done by visualizing with immunofluorescence the localization of other claudins/ tight junction membrane proteins localized to the BTB after NT11 treatment such as Claudin-3 or Occludin.

Optimizing the purity, solubility, and induction of NT11 will be crucial for its clinical utility. Despite efforts to purify NT11 using various methods such as size exclusion chromatography and adjusting buffer conditions, the bacterial contaminants around 80kDa and 24kDa remained with NT11. This limitation emphasizes the need for alternative purification techniques or further optimization of existing methods to effectively isolate NT11 from its contaminants. Moreover, solubility did not improve despite various strategies such as including buffer additives or inducing at lower temperatures. This limitation highlights the need for a new approach such as modifying our current peptide or creating a new version of our peptide to increase the solubility of the unstable protein. Last but not least, I was unable to definitively assess the impact of NT11 alone on the BTB due to the inability to isolate it from bacterial contaminants. Consequently, the observed effects could have been influenced by the presence of these contaminants. This could have contributed to the long incubation time required for NT11 to exert its effect on Claudin-11 compared to the relatively short time (3-5hours) for C-CPE to remove Claudin 3 and 4 from the tight junctions of chick embryo epithelia (Baumholtz et al., 2017). Very minimal amount of the protein being added is actually NT11; thus, the relative dose is much less.

Addressing these limitations in future studies could strengthen our results and further support our findings on NT11-mediated Claudin-11 targeting in BTB disruption. Additionally, investigating the underlying factors influencing NT11's purity and solubility will contribute to the development of peptides with the ability to disrupt cellular barriers.

## **5. Conclusions and Future Directions**

### **5.1 Final Conclusion**

My data demonstrates that NT11 effectively removes Claudin-11 from the BTB of *ex vivo* cultured mouse testis tubules. I observed a significant decrease in Claudin-11 signal localization at the BTB in NT11-treated W/W<sup>v</sup> and busulfan-treated 129/B6 testis samples compared to controls within 16 hours. These experiments highlight NT11's efficacy in targeting Claudin-11 in genetically and induced infertile mouse models. Following the depletion of Claudin-11 from the BTB, a gradual restoration of Claudin-11 was observed over 72 hours following removal of NT11 from the culture medium. Quantitative analysis, including Pearson's correlation coefficient and integrated sum intensities of Claudin-11 over ZO-1, further confirmed the reproducibility and reliability of NT11 in reversibly disrupting the BTB by targeting Claudin-11. These data support the use of NT11 to transiently open the BTB to promote SSC homing in patients seeking fertility restoration post-cancer treatment.

Moving forward, the optimization of NT11 purity, solubility, and induction will be crucial for translating these findings into clinical applications. The troubleshooting that I performed did not improve the yield, solubility or purity of our anti-claudin peptide NT11. Beyond addressing the limitations in purification of the NT11 fusion protein through increasing protein stability, it may be important to consider redesigning the fusion protein so as not to disrupt the beta-sheet sandwich structure. Ultimately, my study contributes towards NT11's therapeutic potential in promoting SSC homing and research on optimization of peptides capable of disrupting cellular barriers.

### **5.2 Optimizing NT11 Stability and BTB Disruption**

To increase NT11 solubility, it will be important to investigate methods of increasing peptide stability and correct folding. One way we can potentially stabilize our protein is the addition of a protein tag on both ends. Currently, NT11 has a His-tag on the N-terminal domain; however, adding tags such as MBP or small ubiquitin related modifier (SUMO) to the C-terminal domain in addition to the His-tag can aid with stabilizing the protein as these larger protein tags fold rapidly (Butt et al., 2005; Costa et al., 2014; Marblestone et al., 2006). The rapid folding of the attached protein tags can drive the folding of NT11, aiding in the solubility and stability of

our peptide while preventing its aggregation in inclusion bodies (Ghosh et al., 2004). Thus, the new construct could be potentially designed as: His::NT::C-CPE::Cldn1 1EL2::SUMO.

Another well-studied method for stabilizing proteins and increasing solubility is the co-production of molecular chaperones and folding modulators along with the target protein (Costa et al., 2014). Initial folding of NT11 can be assisted by molecular chaperones that prevent protein aggregation through binding to the partially folded or misfolded peptide (Ghosh et al., 2004). A low concentration of folding modulators in the cell can improve soluble protein production when co-produced to prevent folding failures (Baneyx & Palumbo, 2003; Gasser et al., 2008; Hoffmann & Rinas, 2004; Kolaj et al., 2009; Schlieker et al., 2002; Thomas et al., 1997). Chaperones such as DnaK and GroEL are commonly co-expressed to assist protein folding and formation of correct tertiary structures (De Marco et al., 2007; De Marco & De Marco, 2004; Deuerling et al., 2003; Nishihara et al., 1998; Schlieker et al., 2002). A drawback to this method could be that the contaminants I observed on the Coomassie-stained SDS-PAGE gel of the purified NT11 product are chaperones, especially the bands at 80kDa; thus, there are already many chaperones assisting with the folding of the soluble fraction of NT11. Therefore, it would be important to determine the identity of these contaminants that are eluting alongside our peptide.

If these described measures do not improve NT11's stability nor solubility, I propose alternative methods involving the use of C-CPE and claudins to transiently disrupt the BTB. The individual  $\beta$ -sheets in the 9-strand  $\beta$ -sandwich play an important role in the stability and proper folding of C-CPE. Thus, rather than completely replacing the claudin-binding domain, it could be interesting to investigate the specific changes in amino acid sequences on C-CPE to enhance its recognition of Claudin-11. C-CPE already recognizes Claudins-3, -4, -6, -7, -8, and -14. Moreover, various research studies have identified the important amino acids that interact between C-CPE and claudins, mainly Claudin-4 (Van Itallie et al., 2008; Kitadokoro et al., 2011; Sharafi et al., 2022; Vecchio et al., 2021; Veshnyakova et al., 2010). Therefore, changing the amino acid sequences one by one through mutagenesis could potentially create an alternate C-CPE that recognizes Claudin-11. This approach has been explored where researchers have created various C-CPE variants to recognize Claudins-1, -2, -3, -4 and -5 more specifically (Beier et al., 2019; Liao et al., 2016; Piontek et al., 2020; Protze et al., 2015; Walther et al., 2012; Winkler et al., 2009). A challenge to this approach is that Claudin-11 is a "non-classic"

claudin that exhibits more variability and differs from the “classic” amino acid sequence of claudins (Krause et al., 2008). Additionally, it has been noted that even a few changes in amino acids have rendered C-CPE insoluble; thus, this approach would be quite a challenge.

Another method for disrupting the BTB using our knowledge on claudins could be the development of a peptide with the sequence of Claudin-11 EL1 and EL2 and a tag: GST::Cldn11EL1::His::CldnEL2. This method is similar to the idea proposed by other researchers; however, it includes both the EL1 and the EL2 (Sauer et al., 2014; Shrestha et al., 2014; Takahashi et al., 2008; Taylor et al., 2021). This peptide could out compete the Claudin-11 trans-interactions and transiently disrupt the BTB although it may not affect the localization of claudins at the tight junction. Alternatively, I propose creating new versions of the NT11 peptide. A group of researchers created a soluble mutant of C-CPE known as C-CPE-Y306A/L315A (C-CPE-YL) that does not exhibit any claudin binding (Neuhaus et al., 2018; Protze et al., 2015; Waldow et al., 2023). We could attach the sequence of the mouse Claudin-11 EL2 to the C-terminal domain of C-CPE-YL such that it would recognize the EL2 of Claudin 11 and disrupt the BTB in a similar manner to our current peptide. Another possible design could be to replace the sequence between strand  $\beta$ 8 and  $\beta$ 9 of C-CPE (9aa) with the sequence for the mouse Claudin-11 EL2 (14aa) to create a new NT11. In this manner, the two ridged  $\beta$ -sheet structures would remain intact for proper protein folding while carrying the sequence that will recognize Claudin-11 in the BTB.

### **5.3 NT11 Treatment on Human Testis Biopsies**

Following the optimization of NT11 and BTB disruption using our current air-liquid interface culture system on an *ex vivo* culture of mouse testis tubules, we would expand upon these findings by exposing human testis biopsies to our peptide. This will likely require optimization of our current *ex vivo* culture system to better suit the survival of a human testis tissue piece. Additionally, while there are various research articles illustrating the role of Claudin-11 in human BTB, the rest of the claudin family members along with their function in the human testes are still largely unknown. Therefore, it would be interesting to further explore claudins in the human BTB through immunofluorescence and functional studies such that we can optimize the utility of our peptides.

## 6. References

- Ahmed, E. A., & de Rooij, D. G. (2009). Staging of Mouse Seminiferous Tubule Cross-Sections. In S. Keeney (Ed.), *Meiosis: Volume 2, Cytological Methods* (pp. 263–277). Humana Press. [https://doi.org/10.1007/978-1-60761-103-5\\_16](https://doi.org/10.1007/978-1-60761-103-5_16)
- Amann, R. P., & Howards, S. S. (1980). Daily spermatozoal production and epididymal spermatozoal reserves of the human male. *The Journal of Urology*, *124*(2), 211–215. [https://doi.org/10.1016/s0022-5347\(17\)55377-x](https://doi.org/10.1016/s0022-5347(17)55377-x)
- Anfinsen, C. B. (1973). Principles that Govern the Folding of Protein Chains. *Science*, *181*(4096), 223–230. <https://doi.org/10.1126/science.181.4096.223>
- Avarbock, M. R., Brinster, C. J., & Brinster, R. L. (1996). Reconstitution of spermatogenesis from frozen spermatogonial stem cells. *Nature Medicine*, *2*(6), 693–696. <https://doi.org/10.1038/nm0696-693>
- Aydin, S., Billur, D., Kizil, S., Ozkavukcu, S., Topal Celikkan, F., Aydos, K., & Erdemli, E. (2020). Evaluation of blood–testis barrier integrity in terms of adhesion molecules in nonobstructive azoospermia. *Andrologia*, *52*(7), e13636. <https://doi.org/10.1111/and.13636>
- Azizi, H., Niazi Tabar, A., & Skutella, T. (2021). Successful transplantation of spermatogonial stem cells into the seminiferous tubules of busulfan-treated mice. *Reproductive Health*, *18*(1), 189. <https://doi.org/10.1186/s12978-021-01242-4>
- Bagnat, M., Cheung, I. D., Mostov, K. E., & Stainier, D. Y. R. (2007). Genetic control of single lumen formation in the zebrafish gut. *Nature Cell Biology*, *9*(8), 954–960. <https://doi.org/10.1038/ncb1621>
- Balda, M. S., Whitney, J. A., Flores, C., González, S., Cerejido, M., & Matter, K. (1996). Functional dissociation of paracellular permeability and transepithelial electrical resistance and disruption of the apical-basolateral intramembrane diffusion barrier by expression of a mutant tight junction membrane protein. *The Journal of Cell Biology*, *134*(4), 1031–1049. <https://doi.org/10.1083/jcb.134.4.1031>
- Baneyx, F., & Palumbo, J. L. (2003). Improving Heterologous Protein Folding via Molecular Chaperone and Foldase Co-Expression. In P. E. Vaillancourt (Ed.), *E. coli Gene Expression Protocols* (pp. 171–197). Humana Press. <https://doi.org/10.1385/1-59259-301-1:171>
- Baumholtz, A. I., Simard, A., Nikolopoulou, E., Oosenbrug, M., Collins, M. M., Piontek, A., Krause, G., Piontek, J., Greene, N. D. E., & Ryan, A. K. (2017). Claudins are essential for cell shape changes and convergent extension movements during neural tube closure. *Developmental Biology*, *428*(1), 25–38. <https://doi.org/10.1016/j.ydbio.2017.05.013>
- Behr, M., Riedel, D., & Schuh, R. (2003). The claudin-like megatrachea is essential in septate junctions for the epithelial barrier function in Drosophila. *Developmental Cell*, *5*(4), 611–620. [https://doi.org/10.1016/s1534-5807\(03\)00275-2](https://doi.org/10.1016/s1534-5807(03)00275-2)
- Beier, L.-S., Rossa, J., Woodhouse, S., Bergmann, S., Kramer, H. B., Protze, J., Eichner, M., Piontek, A., Vidal-Y-Sy, S., Brandner, J. M., Krause, G., Zitzmann, N., & Piontek, J. (2019). Use of Modified Clostridium perfringens Enterotoxin Fragments for Claudin Targeting in Liver and Skin Cells. *International Journal of Molecular Sciences*, *20*(19), 4774. <https://doi.org/10.3390/ijms20194774>
- Bhatwa, A., Wang, W., Hassan, Y. I., Abraham, N., Li, X.-Z., & Zhou, T. (2021). Challenges Associated With the Formation of Recombinant Protein Inclusion Bodies in Escherichia

- coli and Strategies to Address Them for Industrial Applications. *Frontiers in Bioengineering and Biotechnology*, 9, 630551. <https://doi.org/10.3389/fbioe.2021.630551>
- Black, J. D., Lopez, S., Cocco, E., Schwab, C. L., English, D. P., & Santin, A. D. (2015). Clostridium Perfringens Enterotoxin (CPE) and CPE-Binding Domain (c-CPE) for the Detection and Treatment of Gynecologic Cancers. *Toxins*, 7(4), 1116–1125. <https://doi.org/10.3390/toxins7041116>
- Bornhorst, J. A., & Falke, J. J. (2000). [16] Purification of Proteins Using Polyhistidine Affinity Tags. *Methods in Enzymology*, 326, 245–254.
- Brinster, R. L., & Zimmermann, J. W. (1994). Spermatogenesis following male germ-cell transplantation. *Proceedings of the National Academy of Sciences*, 91(24), 11298–11302. <https://doi.org/10.1073/pnas.91.24.11298>
- Butt, T. R., Edavettal, S. C., Hall, J. P., & Mattern, M. R. (2005). SUMO fusion technology for difficult-to-express proteins. *Protein Expression and Purification*, 43(1), 1–9. <https://doi.org/10.1016/j.pep.2005.03.016>
- Carratalá, J. V., Cisneros, A., Hellman, E., Villaverde, A., & Ferrer-Miralles, N. (2021). Title: Insoluble proteins catch heterologous soluble proteins into inclusion bodies by intermolecular interaction of aggregating peptides. *Microbial Cell Factories*, 20(1), 30. <https://doi.org/10.1186/s12934-021-01524-3>
- Chakrabarti, G., Zhou, X., & McClane, B. A. (2003). Death Pathways Activated in CaCo-2 Cells by Clostridium perfringens Enterotoxin. *Infection and Immunity*, 71(8), 4260–4270. <https://doi.org/10.1128/IAI.71.8.4260-4270.2003>
- Chakraborty, P., William Buaas, F., Sharma, M., Smith, B. E., Greenlee, A. R., Eacker, S. M., & Braun, R. E. (2014). Androgen-dependent sertoli cell tight junction remodeling is mediated by multiple tight junction components. *Molecular Endocrinology (Baltimore, Md.)*, 28(7), 1055–1072. <https://doi.org/10.1210/me.2013-1134>
- Cheng, C. Y., & Mruk, D. D. (2012). The Blood-Testis Barrier and Its Implications for Male Contraception. *Pharmacological Reviews*, 64(1), 16. <https://doi.org/10.1124/pr.110.002790>
- Chhetri, G., Kalita, P., & Tripathi, T. (2015). An efficient protocol to enhance recombinant protein expression using ethanol in Escherichia coli. *MethodsX*, 2, 385–391. <https://doi.org/10.1016/j.mex.2015.09.005>
- Chiba, K., Yamaguchi, K., Ando, M., Miyake, H., & Fujisawa, M. (2012). Expression pattern of testicular claudin-11 in infertile men. *Urology*, 80(5), 1161.e13-17. <https://doi.org/10.1016/j.urology.2012.06.036>
- Chihara, M., Otsuka, S., Ichii, O., Hashimoto, Y., & Kon, Y. (2010). Molecular dynamics of the blood–testis barrier components during murine spermatogenesis. *Molecular Reproduction and Development*, 77(7), 630–639. <https://doi.org/10.1002/mrd.21200>
- Chiquoine, A. D. (1964). Observations on the early events of cadmium necrosis of the testis. *The Anatomical Record*, 149(1), 23–35. <https://doi.org/10.1002/ar.1091490104>
- Costa, S., Almeida, A., Castro, A., & Domingues, L. (2014). Fusion tags for protein solubility, purification and immunogenicity in Escherichia coli: The novel Fh8 system. *Frontiers in Microbiology*, 5. <https://doi.org/10.3389/fmicb.2014.00063>
- David, S., & Orwig, K. E. (2020). Spermatogonial Stem Cell Culture in Oncofertility. *The Urologic Clinics of North America*, 47(2), 227–244. <https://doi.org/10.1016/j.ucl.2020.01.001>

- de Kretser, D. M., Loveland, K., & O'Bryan, M. (2016). Chapter 136—Spermatogenesis. In J. L. Jameson, L. J. De Groot, D. M. de Kretser, L. C. Giudice, A. B. Grossman, S. Melmed, J. T. Potts, & G. C. Weir (Eds.), *Endocrinology: Adult and Pediatric (Seventh Edition)* (pp. 2325-2353.e9). W.B. Saunders. <https://doi.org/10.1016/B978-0-323-18907-1.00136-0>
- de Marco, A., & De Marco, V. (2004). Bacteria co-transformed with recombinant proteins and chaperones cloned in independent plasmids are suitable for expression tuning. *Journal of Biotechnology*, *109*(1), 45–52. <https://doi.org/10.1016/j.jbiotec.2003.10.025>
- de Marco, A., Deuerling, E., Mogk, A., Tomoyasu, T., & Bukau, B. (2007). Chaperone-based procedure to increase yields of soluble recombinant proteins produced in *E. coli*. *BMC Biotechnology*, *7*(1), 32. <https://doi.org/10.1186/1472-6750-7-32>
- de Michele, F., Poels, J., Giudice, M. G., De Smedt, F., Ambroise, J., Vermeulen, M., Gruson, D., & Wyns, C. (2018). In vitro formation of the blood–testis barrier during long-term organotypic culture of human prepubertal tissue: Comparison with a large cohort of pre/peripubertal boys. *Molecular Human Reproduction*, *24*(5), 271–282. <https://doi.org/10.1093/molehr/gay012>
- Deuerling, E., Patzelt, H., Vorderwülbecke, S., Rauch, T., Kramer, G., Schaffitzel, E., Mogk, A., Schulze-Specking, A., Langen, H., & Bukau, B. (2003). Trigger Factor and DnaK possess overlapping substrate pools and binding specificities. *Molecular Microbiology*, *47*(5), 1317–1328. <https://doi.org/10.1046/j.1365-2958.2003.03370.x>
- Diao, L., Turek, P. J., John, C. M., Fang, F., & Reijo Pera, R. A. (2022). Roles of Spermatogonial Stem Cells in Spermatogenesis and Fertility Restoration. *Frontiers in Endocrinology*, *13*. <https://www.frontiersin.org/journals/endocrinology/articles/10.3389/fendo.2022.895528>
- Ding, L., Lu, Z., Lu, Q., & Chen, Y.-H. (2013). The claudin family of proteins in human malignancy: A clinical perspective. *Cancer Management and Research*, *5*, 367–375. <https://doi.org/10.2147/CMAR.S38294>
- Dithmer, S., Staat, C., Müller, C., Ku, M.-C., Pohlmann, A., Niendorf, T., Gehne, N., Fallier-Becker, P., Kittel, Á., Walter, F. R., Veszelka, S., Deli, M. A., Blasig, R., Haseloff, R. F., Blasig, I. E., & Winkler, L. (2017). Claudin peptidomimetics modulate tissue barriers for enhanced drug delivery. *Annals of the New York Academy of Sciences*, *1397*(1), 169–184. <https://doi.org/10.1111/nyas.13359>
- Dohle, G. R. (2010). Male infertility in cancer patients: Review of the literature. *International Journal of Urology*, *17*(4), 327–331. <https://doi.org/10.1111/j.1442-2042.2010.02484.x>
- Ebihara, C., Kondoh, M., Harada, M., Fujii, M., Mizuguchi, H., Tsunoda, S., Horiguchi, Y., Yagi, K., & Watanabe, Y. (2007). Role of Tyr306 in the C-terminal fragment of *Clostridium perfringens* enterotoxin for modulation of tight junction. *Biochemical Pharmacology*, *73*(6), 824–830. <https://doi.org/10.1016/j.bcp.2006.11.013>
- English, D. P., & Santin, A. D. (2013). Claudins Overexpression in Ovarian Cancer: Potential Targets for *Clostridium Perfringens* Enterotoxin (CPE) Based Diagnosis and Therapy. *International Journal of Molecular Sciences*, *14*(5), Article 5. <https://doi.org/10.3390/ijms140510412>
- Farshdari, F., Ahmadzadeh, M., Nematollahi, L., & Mohit, E. (2020). The improvement of anti-HER2 scFv soluble expression in *Escherichia coli*. *Brazilian Journal of Pharmaceutical Sciences*, *56*, e17861. <https://doi.org/10.1590/s2175-97902019000317861>
- Fink, C., Weigel, R., Fink, L., Wilhelm, J., Kliesch, S., Zeiler, M., Bergmann, M., & Brehm, R. (2009). Claudin-11 is over-expressed and dislocated from the blood–testis barrier in

- Sertoli cells associated with testicular intraepithelial neoplasia in men. *Histochemistry and Cell Biology*, 131(6), 755–764. <https://doi.org/10.1007/s00418-009-0576-2>
- Forbes, C. M., Flannigan, R., & Schlegel, P. N. (2017). Spermatogonial stem cell transplantation and male infertility: Current status and future directions. *Arab Journal of Urology*, 16(1), 171–180. <https://doi.org/10.1016/j.aju.2017.11.015>
- Fu, J., Liu, X., Yin, B., Shu, P., & Peng, X. (2023). NECL2 regulates blood–testis barrier dynamics in mouse testes. *Cell and Tissue Research*, 392(3), 811–826. <https://doi.org/10.1007/s00441-023-03759-5>
- Fukasawa, M., Nagase, S., Shirasago, Y., Iida, M., Yamashita, M., Endo, K., Yagi, K., Suzuki, T., Wakita, T., Hanada, K., Kuniyasu, H., & Kondoh, M. (2015). Monoclonal antibodies against extracellular domains of claudin-1 block hepatitis C virus infection in a mouse model. *Journal of Virology*, 89(9), 4866–4879. <https://doi.org/10.1128/JVI.03676-14>
- Furuse, M., Fujita, K., Hiragi, T., Fujimoto, K., & Tsukita, S. (1998). Claudin-1 and -2: Novel integral membrane proteins localizing at tight junctions with no sequence similarity to occludin. *The Journal of Cell Biology*, 141(7), 1539–1550. <https://doi.org/10.1083/jcb.141.7.1539>
- Furuse, M., Hirase, T., Itoh, M., Nagafuchi, A., Yonemura, S., Tsukita, S., & Tsukita, S. (1993). Occludin: A novel integral membrane protein localizing at tight junctions. *The Journal of Cell Biology*, 123(6 Pt 2), 1777–1788. <https://doi.org/10.1083/jcb.123.6.1777>
- Gasser, B., Saloheimo, M., Rinas, U., Dragosits, M., Rodríguez-Carmona, E., Baumann, K., Giuliani, M., Parrilli, E., Branduardi, P., Lang, C., Porro, D., Ferrer, P., Tutino, M. L., Mattanovich, D., & Villaverde, A. (2008). Protein folding and conformational stress in microbial cells producing recombinant proteins: A host comparative overview. *Microbial Cell Factories*, 7(1), 11. <https://doi.org/10.1186/1475-2859-7-11>
- Gerber, J., Heinrich, J., & Brehm, R. (2016). Blood–testis barrier and Sertoli cell function: Lessons from SCCx43KO mice. *Reproduction*, 151(2), R15–R27. <https://doi.org/10.1530/REP-15-0366>
- Ghosh, S., Rasheedi, S., Rahim, S. S., Banerjee, S., Choudhary, R. K., Chakhaiyar, P., Ehtesham, N. Z., Mukhopadhyay, S., & Hasnain, S. E. (2004). Method for enhancing solubility of the expressed recombinant proteins in Escherichia coli. *BioTechniques*, 37(3), 418–423. <https://doi.org/10.2144/04373ST07>
- Gow, A., Southwood, C. M., Li, J. S., Pariali, M., Riordan, G. P., Brodie, S. E., Danias, J., Bronstein, J. M., Kachar, B., & Lazzarini, R. A. (1999). CNS Myelin and Sertoli Cell Tight Junction Strands Are Absent in *Osp/Claudin-11* Null Mice. *Cell*, 99(6), 649–659. [https://doi.org/10.1016/S0092-8674\(00\)81553-6](https://doi.org/10.1016/S0092-8674(00)81553-6)
- Günzel, D., & Yu, A. S. L. (2013). Claudins and the Modulation of Tight Junction Permeability. *Physiological Reviews*, 93(2), 525–569. <https://doi.org/10.1152/physrev.00019.2012>
- GYE, M. C. (2003). Expression of Claudin-1 in Mouse Testis. *Archives of Andrology*, 49(4), 271–279. <https://doi.org/10.1080/01485010390204913>
- Hanna, P. C., & McClane, B. A. (1991). A recombinant C-terminal toxin fragment provides evidence that membrane insertion is important for Clostridium perfringens enterotoxin cytotoxicity. *Molecular Microbiology*, 5(1), 225–230. <https://doi.org/10.1111/j.1365-2958.1991.tb01843.x>
- Hanna, P. C., Mietzner, T. A., Schoolnik, G. K., & McClane, B. A. (1991). Localization of the receptor-binding region of Clostridium perfringens enterotoxin utilizing cloned toxin

- fragments and synthetic peptides. The 30 C-terminal amino acids define a functional binding region. *The Journal of Biological Chemistry*, 266(17), 11037–11043.
- Hanna, P. C., Wnek, A. P., & McClane, B. A. (1989). Molecular cloning of the 3' half of the *Clostridium perfringens* enterotoxin gene and demonstration that this region encodes receptor-binding activity. *Journal of Bacteriology*, 171(12), 6815–6820. <https://doi.org/10.1128/jb.171.12.6815-6820.1989>
- Harada, M., Kondoh, M., Ebihara, C., Takahashi, A., Komiya, E., Fujii, M., Mizuguchi, H., Tsunoda, S.-I., Horiguchi, Y., Yagi, K., & Watanabe, Y. (2007). Role of tyrosine residues in modulation of claudin-4 by the C-terminal fragment of *Clostridium perfringens* enterotoxin. *Biochemical Pharmacology*, 73(2), 206–214. <https://doi.org/10.1016/j.bcp.2006.10.002>
- Haverfield, J. T., Meachem, S. J., O'Bryan, M. K., McLachlan, R. I., & Stanton, P. G. (2013). Claudin-11 and connexin-43 display altered spatial patterns of organization in men with primary seminiferous tubule failure compared with controls. *Fertility and Sterility*, 100(3), 658–666.e3. <https://doi.org/10.1016/j.fertnstert.2013.04.034>
- Hermann, B. P., Sukhwani, M., Winkler, F., Pascarella, J. N., Peters, K. A., Sheng, Y., Valli, H., Rodriguez, M., Ezzelarab, M., Dargo, G., Peterson, K., Masterson, K., Ramsey, C., Ward, T., Lienesch, M., Volk, A., Cooper, D. K., Thomson, A. W., Kiss, J. E., ... Orwig, K. E. (2012). Spermatogonial stem cell transplantation into Rhesus testes regenerates spermatogenesis producing functional sperm. *Cell Stem Cell*, 11(5), 715–726. <https://doi.org/10.1016/j.stem.2012.07.017>
- Hoffmann, F., & Rinas, U. (2004). Roles of Heat-Shock Chaperones in the Production of Recombinant Proteins in *Escherichia coli*. In *Physiological Stress Responses in Bioprocesses: -/-* (pp. 143–161). Springer. <https://doi.org/10.1007/b93996>
- Hogarth, C. (2015). 9—Retinoic acid metabolism, signaling, and function in the adult testis. In M. D. Griswold (Ed.), *Sertoli Cell Biology (Second Edition)* (pp. 247–272). Academic Press. <https://doi.org/10.1016/B978-0-12-417047-6.00009-0>
- Hollenbach, J., Jung, K., Noelke, J., Gasse, H., Pfarrer, C., Koy, M., & Brehm, R. (2018). Loss of connexin43 in murine Sertoli cells and its effect on blood-testis barrier formation and dynamics. *PLOS ONE*, 13(6), e0198100. <https://doi.org/10.1371/journal.pone.0198100>
- Horiguchi, Y., Akai, T., & Sakaguchi, G. (1987). Isolation and function of a *Clostridium perfringens* enterotoxin fragment. *Infection and Immunity*, 55(12), 2912–2915. <https://doi.org/10.1128/iai.55.12.2912-2915.1987>
- Ilani, N., Armanious, N., Lue, Y.-H., Swerdloff, R. S., Baravarian, S., Adler, A., Tsang, C., Jia, Y., Cui, Y.-G., Wang, X.-H., Zhou, Z.-M., Sha, J.-H., & Wang, C. (2012). Integrity of the blood–testis barrier in healthy men after suppression of spermatogenesis with testosterone and levonorgestrel†. *Human Reproduction*, 27(12), 3403–3411. <https://doi.org/10.1093/humrep/des340>
- Jiang, S., Xu, Y., Fan, Y., Hu, Y., Zhang, Q., & Su, W. (2022). Busulfan impairs blood–testis barrier and spermatogenesis by increasing noncollagenous 1 domain peptide via matrix metalloproteinase 9. *Andrology*, 10(2), 377–391. <https://doi.org/10.1111/andr.13112>
- Jiang, X.-H., Bukhari, I., Zheng, W., Yin, S., Wang, Z., Cooke, H. J., & Shi, Q.-H. (2014). Blood-testis barrier and spermatogenesis: Lessons from genetically-modified mice. *Asian Journal of Andrology*, 16(4), 572–580. <https://doi.org/10.4103/1008-682X.125401>
- Jin, C., Wang, Z., Li, P., Tang, J., Jiao, T., Li, Y., Ou, J., Zou, D., Li, M., Mang, X., Liu, J., Ma, Y., Wu, X., Shi, J., Chen, S., He, M., Lu, Y., Zhang, N., Miao, S., ... Song, W. (2023).

- Decoding the spermatogonial stem cell niche under physiological and recovery conditions in adult mice and humans. *Science Advances*, 9(31), eabq3173. <https://doi.org/10.1126/sciadv.abq3173>
- Kadam, P., Ntemou, E., Baert, Y., Van Laere, S., Van Saen, D., & Goossens, E. (2018). Co-transplantation of mesenchymal stem cells improves spermatogonial stem cell transplantation efficiency in mice. *Stem Cell Research & Therapy*, 9(1), 317. <https://doi.org/10.1186/s13287-018-1065-0>
- KANATSU-SHINOHARA, M., MORIMOTO, H., WATANABE, S., & SHINOHARA, T. (2018). Reversible inhibition of the blood-testis barrier protein improves stem cell homing in mouse testes. *The Journal of Reproduction and Development*, 64(6), 511–522. <https://doi.org/10.1262/jrd.2018-093>
- Kanatsu-Shinohara, M., Ogonuki, N., Matoba, S., Ogura, A., & Shinohara, T. (2020). Autologous transplantation of spermatogonial stem cells restores fertility in congenitally infertile mice. *Proceedings of the National Academy of Sciences*, 117(14), 7837–7844. <https://doi.org/10.1073/pnas.1914963117>
- Kanatsu-Shinohara, M., Takehashi, M., Takashima, S., Lee, J., Morimoto, H., Chuma, S., Raducanu, A., Nakatsuji, N., Fässler, R., & Shinohara, T. (2008). Homing of mouse spermatogonial stem cells to germline niche depends on beta1-integrin. *Cell Stem Cell*, 3(5), 533–542. <https://doi.org/10.1016/j.stem.2008.08.002>
- Katahira, J., Inoue, N., Horiguchi, Y., Matsuda, M., & Sugimoto, N. (1997). Molecular Cloning and Functional Characterization of the Receptor for Clostridium perfringens Enterotoxin. *Journal of Cell Biology*, 136(6), 1239–1247. <https://doi.org/10.1083/jcb.136.6.1239>
- Kato-Nakano, M., Suzuki, M., Kawamoto, S., Furuya, A., Ohta, S., Nakamura, K., & Ando, H. (2010). Characterization and evaluation of the antitumour activity of a dual-targeting monoclonal antibody against claudin-3 and claudin-4. *Anticancer Research*, 30(11), 4555–4562.
- Kimura, J., Abe, H., Kamitani, S., Toshima, H., Fukui, A., Miyake, M., Kamata, Y., Sugita-Konishi, Y., Yamamoto, S., & Horiguchi, Y. (2010). Clostridium perfringens Enterotoxin Interacts with Claudins via Electrostatic Attraction. *The Journal of Biological Chemistry*, 285(1), 401–408. <https://doi.org/10.1074/jbc.M109.051417>
- Kitadokoro, K., Nishimura, K., Kamitani, S., Fukui-Miyazaki, A., Toshima, H., Abe, H., Kamata, Y., Sugita-Konishi, Y., Yamamoto, S., Karatani, H., & Horiguchi, Y. (2011). Crystal Structure of Clostridium perfringens Enterotoxin Displays Features of  $\beta$ -Pore-forming Toxins. *The Journal of Biological Chemistry*, 286(22), 19549–19555. <https://doi.org/10.1074/jbc.M111.228478>
- Kojima, T., Kondoh, M., Keira, T., Takano, K.-I., Kakuki, T., Kaneko, Y., Miyata, R., Nomura, K., Obata, K., Kohno, T., Konno, T., Sawada, N., & Himi, T. (2016). Claudin-binder C-CPE mutants enhance permeability of insulin across human nasal epithelial cells. *Drug Delivery*, 23(8), 2703–2710. <https://doi.org/10.3109/10717544.2015.1050530>
- Kokai-Kun, J. F., Benton, K., Wieckowski, E. U., & McClane, B. A. (1999). Identification of a Clostridium perfringens Enterotoxin Region Required for Large Complex Formation and Cytotoxicity by Random Mutagenesis. *Infection and Immunity*, 67(11), 5634–5641. <https://doi.org/10.1128/iai.67.11.5634-5641.1999>
- Kokai-Kun, J. F., & McClane, B. A. (1997). Deletion analysis of the Clostridium perfringens enterotoxin. *Infection and Immunity*, 65(3), 1014–1022.

- Kolaj, O., Spada, S., Robin, S., & Wall, J. G. (2009). Use of folding modulators to improve heterologous protein production in *Escherichia coli*. *Microbial Cell Factories*, 8(1), 9. <https://doi.org/10.1186/1475-2859-8-9>
- Komljenovic, D., Sandhoff, R., Teigler, A., Heid, H., Just, W. W., & Gorgas, K. (2009). Disruption of blood-testis barrier dynamics in ether-lipid-deficient mice. *Cell and Tissue Research*, 337(2), 281–299. <https://doi.org/10.1007/s00441-009-0809-7>
- Kondoh, M., Masuyama, A., Takahashi, A., Asano, N., Mizuguchi, H., Koizumi, N., Fujii, M., Hayakawa, T., Horiguchi, Y., & Watanabe, Y. (2005). A Novel Strategy for the Enhancement of Drug Absorption Using a Claudin Modulator. *Molecular Pharmacology*, 67(3), 749–756. <https://doi.org/10.1124/mol.104.008375>
- Kramer, R. M., Shende, V. R., Motl, N., Pace, C. N., & Scholtz, J. M. (2012). Toward a Molecular Understanding of Protein Solubility: Increased Negative Surface Charge Correlates with Increased Solubility. *Biophysical Journal*, 102(8), 1907–1915. <https://doi.org/10.1016/j.bpj.2012.01.060>
- Krause, G., Winkler, L., Mueller, S. L., Haseloff, R. F., Piontek, J., & Blasig, I. E. (2008). Structure and function of claudins. *Biochimica Et Biophysica Acta*, 1778(3), 631–645. <https://doi.org/10.1016/j.bbamem.2007.10.018>
- Kronqvist, N., Rising, A., & Johansson, J. (2022). A Novel Approach for the Production of Aggregation-Prone Proteins Using the Spidroin-Derived NT\* Tag. *Methods in Molecular Biology (Clifton, N.J.)*, 2406, 113–130. [https://doi.org/10.1007/978-1-0716-1859-2\\_6](https://doi.org/10.1007/978-1-0716-1859-2_6)
- Kronqvist, N., Sarr, M., Lindqvist, A., Nordling, K., Otikovs, M., Venturi, L., Pioselli, B., Purhonen, P., Landreh, M., Biverstål, H., Toleikis, Z., Sjöberg, L., Robinson, C. V., Pelizzi, N., Jörnvall, H., Hebert, H., Jaudzems, K., Curstedt, T., Rising, A., & Johansson, J. (2017). Efficient protein production inspired by how spiders make silk. *Nature Communications*, 8, 15504. <https://doi.org/10.1038/ncomms15504>
- Kubota, H., Avarbock, M. R., & Brinster, R. L. (2004). Growth factors essential for self-renewal and expansion of mouse spermatogonial stem cells. *Proceedings of the National Academy of Sciences*, 101(47), 16489–16494. <https://doi.org/10.1073/pnas.0407063101>
- Kubota, H., & Brinster, R. L. (2018). Spermatogonial stem cells†. *Biology of Reproduction*, 99(1), 52–74. <https://doi.org/10.1093/biolre/i0y077>
- Lal-Nag, M., & Morin, P. J. (2009). The claudins. *Genome Biology*, 10(8), 235. <https://doi.org/10.1186/gb-2009-10-8-235>
- Lee, N. P. Y., Wong, E. W. P., Mruk, D. D., & Cheng, C. Y. (2009). Testicular cell junction: A novel target for male contraception. *Current Medicinal Chemistry*, 16(7), 906–915. <https://doi.org/10.2174/092986709787549262>
- Li, X.-Y., Zhang, Y., Wang, X.-X., Jin, C., Wang, Y.-Q., Sun, T.-C., Li, J., Tang, J.-X., Batool, A., Deng, S.-L., Chen, S.-R., Yan Cheng, C., & Liu, Y.-X. (2018). Regulation of blood-testis barrier assembly in vivo by germ cells. *The FASEB Journal*, 32(3), 1653–1664. <https://doi.org/10.1096/fj.201700681R>
- Liao, Z., Yang, Z., Piontek, A., Eichner, M., Krause, G., Li, L., Piontek, J., & Zhang, J. (2016). Specific binding of a mutated fragment of *Clostridium perfringens* enterotoxin to endothelial claudin-5 and its modulation of cerebral vascular permeability. *Neuroscience*, 327, 53–63. <https://doi.org/10.1016/j.neuroscience.2016.04.013>
- Lopes, F., Tholeti, P., Adiga, S. K., Anderson, R. A., Mitchell, R. T., & Spears, N. (2020). Chemotherapy induced damage to spermatogonial stem cells in prepubertal mouse in

- vitro impairs long-term spermatogenesis. *Toxicology Reports*, 8, 114–123.  
<https://doi.org/10.1016/j.toxrep.2020.12.023>
- Loveland, K. L. (2018). Activins in Male Reproduction. In M. K. Skinner (Ed.), *Encyclopedia of Reproduction (Second Edition)* (pp. 208–214). Academic Press.  
<https://doi.org/10.1016/B978-0-12-801238-3.64581-6>
- Luaces, J. P., Toro-Urrego, N., Otero-Losada, M., & Capani, F. (2023). What do we know about blood-testis barrier? Current understanding of its structure and physiology. *Frontiers in Cell and Developmental Biology*, 11. <https://doi.org/10.3389/fcell.2023.1114769>
- Lui, W.-Y., Mruk, D., Lee, W. M., & Cheng, C. Y. (2003). Sertoli Cell Tight Junction Dynamics: Their Regulation During Spermatogenesis1. *Biology of Reproduction*, 68(4), 1087–1097. <https://doi.org/10.1095/biolreprod.102.010371>
- Manku, G., Hueso, A., Brimo, F., Chan, P., Gonzalez-Peramato, P., Jabado, N., Gayden, T., Bourgey, M., Riazalhosseini, Y., & Culty, M. (2016). Changes in the expression profiles of claudins during gonocyte differentiation and in seminomas. *Andrology*, 4(1), 95–110. <https://doi.org/10.1111/andr.12122>
- Marblestone, J. G., Edavettal, S. C., Lim, Y., Lim, P., Zuo, X., & Butt, T. R. (2006). Comparison of SUMO fusion technology with traditional gene fusion systems: Enhanced expression and solubility with SUMO. *Protein Science : A Publication of the Protein Society*, 15(1), 182. <https://doi.org/10.1110/ps.051812706>
- Matsumoto, A. M., & Bremner, W. J. (2016). Chapter 19—Testicular Disorders. In S. Melmed, K. S. Polonsky, P. R. Larsen, & H. M. Kronenberg (Eds.), *Williams Textbook of Endocrinology (Thirteenth Edition)* (pp. 694–784). Elsevier.  
<https://doi.org/10.1016/B978-0-323-29738-7.00019-8>
- Mazaud-Guittot, S., Meugnier, E., Pesenti, S., Wu, X., Vidal, H., Gow, A., & Le Magueresse-Battistoni, B. (2010). Claudin 11 Deficiency in Mice Results in Loss of the Sertoli Cell Epithelial Phenotype in the Testis1. *Biology of Reproduction*, 82(1), 202–213. <https://doi.org/10.1095/biolreprod.109.078907>
- McCabe, M. J., Tarulli, G. A., Laven-Law, G., Matthiesson, K. L., Meachem, S. J., McLachlan, R. I., Dinger, M. E., & Stanton, P. G. (2016). Gonadotropin suppression in men leads to a reduction in claudin-11 at the Sertoli cell tight junction. *Human Reproduction*, 31(4), 875–886. <https://doi.org/10.1093/humrep/dew009>
- Meng, J., Holdcraft, R. W., Shima, J. E., Griswold, M. D., & Braun, R. E. (2005). Androgens regulate the permeability of the blood–testis barrier. *Proceedings of the National Academy of Sciences*, 102(46), 16696–16700. <https://doi.org/10.1073/pnas.0506084102>
- Meoli, L., & Günzel, D. (2020). Channel functions of claudins in the organization of biological systems. *Biochimica et Biophysica Acta (BBA) - Biomembranes*, 1862(9), 183344. <https://doi.org/10.1016/j.bbamem.2020.183344>
- Mok, K. W., Mruk, D. D., & Cheng, C. Y. (2013). Chapter Six—Regulation of Blood–Testis Barrier (BTB) Dynamics during Spermatogenesis via the “Yin” and “Yang” Effects of Mammalian Target of Rapamycin Complex 1 (mTORC1) and mTORC2. In K. W. Jeon (Ed.), *International Review of Cell and Molecular Biology* (Vol. 301, pp. 291–358). Academic Press. <https://doi.org/10.1016/B978-0-12-407704-1.00006-3>
- Morales, E. S., Parcerisa, I. L., & Ceccarelli, E. A. (2019). A novel method for removing contaminant Hsp70 molecular chaperones from recombinant proteins. *Protein Science : A Publication of the Protein Society*, 28(4), 800. <https://doi.org/10.1002/pro.3574>

- Morita, K., Furuse, M., Fujimoto, K., & Tsukita, S. (1999). Claudin multigene family encoding four-transmembrane domain protein components of tight junction strands. *Proceedings of the National Academy of Sciences*, *96*(2), 511–516. <https://doi.org/10.1073/pnas.96.2.511>
- Morita, K., Sasaki, H., Fujimoto, K., Furuse, M., & Tsukita, S. (1999). Claudin-11/OSP-based tight junctions of myelin sheaths in brain and Sertoli cells in testis. *The Journal of Cell Biology*, *145*(3), 579–588. <https://doi.org/10.1083/jcb.145.3.579>
- Moroi, S., Saitou, M., Fujimoto, K., Sakakibara, A., Furuse, M., Yoshida, O., & Tsukita, S. (1998). Occludin is concentrated at tight junctions of mouse/rat but not human/guinea pig Sertoli cells in testes. *The American Journal of Physiology*, *274*(6), C1708–1717. <https://doi.org/10.1152/ajpcell.1998.274.6.C1708>
- Morrow, C. M. K., Mruk, D., Cheng, C. Y., & Hess, R. A. (2010). Claudin and occludin expression and function in the seminiferous epithelium. *Philosophical Transactions of the Royal Society B: Biological Sciences*, *365*(1546), 1679–1696. <https://doi.org/10.1098/rstb.2010.0025>
- Mruk, D. D., & Cheng, C. Y. (2015). The Mammalian Blood-Testis Barrier: Its Biology and Regulation. *Endocrine Reviews*, *36*(5), 564–591. <https://doi.org/10.1210/er.2014-1101>
- Nagano, M., Avarbock, M. R., & Brinster, R. L. (1999). Pattern and Kinetics of Mouse Donor Spermatogonial Stem Cell Colonization in Recipient Testes1. *Biology of Reproduction*, *60*(6), 1429–1436. <https://doi.org/10.1095/biolreprod60.6.1429>
- Nagano, M. C. (2003). Homing Efficiency and Proliferation Kinetics of Male Germ Line Stem Cells Following Transplantation in Mice1. *Biology of Reproduction*, *69*(2), 701–707. <https://doi.org/10.1095/biolreprod.103.016352>
- Nah, W. H., Lee, J. E., Park, H. J., Park, N. C., & Gye, M. C. (2011). Claudin-11 expression increased in spermatogenic defect in human testes. *Fertility and Sterility*, *95*(1), 385–388. <https://doi.org/10.1016/j.fertnstert.2010.08.023>
- Nasako, H., Akizuki, R., Takashina, Y., Ishikawa, Y., Shinoda, T., Shirouzu, M., Asai, T., Matsunaga, T., Endo, S., & Ikari, A. (2020). Claudin-2 binding peptides, VPDSM and DSMKF, down-regulate claudin-2 expression and anticancer resistance in human lung adenocarcinoma A549 cells. *Biochimica Et Biophysica Acta. Molecular Cell Research*, *1867*(4), 118642. <https://doi.org/10.1016/j.bbamcr.2019.118642>
- Nelson, K. S., Furuse, M., & Beitel, G. J. (2010). The Drosophila Claudin Kune-kune is required for septate junction organization and tracheal tube size control. *Genetics*, *185*(3), 831–839. <https://doi.org/10.1534/genetics.110.114959>
- Neuhaus, W., Piontek, A., Protze, J., Eichner, M., Mahringer, A., Subileau, E.-A., Lee, I.-F. M., Schulzke, J. D., Krause, G., & Piontek, J. (2018). Reversible opening of the blood-brain barrier by claudin-5-binding variants of Clostridium perfringens enterotoxin's claudin-binding domain. *Biomaterials*, *161*, 129–143. <https://doi.org/10.1016/j.biomaterials.2018.01.028>
- Niiranen, L., Espelid, S., Karlsen, C. R., Mustonen, M., Paulsen, S. M., Heikinheimo, P., & Willassen, N. P. (2007). Comparative expression study to increase the solubility of cold adapted *Vibrio* proteins in *Escherichia coli*. *Protein Expression and Purification*, *52*(1), 210–218. <https://doi.org/10.1016/j.pep.2006.09.005>
- Nishihara, K., Kanemori, M., Kitagawa, M., Yanagi, H., & Yura, T. (1998). Chaperone Coexpression Plasmids: Differential and Synergistic Roles of DnaK-DnaJ-GrpE and GroEL-GroES in Assisting Folding of an Allergen of Japanese Cedar Pollen, Cryj2,

- in *Escherichia coli*. *Applied and Environmental Microbiology*, 64(5), 1694–1699.  
<https://doi.org/10.1128/AEM.64.5.1694-1699.1998>
- Nomme, J., Antanasijevic, A., Caffrey, M., Van Itallie, C. M., Anderson, J. M., Fanning, A. S., & Lavie, A. (2015). Structural Basis of a Key Factor Regulating the Affinity between the Zonula Occludens First PDZ Domain and Claudins. *The Journal of Biological Chemistry*, 290(27), 16595–16606. <https://doi.org/10.1074/jbc.M115.646695>
- Oduwole, O. O., Huhtaniemi, I. T., & Misrahi, M. (2021). The Roles of Luteinizing Hormone, Follicle-Stimulating Hormone and Testosterone in Spermatogenesis and Folliculogenesis Revisited. *International Journal of Molecular Sciences*, 22(23), 12735.  
<https://doi.org/10.3390/ijms222312735>
- Ó'Fágáin, C., Cummins, P. M., & O'Connor, B. F. (2016). Gel-Filtration Chromatography. *Protein Chromatography*, 1485, 15–25. [https://doi.org/10.1007/978-1-4939-6412-3\\_2](https://doi.org/10.1007/978-1-4939-6412-3_2)
- Ogawa, T., Arechaga, J. M., Avarbock, M. R., & Brinster, R. L. (1997). Transplantation of testis germinal cells into mouse seminiferous tubules. *The International Journal of Developmental Biology*, 41(1), Article 1. <https://doi.org/10.1387/ijdb.9074943>
- Ogawa, T., Dobrinski, I., Avarbock, M. R., & Brinster, R. L. (2000). Transplantation of male germ line stem cells restores fertility in infertile mice. *Nature Medicine*, 6(1), Article 1. <https://doi.org/10.1038/71496>
- Okai, K., Ichikawa-Tomikawa, N., Saito, A. C., Watabe, T., Sugimoto, K., Fujita, D., Ono, C., Fukuhara, T., Matsuura, Y., Ohira, H., & Chiba, H. (2018). A novel occludin-targeting monoclonal antibody prevents hepatitis C virus infection in vitro. *Oncotarget*, 9(24), 16588–16598. <https://doi.org/10.18632/oncotarget.24742>
- Osterberg, E. C., Ramasamy, R., Masson, P., & Brannigan, R. E. (2014). Current practices in fertility preservation in male cancer patients. *Urology Annals*, 6(1), 13–17.  
<https://doi.org/10.4103/0974-7796.127008>
- Overgaard, C. E., Daugherty, B. L., Mitchell, L. A., & Koval, M. (2011). Claudins: Control of Barrier Function and Regulation in Response to Oxidant Stress. *Antioxidants & Redox Signaling*, 15(5), 1179–1193. <https://doi.org/10.1089/ars.2011.3893>
- Pace, C. N., Treviño, S., Prabhakaran, E., & Scholtz, J. M. (2004). Protein structure, stability and solubility in water and other solvents. *Philosophical Transactions of the Royal Society B: Biological Sciences*, 359(1448), 1225–1235. <https://doi.org/10.1098/rstb.2004.1500>
- Palmer, I., & Wingfield, P. T. (2012). Preparation and Extraction of Insoluble (Inclusion-Body) Proteins from *Escherichia coli*. *Current Protocols in Protein Science / Editorial Board, John E. Coligan ... [et Al.]*, 0 6, 10.1002/0471140864.ps0603s70.  
<https://doi.org/10.1002/0471140864.ps0603s70>
- Park, C. J., Lee, J. E., Oh, Y., Shim, S., Kim, D., Park, N., Park, H., & Gye, M.-C. (2010). Postnatal Changes in the Expression of Claudin-11 in the Testes and Excurrent Ducts of the Domestic Rabbit (*Oryctolagus cuniculus domesticus*). *Journal of Andrology*, 32, 295–306. <https://doi.org/10.2164/jandrol.110.010611>
- Pelegrine, D. H. G., & Gasparetto, C. A. (2005). Whey proteins solubility as function of temperature and pH. *LWT - Food Science and Technology*, 38(1), 77–80.  
<https://doi.org/10.1016/j.lwt.2004.03.013>
- Peti, W., & Page, R. (2007). Strategies to maximize heterologous protein expression in *Escherichia coli* with minimal cost. *Protein Expression and Purification*, 51(1), 1–10.  
<https://doi.org/10.1016/j.pep.2006.06.024>

- Phillips, B. T., Gassei, K., & Orwig, K. E. (2010). Spermatogonial stem cell regulation and spermatogenesis. *Philosophical Transactions of the Royal Society B: Biological Sciences*, 365(1546), 1663–1678. <https://doi.org/10.1098/rstb.2010.0026>
- Piontek, A., Eichner, M., Zwanziger, D., Beier, L.-S., Protze, J., Walther, W., Theurer, S., Schmid, K. W., Führer-Sakel, D., Piontek, J., & Krause, G. (2020). Targeting claudin-overexpressing thyroid and lung cancer by modified *Clostridium perfringens* enterotoxin. *Molecular Oncology*, 14(2), 261–276. <https://doi.org/10.1002/1878-0261.12615>
- Protze, J., Eichner, M., Piontek, A., Dinter, S., Rossa, J., Blecharz, K. G., Vajkoczy, P., Piontek, J., & Krause, G. (2015). Directed structural modification of *Clostridium perfringens* enterotoxin to enhance binding to claudin-5. *Cellular and Molecular Life Sciences*, 72(7), 1417–1432. <https://doi.org/10.1007/s00018-014-1761-6>
- QIAGEN. (2003). *The QIAexpressionist. 5th Edition.*  
[https://kirschner.med.harvard.edu/files/protocols/QIAGEN\\_QIAexpressionist\\_EN.pdf](https://kirschner.med.harvard.edu/files/protocols/QIAGEN_QIAexpressionist_EN.pdf)
- Qin, Y., Liu, L., He, Y., Wang, C., Liang, M., Chen, X., Hao, H., Qin, T., Zhao, X., & Wang, D. (2016). Testicular Busulfan Injection in Mice to Prepare Recipients for Spermatogonial Stem Cell Transplantation Is Safe and Non-Toxic. *PLoS ONE*, 11(2), e0148388. <https://doi.org/10.1371/journal.pone.0148388>
- Robertson, S. L., Smedley, J. G., Singh, U., Chakrabarti, G., Van Itallie, C. M., Anderson, J. M., & McClane, B. A. (2007). Compositional and stoichiometric analysis of *Clostridium perfringens* enterotoxin complexes in Caco-2 cells and claudin 4 fibroblast transfectants. *Cellular Microbiology*, 9(11), 2734–2755. <https://doi.org/10.1111/j.1462-5822.2007.00994.x>
- Russell, L. D., Ettlin, R. A., Hikim, A. P. S., & Clegg, E. D. (1993). Histological and Histopathological Evaluation of the Testis. *International Journal of Andrology*, 16(1), 83–83. <https://doi.org/10.1111/j.1365-2605.1993.tb01156.x>
- Sadeghian-Rizi, T., Ebrahimi, A., Moazzen, F., Yousefian, H., & Jahanian-Najafabadi, A. (2019). Improvement of solubility and yield of recombinant protein expression in *E. coli* using a two-step system. *Research in Pharmaceutical Sciences*, 14(5), 400. <https://doi.org/10.4103/1735-5362.268200>
- Saitou, M., Furuse, M., Sasaki, H., Schulzke, J.-D., Fromm, M., Takano, H., Noda, T., & Tsukita, S. (2000). Complex Phenotype of Mice Lacking Occludin, a Component of Tight Junction Strands. *Molecular Biology of the Cell*, 11(12), 4131–4142.
- Samuelson, J. C. (2016). Purifying Recombinant His-Tagged Proteins: Improving the Process with Use of Genetically Tailored Expression Host NiCo21(DE3). *Genetic Engineering & Biotechnology News*, 36(5), 26–27. <https://doi.org/10.1089/gen.36.05.15>
- San-Miguel, T., Pérez-Bermúdez, P., & Gavidia, I. (2013). Production of soluble eukaryotic recombinant proteins in *E. coli* is favoured in early log-phase cultures induced at low temperature. *SpringerPlus*, 2(1), 89. <https://doi.org/10.1186/2193-1801-2-89>
- Sauer, R.-S., Krug, S. M., Hackel, D., Staat, C., Konasin, N., Yang, S., Niedermirtl, B., Bosten, J., Günther, R., Dabrowski, S., Doppler, K., Sommer, C., Blasig, I. E., Brack, A., & Rittner, H. L. (2014). Safety, efficacy, and molecular mechanism of claudin-1-specific peptides to enhance blood-nerve-barrier permeability. *Journal of Controlled Release: Official Journal of the Controlled Release Society*, 185, 88–98. <https://doi.org/10.1016/j.jconrel.2014.04.029>
- Schlieker, C., Bukau, B., & Mogk, A. (2002). Prevention and reversion of protein aggregation by molecular chaperones in the *E. coli* cytosol: Implications for their applicability in

- biotechnology. *Journal of Biotechnology*, 96(1), 13–21. [https://doi.org/10.1016/S0168-1656\(02\)00033-0](https://doi.org/10.1016/S0168-1656(02)00033-0)
- Sharafi, Y., Mirhosseini, S. A., & Amani, J. (2022). In silico prediction of amino acids involved in cCPE290-319 interaction with claudin 4. *Veterinary Research Forum*, 13(4), 501–506. <https://doi.org/10.30466/vrf.2021.527750.3161>
- Sharma, R., & Agarwal, A. (2011). Spermatogenesis: An Overview. In A. Zini & A. Agarwal (Eds.), *Sperm Chromatin* (pp. 19–44). Springer New York. [https://doi.org/10.1007/978-1-4419-6857-9\\_2](https://doi.org/10.1007/978-1-4419-6857-9_2)
- Shihan, M. H., Novo, S. G., Le Marchand, S. J., Wang, Y., & Duncan, M. K. (2021). A simple method for quantitating confocal fluorescent images. *Biochemistry and Biophysics Reports*, 25, 100916. <https://doi.org/10.1016/j.bbrep.2021.100916>
- Shinohara, T., Orwig, K. E., Avarbock, M. R., & Brinster, R. L. (2001). Remodeling of the postnatal mouse testis is accompanied by dramatic changes in stem cell number and niche accessibility. *Proceedings of the National Academy of Sciences of the United States of America*, 98(11), 6186–6191. <https://doi.org/10.1073/pnas.111158198>
- Shrestha, A., Robertson, S. L., Garcia, J., Beingasser, J., McClane, B. A., & Uzal, F. A. (2014). A Synthetic Peptide Corresponding to the Extracellular Loop 2 Region of Claudin-4 Protects against Clostridium perfringens Enterotoxin In Vitro and In Vivo. *Infection and Immunity*, 82(11), 4778–4788. <https://doi.org/10.1128/IAI.02453-14>
- Shrestha, A., Uzal, F. A., & McClane, B. A. (2016). The interaction of Clostridium perfringens enterotoxin with receptor claudins. *Anaerobe*, 41, 18–26. <https://doi.org/10.1016/j.anaerobe.2016.04.011>
- Siddiqui, M., Sheikh, H., Tran, C., & Bruce, A. E. E. (2010). The tight junction component Claudin E is required for zebrafish epiboly. *Developmental Dynamics: An Official Publication of the American Association of Anatomists*, 239(2), 715–722. <https://doi.org/10.1002/dvdy.22172>
- Siegel, R. L., Giaquinto, A. N., & Jemal, A. (2024). Cancer statistics, 2024. *CA: A Cancer Journal for Clinicians*, 74(1), 12–49. <https://doi.org/10.3322/caac.21820>
- Singh, A. P., Cummings, C. A., Mishina, Y., & Archer, T. K. (2013). SOX8 regulates permeability of the blood-testes barrier that affects adult male fertility in the mouse. *Biology of Reproduction*, 88(5), 133. <https://doi.org/10.1095/biolreprod.112.107284>
- Singh, A. P., Harada, S., & Mishina, Y. (2009). Downstream Genes of Sox8 That Would Affect Adult Male Fertility. *Sexual Development*, 3(1), 16–25. <https://doi.org/10.1159/000200078>
- Singh, U., Van Itallie, C. M., Mitic, L. L., Anderson, J. M., & McClane, B. A. (2000). CaCo-2 cells treated with Clostridium perfringens enterotoxin form multiple large complex species, one of which contains the tight junction protein occludin. *The Journal of Biological Chemistry*, 275(24), 18407–18417. <https://doi.org/10.1074/jbc.M001530200>
- Smedley, J. G., & McClane, B. A. (2004). Fine mapping of the N-terminal cytotoxicity region of Clostridium perfringens enterotoxin by site-directed mutagenesis. *Infection and Immunity*, 72(12), 6914–6923. <https://doi.org/10.1128/IAI.72.12.6914-6923.2004>
- Smedley, J. G., Uzal, F. A., & McClane, B. A. (2007). Identification of a Prepore Large-Complex Stage in the Mechanism of Action of Clostridium perfringens Enterotoxin. *Infection and Immunity*, 75(5), 2381–2390. <https://doi.org/10.1128/iai.01737-06>
- Smith, B. E., & Braun, R. E. (2012). Germ cell migration across Sertoli cell tight junctions. *Science (New York, N.Y.)*, 338(6108), 798–802. <https://doi.org/10.1126/science.1219969>

- Smith, L. B., & Walker, W. H. (2014). The Regulation of Spermatogenesis by Androgens. *Seminars in Cell & Developmental Biology*, 0, 2–13. <https://doi.org/10.1016/j.semcdb.2014.02.012>
- Sofikitis, N., Giotitsas, N., Tsounapi, P., Baltogiannis, D., Giannakis, D., & Pardalidis, N. (2008). Hormonal regulation of spermatogenesis and spermiogenesis. *The Journal of Steroid Biochemistry and Molecular Biology*, 109(3–5), 323–330. <https://doi.org/10.1016/j.jsbmb.2008.03.004>
- Song, H., Park, H.-J., Lee, W.-Y., & Lee, K. H. (2022). Models and Molecular Markers of Spermatogonial Stem Cells in Vertebrates: To Find Models in Nonmammals. *Stem Cells International*, 2022, 4755514. <https://doi.org/10.1155/2022/4755514>
- Song, J. M., An, Y. J., Kang, M. H., Lee, Y.-H., & Cha, S.-S. (2012). Cultivation at 6–10 °C is an effective strategy to overcome the insolubility of recombinant proteins in *Escherichia coli*. *Protein Expression and Purification*, 82(2), 297–301. <https://doi.org/10.1016/j.pep.2012.01.020>
- Sonoda, N., Furuse, M., Sasaki, H., Yonemura, S., Katahira, J., Horiguchi, Y., & Tsukita, S. (1999). Clostridium perfringens Enterotoxin Fragment Removes Specific Claudins from Tight Junction Strands: Evidence for Direct Involvement of Claudins in Tight Junction Barrier. *Journal of Cell Biology*, 147(1), 195–204. <https://doi.org/10.1083/jcb.147.1.195>
- Sørensen, H. P., & Mortensen, K. K. (2005). Soluble expression of recombinant proteins in the cytoplasm of *Escherichia coli*. *Microbial Cell Factories*, 4(1), 1. <https://doi.org/10.1186/1475-2859-4-1>
- Sourdaine, P., Gautier, A., & Gribouval, L. (2018). Spermatogenesis and Spermiogenesis in Elasmobranchs, a Short Overview. In M. K. Skinner (Ed.), *Encyclopedia of Reproduction (Second Edition)* (pp. 305–312). Academic Press. <https://doi.org/10.1016/B978-0-12-809633-8.20572-4>
- Staat, C., Coisne, C., Dabrowski, S., Stamatovic, S. M., Andjelkovic, A. V., Wolburg, H., Engelhardt, B., & Blasig, I. E. (2015). Mode of action of claudin peptidomimetics in the transient opening of cellular tight junction barriers. *Biomaterials*, 54, 9–20. <https://doi.org/10.1016/j.biomaterials.2015.03.007>
- Stammler, A., Lüftner, B. U., Kliesch, S., Weidner, W., Bergmann, M., Middendorff, R., & Konrad, L. (2016). Highly Conserved Testicular Localization of Claudin-11 in Normal and Impaired Spermatogenesis. *PLOS ONE*, 11(8), e0160349. <https://doi.org/10.1371/journal.pone.0160349>
- Stanton, P. G. (2016). Regulation of the blood-testis barrier. *Seminars in Cell & Developmental Biology*, 59, 166–173. <https://doi.org/10.1016/j.semcdb.2016.06.018>
- Studier, F. W. (2005). Protein production by auto-induction in high-density shaking cultures. *Protein Expression and Purification*, 41(1), 207–234. <https://doi.org/10.1016/j.pep.2005.01.016>
- Studier, F. W. (2014). Stable Expression Clones and Auto-Induction for Protein Production in *E. coli*. In Y. W. Chen (Ed.), *Structural Genomics: General Applications* (pp. 17–32). Humana Press. [https://doi.org/10.1007/978-1-62703-691-7\\_2](https://doi.org/10.1007/978-1-62703-691-7_2)
- Studier, F. W. (2018). T7 Expression Systems for Inducible Production of Proteins from Cloned Genes in *E. coli*. *Current Protocols in Molecular Biology*, 124(1), e63. <https://doi.org/10.1002/cpmb.63>
- Suede, S. H., Malik, A., & Sapra, A. (2023). Histology, Spermatogenesis. In *StatPearls*. StatPearls Publishing. <http://www.ncbi.nlm.nih.gov/books/NBK553142/>

- Suzuki, H., Tani, K., & Fujiyoshi, Y. (2017). Crystal structures of claudins: Insights into their intermolecular interactions. *Annals of the New York Academy of Sciences*, 1397(1), 25–34. <https://doi.org/10.1111/nyas.13371>
- Takahashi, A., Komiya, E., Kakutani, H., Yoshida, T., Fujii, M., Horiguchi, Y., Mizuguchi, H., Tsutsumi, Y., Tsunoda, S., Koizumi, N., Isoda, K., Yagi, K., Watanabe, Y., & Kondoh, M. (2008). Domain mapping of a claudin-4 modulator, the C-terminal region of C-terminal fragment of Clostridium perfringens enterotoxin, by site-directed mutagenesis. *Biochemical Pharmacology*, 75(8), 1639–1648. <https://doi.org/10.1016/j.bcp.2007.12.016>
- Takahashi, A., Kondoh, M., Masuyama, A., Fujii, M., Mizuguchi, H., Horiguchi, Y., & Watanabe, Y. (2005). Role of C-terminal regions of the C-terminal fragment of Clostridium perfringens enterotoxin in its interaction with claudin-4. *Journal of Controlled Release: Official Journal of the Controlled Release Society*, 108(1), 56–62. <https://doi.org/10.1016/j.jconrel.2005.07.008>
- Takashima, S., Kanatsu-Shinohara, M., Tanaka, T., Takehashi, M., Morimoto, H., & Shinohara, T. (2011). Rac Mediates Mouse Spermatogonial Stem Cell Homing to Germline Niches by Regulating Transmigration through the Blood-Testis Barrier. *Cell Stem Cell*, 9(5), 463–475. <https://doi.org/10.1016/j.stem.2011.08.011>
- Takashima, S., & Shinohara, T. (2018). Culture and transplantation of spermatogonial stem cells. *Stem Cell Research*, 29, 46–55. <https://doi.org/10.1016/j.scr.2018.03.006>
- Tang, L., Rodriguez-Sosa, J. R., & Dobrinski, I. (2012). Germ Cell Transplantation and Testis Tissue Xenografting in Mice. *Journal of Visualized Experiments : JoVE*, 60, 3545. <https://doi.org/10.3791/3545>
- Tarulli, G. A., Stanton, P. G., Loveland, K. L., Meyts, E. R.-D., McLachlan, R. I., & Meachem, S. J. (2013). A survey of Sertoli cell differentiation in men after gonadotropin suppression and in testicular cancer. *Spermatogenesis*, 3(1), e24014. <https://doi.org/10.4161/spmg.24014>
- Taylor, A., Warner, M., Mendoza, C., Memmott, C., LeCheminant, T., Bailey, S., Christensen, C., Keller, J., Suli, A., & Mizrachi, D. (2021). Chimeric Claudins: A New Tool to Study Tight Junction Structure and Function. *International Journal of Molecular Sciences*, 22(9), 4947. <https://doi.org/10.3390/ijms22094947>
- Thomas, J. G., Ayling, A., & Baneyx, F. (1997). Molecular chaperones, folding catalysts, and the recovery of active recombinant proteins from E. coli. *Applied Biochemistry and Biotechnology*, 66(3), 197–238. <https://doi.org/10.1007/BF02785589>
- Tokunaga, Y., Kojima, T., Osanai, M., Murata, M., Chiba, H., Tobioka, H., & Sawada, N. (2007). A novel monoclonal antibody against the second extracellular loop of occludin disrupts epithelial cell polarity. *The Journal of Histochemistry and Cytochemistry: Official Journal of the Histochemistry Society*, 55(7), 735–744. <https://doi.org/10.1369/jhc.6A7165.2007>
- Toor, J. S., & Sikka, S. C. (2017). Chapter 59—Developmental and Reproductive Disorders—Role of Endocrine Disruptors in Testicular Toxicity. In R. C. Gupta (Ed.), *Reproductive and Developmental Toxicology (Second Edition)* (pp. 1111–1121). Academic Press. <https://doi.org/10.1016/B978-0-12-804239-7.00059-7>
- Tournaye, H., & Goossens, E. (2011). Spermatogonial stem cells: What does the future hold? *Facts, Views & Vision in ObGyn*, 3(1), 36–40.
- Trimpin, S., & Brizzard, B. (2009). Analysis of insoluble proteins. *BioTechniques*, 46(6), 409–419. <https://doi.org/10.2144/000113168>

- Tsukita, S., Furuse, M., & Itoh, M. (2001). Multifunctional strands in tight junctions. *Nature Reviews Molecular Cell Biology*, 2(4), Article 4. <https://doi.org/10.1038/35067088>
- Tsumoto, K., Ejima, D., Kumagai, I., & Arakawa, T. (2003). Practical considerations in refolding proteins from inclusion bodies. *Protein Expression and Purification*, 28(1), 1–8. [https://doi.org/10.1016/S1046-5928\(02\)00641-1](https://doi.org/10.1016/S1046-5928(02)00641-1)
- Van Itallie, C. M. V., Betts, L., Smedley, J. G., McClane, B. A., & Anderson, J. M. (2008). Structure of the Claudin-binding Domain of Clostridium perfringens Enterotoxin \*. *Journal of Biological Chemistry*, 283(1), 268–274. <https://doi.org/10.1074/jbc.M708066200>
- Vakalopoulos, I., Dimou, P., Anagnostou, I., & Zeginiadou, T. (2015). Impact of cancer and cancer treatment on male fertility. *Hormones*, 14(4), 579–589. <https://doi.org/10.14310/horm.2002.1620>
- Vecchio, A. J., Rathnayake, S. S., & Stroud, R. M. (2021). Structural basis for Clostridium perfringens enterotoxin targeting of claudins at tight junctions in mammalian gut. *Proceedings of the National Academy of Sciences*, 118(15), e2024651118. <https://doi.org/10.1073/pnas.2024651118>
- Vera, A., González-Montalbán, N., Arís, A., & Villaverde, A. (2007). The conformational quality of insoluble recombinant proteins is enhanced at low growth temperatures. *Biotechnology and Bioengineering*, 96(6), 1101–1106. <https://doi.org/10.1002/bit.21218>
- Veshnyakova, A., Protze, J., Rossa, J., Blasig, I. E., Krause, G., & Piontek, J. (2010). On the Interaction of Clostridium perfringens Enterotoxin with Claudins. *Toxins*, 2(6), 1336–1356. <https://doi.org/10.3390/toxins2061336>
- Vihinen, M. (2020). Solubility of proteins. *ADMET & DMPK*, 8(4), 391–399. <https://doi.org/10.5599/admet.831>
- Waldow, A., Beier, L.-S., Arndt, J., Schallenberg, S., Vollbrecht, C., Bischoff, P., Farrera-Sal, M., Loch, F. N., Bojarski, C., Schumann, M., Winkler, L., Kamphues, C., Ehlen, L., & Piontek, J. (2023). cCPE Fusion Proteins as Molecular Probes to Detect Claudins and Tight Junction Dysregulation in Gastrointestinal Cell Lines, Tissue Explants and Patient-Derived Organoids. *Pharmaceutics*, 15(7), 1980. <https://doi.org/10.3390/pharmaceutics15071980>
- Walther, W., Petkov, S., Kuvardina, O. N., Aumann, J., Kobelt, D., Fichtner, I., Lemm, M., Piontek, J., Blasig, I. E., Stein, U., & Schlag, P. M. (2012). Novel Clostridium perfringens enterotoxin suicide gene therapy for selective treatment of claudin-3- and -4-overexpressing tumors. *Gene Therapy*, 19(5), 494–503. <https://doi.org/10.1038/gt.2011.136>
- Wang, X., Zhang, X., Hu, L., & Li, H. (2018). Exogenous leptin affects sperm parameters and impairs blood testis barrier integrity in adult male mice. *Reproductive Biology and Endocrinology*, 16(1), 55. <https://doi.org/10.1186/s12958-018-0368-4>
- Wieckowski, E. U., Wnek, A. P., & McClane, B. A. (1994). Evidence that an approximately 50-kDa mammalian plasma membrane protein with receptor-like properties mediates the amphiphilicity of specifically bound Clostridium perfringens enterotoxin. *The Journal of Biological Chemistry*, 269(14), 10838–10848.
- Wingfield, P. T. (2015). Overview of the Purification of Recombinant Proteins. *Current Protocols in Protein Science / Editorial Board, John E. Coligan ... [et Al.]*, 80, 6.1.1-6.1.35. <https://doi.org/10.1002/0471140864.ps0601s80>

- Wingfield, P. T., Palmer, I., & Liang, S.-M. (2014). Folding and Purification of Insoluble (Inclusion Body) Proteins from Escherichia coli. *Current Protocols in Protein Science*, 78, 6.5.1-6.5.30. <https://doi.org/10.1002/0471140864.ps0605s78>
- Winkler, L., Gehring, C., Wenzel, A., Müller, S. L., Piehl, C., Krause, G., Blasig, I. E., & Piontek, J. (2009). Molecular determinants of the interaction between Clostridium perfringens enterotoxin fragments and claudin-3. *The Journal of Biological Chemistry*, 284(28), 18863–18872. <https://doi.org/10.1074/jbc.M109.008623>
- Wong, E. W. P., Yan, H. H. N., Li, M. W. M., Lie, P. P. Y., Mruk, D. D., & Cheng, C. Y. (2010). 11.09—Cell Junctions in the Testis as Targets for Toxicants. In C. A. McQueen (Ed.), *Comprehensive Toxicology (Second Edition)* (pp. 167–188). Elsevier. <https://doi.org/10.1016/B978-0-08-046884-6.01111-8>
- Wong, V., & Gumbiner, B. M. (1997). A Synthetic Peptide Corresponding to the Extracellular Domain of Occludin Perturbs the Tight Junction Permeability Barrier. *The Journal of Cell Biology*, 136(2), 399–409.
- Wu, S., & Cheng, C. Y. (2020). Blood-Testis Barrier. In S. Offermanns & W. Rosenthal (Eds.), *Encyclopedia of Molecular Pharmacology* (pp. 1–6). Springer International Publishing. [https://doi.org/10.1007/978-3-030-21573-6\\_10017-1](https://doi.org/10.1007/978-3-030-21573-6_10017-1)
- Wu, V. M., Schulte, J., Hirschi, A., Tepass, U., & Beitel, G. J. (2004). Sinuous is a Drosophila claudin required for septate junction organization and epithelial tube size control. *The Journal of Cell Biology*, 164(2), 313–323. <https://doi.org/10.1083/jcb.200309134>
- Xu, J., Anuar, F., Mohamed Ali, S., Ng, M. Y., Phua, D. C. Y., & Hunziker, W. (2009). Zona Occludens-2 Is Critical for Blood–Testis Barrier Integrity and Male Fertility. *Molecular Biology of the Cell*, 20(20), 4268–4277. <https://doi.org/10.1091/mbc.e08-12-1236>
- Xu, J., Lu, H., Li, H., Yan, C., Wang, X., Zang, M., Rooij, D. G. de, Madabhushi, A., & Xu, E. Y. (2021). Computerized spermatogenesis staging (CSS) of mouse testis sections via quantitative histomorphological analysis. *Medical Image Analysis*, 70, 101835. <https://doi.org/10.1016/j.media.2020.101835>
- Yan Cheng, C., & Mruk, D. D. (2015). 12—Biochemistry of Sertoli cell/germ cell junctions, germ cell transport, and spermiation in the seminiferous epithelium. In M. D. Griswold (Ed.), *Sertoli Cell Biology (Second Edition)* (pp. 333–383). Academic Press. <https://doi.org/10.1016/B978-0-12-417047-6.00012-0>
- Yang, Q., Hao, J., Chen, M., & Li, G. (2014). Dermatopontin is a novel regulator of the CdCl<sub>2</sub>-induced decrease in claudin-11 expression. *Toxicology in Vitro*, 28(6), 1158–1164. <https://doi.org/10.1016/j.tiv.2014.05.013>
- Yuan, Y., Zhou, Q., Wan, H., Shen, B., Wang, X., Wang, M., Feng, C., Xie, M., Gu, T., Zhou, T., Fu, R., Huang, X., Zhou, Q., Sha, J., & Zhao, X.-Y. (2015). Generation of fertile offspring from Kitw/Kitwv mice through differentiation of gene corrected nuclear transfer embryonic stem cells. *Cell Research*, 25(7), Article 7. <https://doi.org/10.1038/cr.2015.74>
- Zhao, X., Wan, W., Zhang, X., Wu, Z., & Yang, H. (2021). Spermatogonial Stem Cell Transplantation in Large Animals. *Animals : An Open Access Journal from MDPI*, 11(4), 918. <https://doi.org/10.3390/ani11040918>
- Zohni, K., Zhang, X., Tan, S. L., Chan, P., & Nagano, M. (2012). CD9 is expressed on human male germ cells that have a long-term repopulation potential after transplantation into mouse testes. *Biology of Reproduction*, 87(2), 27. <https://doi.org/10.1095/biolreprod.112.098913>

Zwanziger, D., Hackel, D., Staat, C., Böcker, A., Brack, A., Beyermann, M., Rittner, H., & Blasig, I. E. (2012). A peptidomimetic tight junction modulator to improve regional analgesia. *Molecular Pharmaceutics*, 9(6), 1785–1794.  
<https://doi.org/10.1021/mp3000937>

## 7. Appendix

### 7.1 Animal Ethics Certificate



August 31, 2023

#### Animal Certificate

This is to certify that **Dr Makoto Nagano, Glen site of the RI-MUHC**, currently holds an approved **Animal Use Protocol # MUHC-7376** with McGill University and its Affiliated Hospital's Research Institutes for the following project:

**Animal Use Protocol Title:** Improving colonization of spermatogonial stem cells by disrupting the blood-testis barrier

**Start date:** August 31, 2023

**Expiration date:** August 30, 2024

McGill University and Affiliated Hospitals Research Institutes recognize the importance of animal research in our efforts to further our knowledge of natural processes, diseases and conservation. Research, educational and testing projects are conducted with full commitment to the wellbeing of the animal subjects. In order to limit animal use to meritorious research or educational projects, the institution relies on stringent peer review processes, along with assessment of ethical issues by the Animal Care Committee. McGill University recognizes that the use of animals in research, teaching and testing carries significant responsibilities. The institution will continue to develop and maintain guidelines and regulations, following the high standards established by the Canadian Council on Animal Care. It is committed to conducting the highest-quality research and to providing animals with the best care.

A handwritten signature in blue ink that reads "Cynthia Lavoie".

**Cynthia Lavoie**

Animal Ethics and Compliance Administrator  
Animal Compliance Office  
Office of Vice-Principal (Research and Innovation)  
Suite 325, James Administration Building, McGill University  
845 Sherbrooke Street West, Montreal, Quebec, Canada H3A 0G4  
[animal\\_approvals@mcgill.ca](mailto:animal_approvals@mcgill.ca)